Journal of Medicinal Chemistry

pubs.acs.org/jmc

Article

Design, Synthesis, and Evaluation of Antifibrotic Activity of Nonsteroidal VDR Agonists Featuring 1,6-Naphthol as a CD-Ring Surrogate

Yi Gao,[#] Yue Wu,[#] Chun Guan, Nuo Cheng, Yu Tong, Cong Wang,[*] and Can Zhang[*]

Cite This: *J. Med. Chem.* 2025, 68, 20561−20585

Read Online

ACCESS | Metrics & More | Article Recommendations | Supporting Information

ABSTRACT: Chronic liver diseases activate hepatic stellate cells (HSCs), driving excessive deposition of extracellular matrix (ECM) and leading to liver fibrosis. Despite being a crucial precursor to cirrhosis, effective targeted antifibrotic therapies are lacking. Activation of the vitamin D receptor (VDR) has been shown to effectively alleviate liver fibrosis, yet prolonged use of currently available steroidal VDR agonists can lead to hypercalcemia. To address this issue, we performed structural optimization targeting the CD-ring and conjugated triene moiety, while preserving the A-ring and side chains, yielding 52 novel nonsteroidal VDR modulators. Among them, compounds **A17**, **B15**, and **B20** demonstrated favorable VDR binding affinity and potent antifibrotic activity *in vitro*. Notably, compound **B15** significantly reduced fibrosis without inducing hypercalcemia in a murine model of carbon tetrachloride (CCl_4)-induced liver fibrosis. These findings highlight the potential of these nonsteroidal VDR modulators and warrant further investigation as promising therapeutics for liver fibrosis.

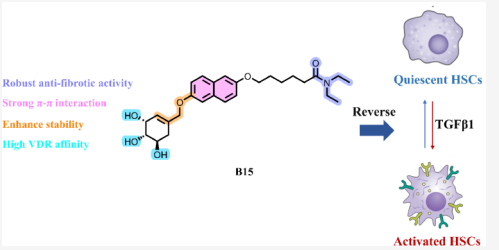

INTRODUCTION

The progression of various chronic liver diseases, such as those resulting from viral infections, alcoholism, drug abuse, cholestasis, and autoimmune disorders, ultimately culminates in the development of liver fibrosis.[1,2] Liver fibrosis is a pivotal factor in the pathogenesis of clinical complications, including chronic portal hypertension, decompensated ascites, gastrointestinal bleeding, and hepatic encephalopathy, contributing to nearly one million deaths globally each year.[3,4] Despite this significant impact, no pharmacological agents specifically targeting liver fibrosis have been successfully developed to date.

Hepatocellular injury triggers an inflammatory response characterized by the activation of quiescent hepatic stellate cells (HSCs) through inflammatory mediators, notably transforming growth factor-beta (TGFβ). Upon activation, HSCs release proinflammatory factors that sustain and amplify their activated state. Furthermore, these activated HSCs undergo differentiation into proliferative and migratory myofibroblasts, marked by the expression of α-smooth muscle actin (α-SMA) and the production of extracellular matrix (ECM) components, particularly type I collagen, thereby contributing to the development of liver fibrosis.[5−8] Activated HSCs play a pivotal role in the pathogenesis of liver fibrosis, and their reversion to a quiescent state is considered a promising therapeutic approach for hepatic fibrosis.[9−11] Numerous studies have identified the TGFβ/Sma- and Mad-related protein 3 (SMAD3) signaling pathway as the primary molecular cascade governing HSC activation.[12]

Activation of the TGFβ/SMAD3 signaling pathway results in the upregulation of multiple profibrotic genes, thereby exacerbating liver fibrosis. Conversely, inhibition of this pathway has been demonstrated to significantly ameliorate liver fibrosis.[13−15] Nonetheless, direct inhibition of TGFβ may result in the onset of autoimmune disorders and cardiotoxicity,[16] thereby presenting substantial challenges for its therapeutic application. Research suggests that activation of the vitamin D receptor (VDR) can effectively mitigate liver fibrosis by suppressing the TGFβ/SMAD3 signaling pathway.[17,18] The VDR is a nuclear receptor that functions as the primary effector protein, mediating the biological actions of VD_3. Upon ligand (such as calcitriol, Figure 1) binding, VDR not only regulates calcium and phosphorus homeostasis, promotes bone development, modulates immune responses, and inhibits cell proliferation[19,20] but also plays a critical role in HSCs, which exhibit high levels of VDR expression. The VDR agonist calcipotriol (Figure 1) has shown efficacy in improving liver fibrosis and remodeling the tumor microenvironment through inhibition of the TGFβ/SMAD3 signaling pathway.[21] Furthermore, several other vitamin D analogs have demonstrated beneficial effects on liver fibrosis.[22] Despite advance-

Received: June 25, 2025
Revised: September 6, 2025
Accepted: September 15, 2025
Published: September 19, 2025

https://doi.org/10.1021/acs.jmedchem.5c01753
J. Med. Chem. 2025, 68, 20561−20585

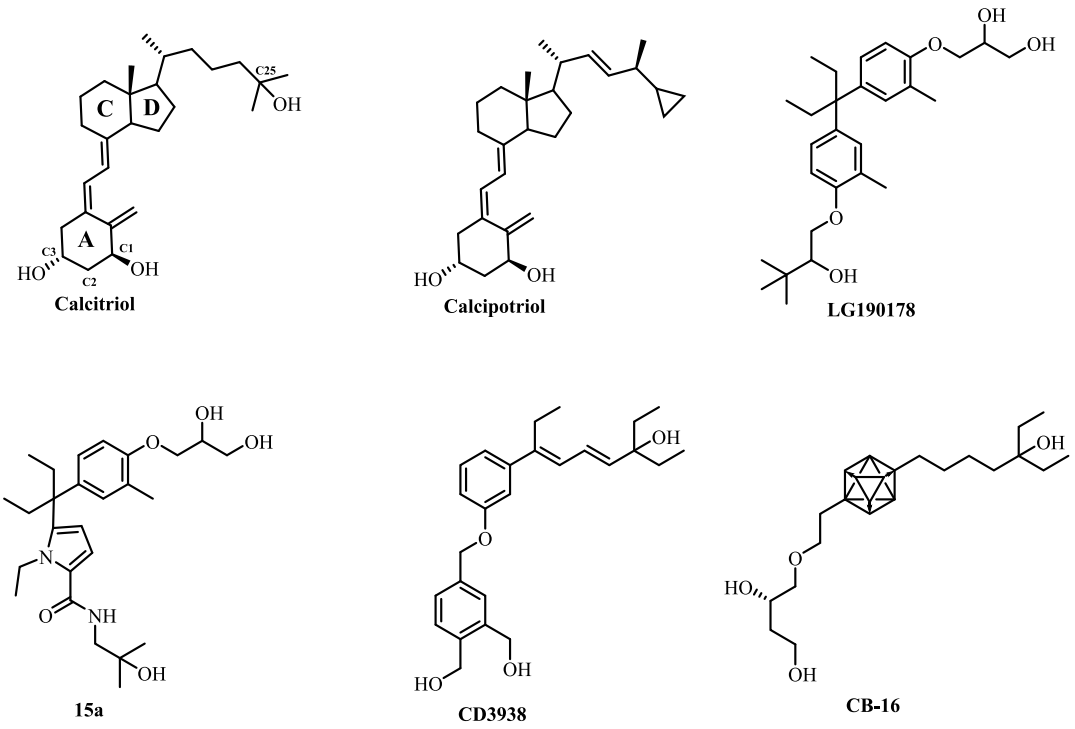

Figure 1. Chemical structures of representative steroidal and nonsteroidal VDR ligands.

ments, several significant challenges persist for these VDR agonists in the clinical management of liver fibrosis.

Currently, VDR agonists encompass over a dozen drugs available on the market, primarily used for treating osteoporosis and psoriasis.[23,24] These compounds predominantly exhibit steroidal structures, are sensitive to ultraviolet radiation, and have the capacity to bind to plasma vitamin D-binding proteins (DBPs). Consequently, their application in treating cancer and fibrosis is constrained by several critical factors, including their complex molecular structure, photodegradation instability, and potential to induce hypercalcemia due to their diverse biological activities.[25] The treatment of liver fibrosis requires prolonged drug administration, which raises significant concerns about the occurrence of hypercalcemia-related side effects, given their potential severity. To address these limitations, particularly hypercalcemia, numerous nonsteroidal VDR agonists have been developed, demonstrating promising biological activity.[26,27] Compared with steroidal VDR agonists, nonsteroidal counterparts are devoid of both the conjugated triene moiety and the cyclopentane polyhydrophenanthrene core. This structural distinction allows them to retain biological activity while reducing binding to DBPs, thereby improving activity selectivity and mitigating side effects such as hypercalcemia. As shown in Figure 1, the derivatives under consideration include bisphenol cyclo methanes[28] (LG190178), phenylpyrrole pentanes[29] (**15a**), trichromatic cycloalcohols[30] (CD3938), and carboranes[31] (CB-16). Among these, bisphenol cyclo methanes demonstrate the highest affinity for the VDR and exhibit the most potent agonistic activity, suggesting their significant potential in drug development.

Utilizing bioelectronic isosteric replacement strategies with bisphenol cyclo-methanes as lead compounds, we have previously designed and synthesized a series of VDR agonists characterized by a phenyl-pyrrolyl-pentane core scaffold.[32−34] These compounds have been shown to effectively inhibit HSC activation without altering blood calcium levels, and they display notable antifibrotic activity in murine models. Recently, we further extensively modified the CD-ring to improve both VDR binding affinity and antifibrotic efficacy, such as **16i** and **E15**.[35,36] However, these structural alterations did not deliver the anticipated gains in overall potency. Consequently, there remains potential to enhance the affinity and agonistic activity of these nonsteroidal VDR agonists to further improve their antifibrotic efficacy.

Building upon a comprehensive review of previous research, we have refined the design of the VDR agonist structure to meet the therapeutic requirements for liver fibrosis treatment. A total of 52 compounds were synthesized following two rounds of structural optimization. Among these, compound **B15** demonstrated a unique binding affinity for the VDR and inhibited HSC activation comparably to **15a**,[34] a nonsteroidal VDR agonist renowned for its potent antihepatic fibrosis properties. In a CCl_4-induced liver fibrosis mouse model, **B15** exhibited a significant antifibrotic effect, akin to that of the positive control calcipotriol.

RESULTS AND DISCUSSION

Design and Synthesis of Novel Nonsteroidal VDR Agonists. Steroidal VDR agonists are characterized by their cyclopentane polyhydrophenanthrene core, which enhances their binding to the DBP in plasma, consequently leading to hypercalcemia. To address this adverse effect, numerous nonsteroidal VDR agonists have been developed. These nonsteroidal agonists feature a more stable structure that is easier to synthesize and, most importantly, completely avoid hypercalcemia due to structural modifications that prevent binding to DBP.[37] Many nonsteroidal VDR agonists have demonstrated favorable VDR affinity and biological activity *in vitro*. However, they still present certain limitations compared with calcitriol.

https://doi.org/10.1021/acs.jmedchem.5c01753
J. Med. Chem. 2025, 68, 20561−20585

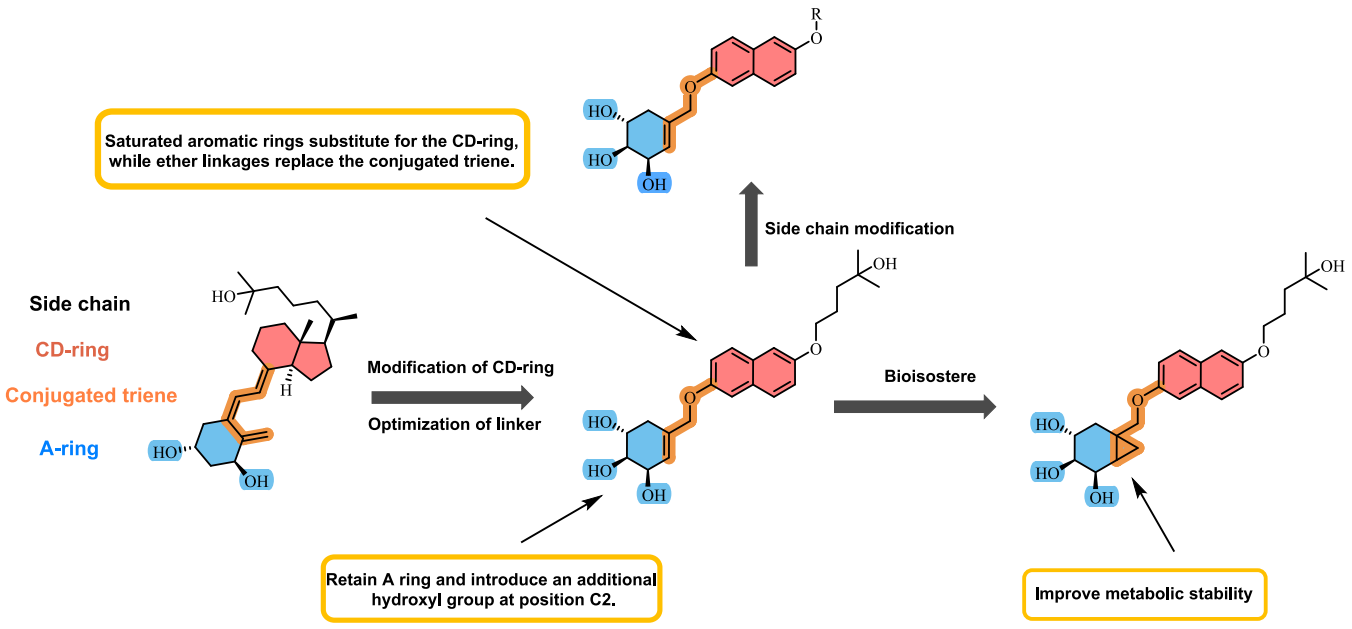

Figure 2. Design of nonsteroidal VDR modulators with 1,6-dinaphthol skeletons.

Scheme 1. Synthesis of Intermediates 3 and 6 Reagents and Conditions: (a) $SOCl_2$, MeOH, 65°C, 6 h; (b) TBSCl, Imidazole, DMF, 60°C, 6 h; (c) DIBAL-H, THF, 0−25°C, Overnight; (d) CH_2N_2, Et_2O, rt, 5 h; (e) DMSO, 150°C, 1 h; (f) DIBAL-H, THF, 0−25°C, Overnight

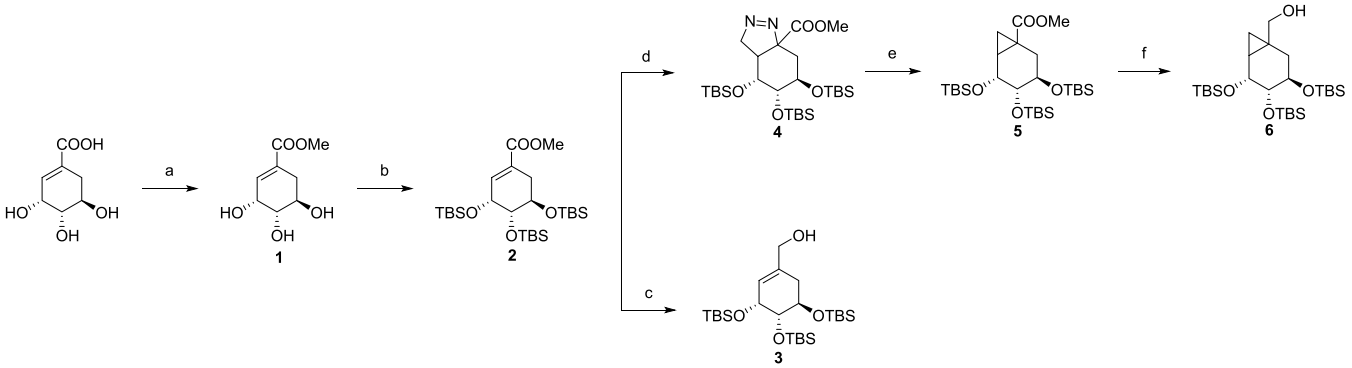

Through comprehensive structural analysis, we determined that the conjugated triene structure in steroid agonists not only contributes to structural instability but also serves as the critical pharmacophore enabling hypercalcemia via hydrophobic interactions with DBP.[38] To address these issues and enhance the VDR affinity and antifibrotic efficacy of these compounds, we designed and synthesized a series of VDR agonists using 1,6-dinaphthol as the core scaffold (Figure 2). Analysis of previously designed compounds has indicated that nonsteroidal VDR agonists, despite their high affinity, frequently lack the A-ring structural component—a major determinant of binding.[39] Therefore, incorporating an A-ring-like moiety represents a rational strategy for enhancing the affinity. To preserve the hydrogen bonding capabilities at the C1 and C3 positions, we replaced the A-ring with shikimic acid, which structurally mimics these functionalities. Additionally, introducing a hydroxyl group at the C2 position improved the binding affinity of VDR while substituting the conjugated triene structure with a more stable ether linkage. Moreover, the CD-ring is replaced by 1,6-dinaphthol, which enhances the structural stability and facilitates easier synthesis. In conclusion, we innovatively replaced the CD-ring with 1,6-dinaphthol and substituted the conjugated trienes with flexible ether linkages while essentially preserving the A-ring and side chain structure. Positioned on the CD-ring, the 1,6- dinaphthol substituent optimally occupies the VDR LBD hydrophobic cavity—a well-characterized determinant of binding affinity enhancement.[40] The naphthalene moiety further stabilizes this interaction through $\pi-\pi$ stacking with cavity residues. Crucially, A-ring retention significantly enhances biological activity.[41] Our structural strategy replaces this A-ring with a shikimic acid analog to functionally emulate its role, yielding compounds with demonstrated robust VDR affinity and potent agonist properties. We subsequently designed and synthesized a series of compounds aimed at discovering more potent VDR agonists.

The synthetic pathways for intermediates **3** and **6** are illustrated in Scheme 1. Shikimic acid underwent methylation via $SOCl_2$ in methanol to afford intermediate **1**. The hydroxyl group of intermediate **1** was protected with TBSCl in the presence of imidazole in DMF, yielding intermediate **2**. Intermediate **2** was then reduced with DIBAL-H in dichloromethane at −20 °C to afford intermediate **3**. Additionally, the reaction of intermediate **2** with CH_2N_2 in Et_2O produced

https://doi.org/10.1021/acs.jmedchem.5c01753
J. Med. Chem. 2025, 68, 20561−20585

Scheme 2. Synthesis of Compounds A1−A24, B1−B3, B9−B12, B13, and B21−B23 Reagents and Conditions: (a) NaH, DMF, 0−60°C, 5 h; (b) Intermediate 3, DEAD, Ph_3P, THF, 0−25°C, Overnight (intermediate 10) or Intermediate 6, DEAD, Ph_3P, THF, 0−25°C, Overnight (Intermediate 8); (c) RMgBr, THF, rt, 2 h; (d) TsOH, CH_3OH, rt, Overnight; (e) H_2, Pd/C, CH_3OH, rt, 48 h

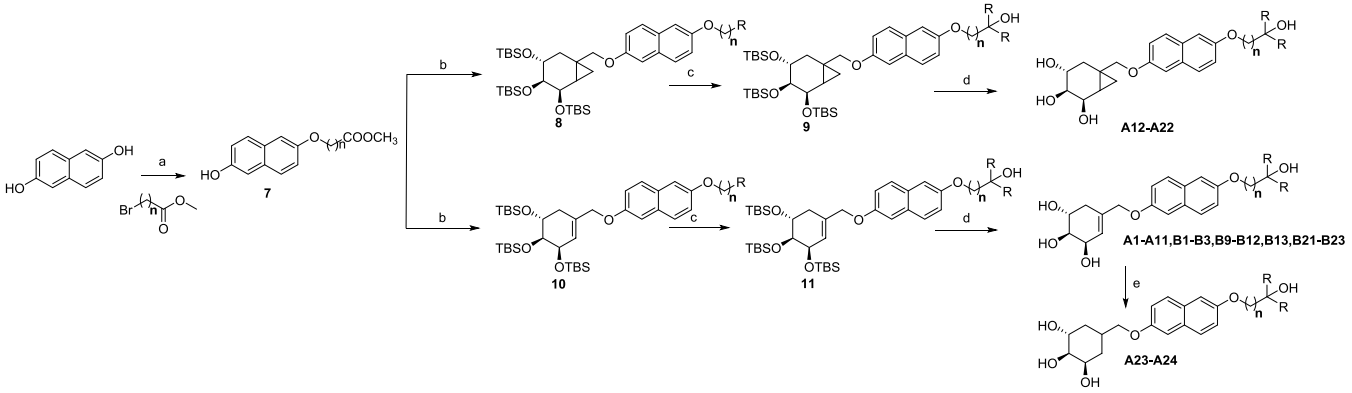

Scheme 3. Synthesis of Compounds B5−B8, B14−B20, and B25−B28 Reagents and Conditions: (a) NaOH, THF, H_2O, 70°C, 5 h; (b) RNH_2, HATU, DCM, rt, Overnight; (c) TsOH, CH_3OH, rt, Overnight

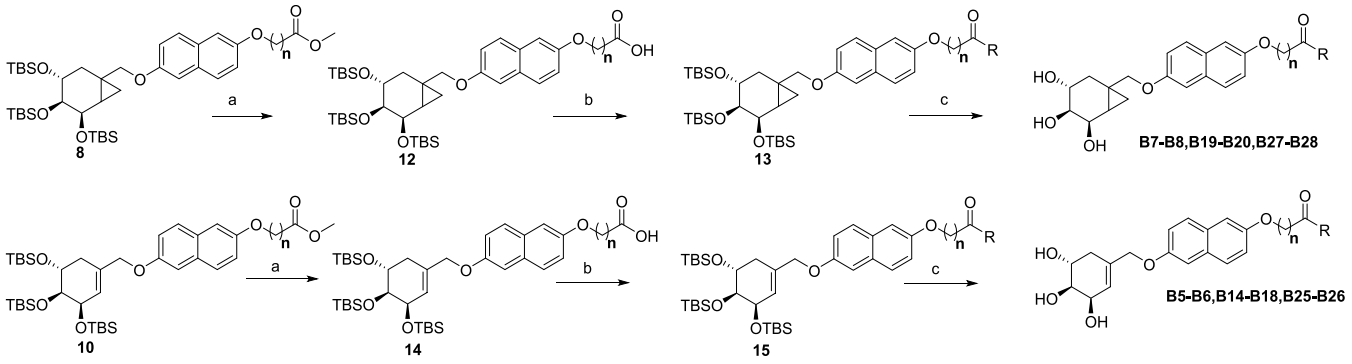

intermediate **3**, which underwent rearrangement upon heating at 150 °C and subsequent reduction by DIBAL-H to yield intermediate **6**. The synthetic route of compounds **A1−A24** is shown in Scheme 2. 1,6-Dinaphthol was dissolved in DMF and reacted with various brominated esters in the presence of NaH as a base to generate intermediate **7**. Intermediate **7** subsequently underwent a Mitsunobu reaction with intermediate **3** to afford intermediate **8**. Intermediate **8** further reacted with appropriate Grignard reagents to form intermediate **9**, which was deprotected with TsOH to afford compounds **A1−A11**, **B1−B4**, **B9−B13**, and **B21−B24**. Similarly, compounds **A12−A22** were synthesized, whereas **A23−A24** were obtained through the hydrogenation of **A11** and **A12** under Pd/C catalysis. Intermediate **8** was hydrolyzed with sodium hydroxide to yield intermediate **12**, which then reacted with various amines in the presence of HATU to form intermediate **13**. Deprotection of these intermediates afforded compounds **B5−B6**, **B14−B18**, and **B25−B26**. Compounds **B7−B8**, **B19−B20**, and **B27−B28** were similarly synthesized (Scheme 3).

VDR Binding Affinity. The binding affinity of the compound for the VDR was investigated, and its structural characteristics, along with the associated data, are summarized in Table 1. Ligand competitive binding assays were conducted to evaluate the VDR binding capacity of these compounds, with calcipotriol serving as the positive control and its binding efficacy set at 100%. Preliminary structural design revealed a substantial influence of side chain length on VDR binding activity. Specifically, when the terminal substituent is dimethyl or diethyl, the relationship between the carbon chain length and activity follows this order: 5 > 6 ≈ 4 > 7 ≈ 3 > 2. Notably, compounds **A7** and **A17**, both featuring a carbon chain length of 5, demonstrated superior VDR binding capacity. Furthermore, modifications to the A-ring structure also impact the binding ability of VDR. The presence of a double bond in the A-ring was found to be critical for activity; reducing this double bond significantly diminished the binding ability of VDR, whereas substituting it with an isopropyl cyclopropyl group had a minimal effect on compound activity. Based on these findings, we selected side chain lengths of 4, 5, and 6 for further structural optimization. In the previous round of optimization, variations in activity were observed between the dimethyl and diethyl end groups, suggesting that steric hindrance from the terminal substituent may play a crucial role in influencing the binding capability of VDR. Building on this foundation, an amide bond was introduced at the terminus to increase the water solubility and stability of the compound while potentially improving hydrogen bonding between the side chain's terminal moiety and amino acids within the VDR. The introduction of amide substituents in the side chain significantly enhanced the VDR binding ability of compounds **B15**, **B19**, and **B20**, indicating the effectiveness of this modification. Additionally, when the side chain length was 5, the compound exhibited the highest affinity for the VDR. In summary, the VDR agonist based on the 1,6-dinaphthol core scaffold exhibits significant VDR affinity. The compounds

https://doi.org/10.1021/acs.jmedchem.5c01753
J. Med. Chem. 2025, 68, 20561−20585

Table 1. Chemical Structures of Synthesized Novel Nonsteroidal VDR Agonists

Comp	A	n	R	VDR Binding affinity (100%)	Comp	A	n	R	VDR Binding affinity (100%)
A1		2		25	B1		4		45
A2		3		35	B2		4		35
A3		3		38	B3		4		46
A4		4		46	B4		4		46
A5		4		52	B5		4		51
A6		5		67	B6		4		56
A7		5		76	B7		4		38
A8		6		49	B8		4		49
A9		6		52	B9		4		42
A10		7		31	B10		4		31
A11		7		26	B11		5		26
A12		2		22	B12		5		22
A13		3		36	B13		5		36
A14		3		48	B14		5		58
A15		4		46	B15		5		67
A16		4		45	B16		5		42
A17		5		65	B17		5		46
A18		5		58	B18		5		58
A19		6		54	B19		5		65
A20		6		50	B20		5		72
A21		7		32	B21		6		54
A22		7		24	B22		6		50
A23		4		26	B23		6		32
A24		4		24	B24		6		24
					B25		6		26
					B26		6		24
					B27		6		28
					B28		6		34

featuring a five-carbon side chain terminating in an amide group, particularly those with dimethylamino or diethylamino substituents, demonstrated the highest affinity for VDR. Structurally, the A-ring in our compounds closely resembles that of calcitriol, with both adopting a hydroxyl-substituted cyclohexane scaffold. This stands in sharp contrast to certain

https://doi.org/10.1021/acs.jmedchem.5c01753
J. Med. Chem. 2025, 68, 20561−20585

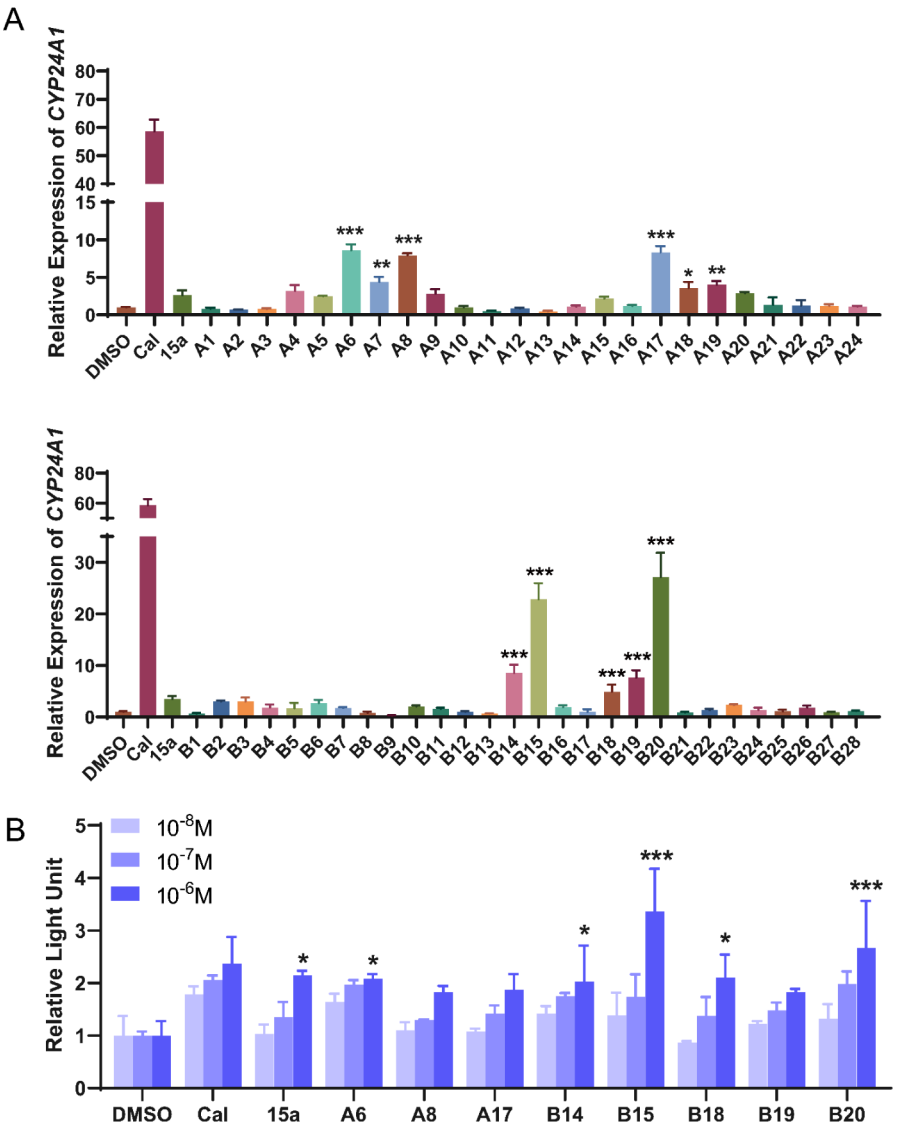

Figure 3. VDR activation ability of the compounds. (A) The relative expression of *CYP24A1* in LX-2 cells was detected by qPCR after treatment with different compounds at a final concentration of 0.1 μM, with calcipotriol and **15a** as positive controls and DMSO as a negative control (mean ± SD; *p < 0.05 vs DMSO, **p < 0.01 vs DMSO, ***p < 0.001 vs DMSO). (B) The VDR transactivation activities of 8 preferred compounds were detected in HEK293 cells via dual-luciferase reporter genes, with calcipotriol and **15a** used as positive controls and DMSO used as a negative control. Transcriptional activities of the 8 preferred compounds at 0.01 μM, 0.1 μM, and 1 μM (mean ± SD; *p < 0.05 vs DMSO, ***p < 0.001 vs DMSO).

nonsteroidal VDR agonists, such as **15a**, that replace the A-ring with an open-chain alcohol moiety. Such structural mimicry likely facilitates the formation of multiple stable hydrogen bonds with key residues within the VDR LBD, thereby reinforcing receptor−ligand interactions. Moreover, incorporation of an amide side chain may potentiate VDR affinity through additional hydrogen bonding and reinforced hydrophobic interactions.

Relative VDR binding affinity (%) = (mP DMSO—mP Testing Compound)/(mP DMSO—mP calcipotriol) × 100%. Calcipotriol is assigned a value of 100%.

VDR Activation Ability of the Compounds. The activation of HSCs serves as the pivotal mechanism underlying liver fibrosis. To further validate the therapeutic efficacy of the compound in treating liver fibrosis, we used human LX-2 cells to assess VDR activation in HSCs. Using the Cell Counting Kit -8 (CCK-8) assay as a quantitative measure of cell viability based on mitochondrial dehydrogenase activity, all compounds were screened in LX-2 cells, with resulting IC_{50} values >50 μM (Table S1 and Figure S1), confirming their safety. Considering the favorable safety profile and our previous research experience,[32,33] a concentration of 0.1 μM was chosen to achieve optimal activation of the VDR. *CYP24A1*, a downstream signature gene that is widely used as an indicator of VDR excitatory activity,[36] was assessed for its expression in LX-2 cells via quantitative polymerase chain reaction (qPCR) to confirm the VDR activity of the compound.

The results are presented in Figure 3A. When the terminal substituent is a tertiary alcohol, the compound's VDR activation activity clearly follows the order of 5 > 6 ≈ 4 > 7 ≈ 3 > 2, and there is a distinction between dimethyl tertiary alcohol and diethyl tertiary alcohol, indicating the influence of steric hindrance from the terminal substituent. Moreover, the A-ring structure also has a certain effect on the compound's

https://doi.org/10.1021/acs.jmedchem.5c01753
J. Med. Chem. 2025, 68, 20561−20585

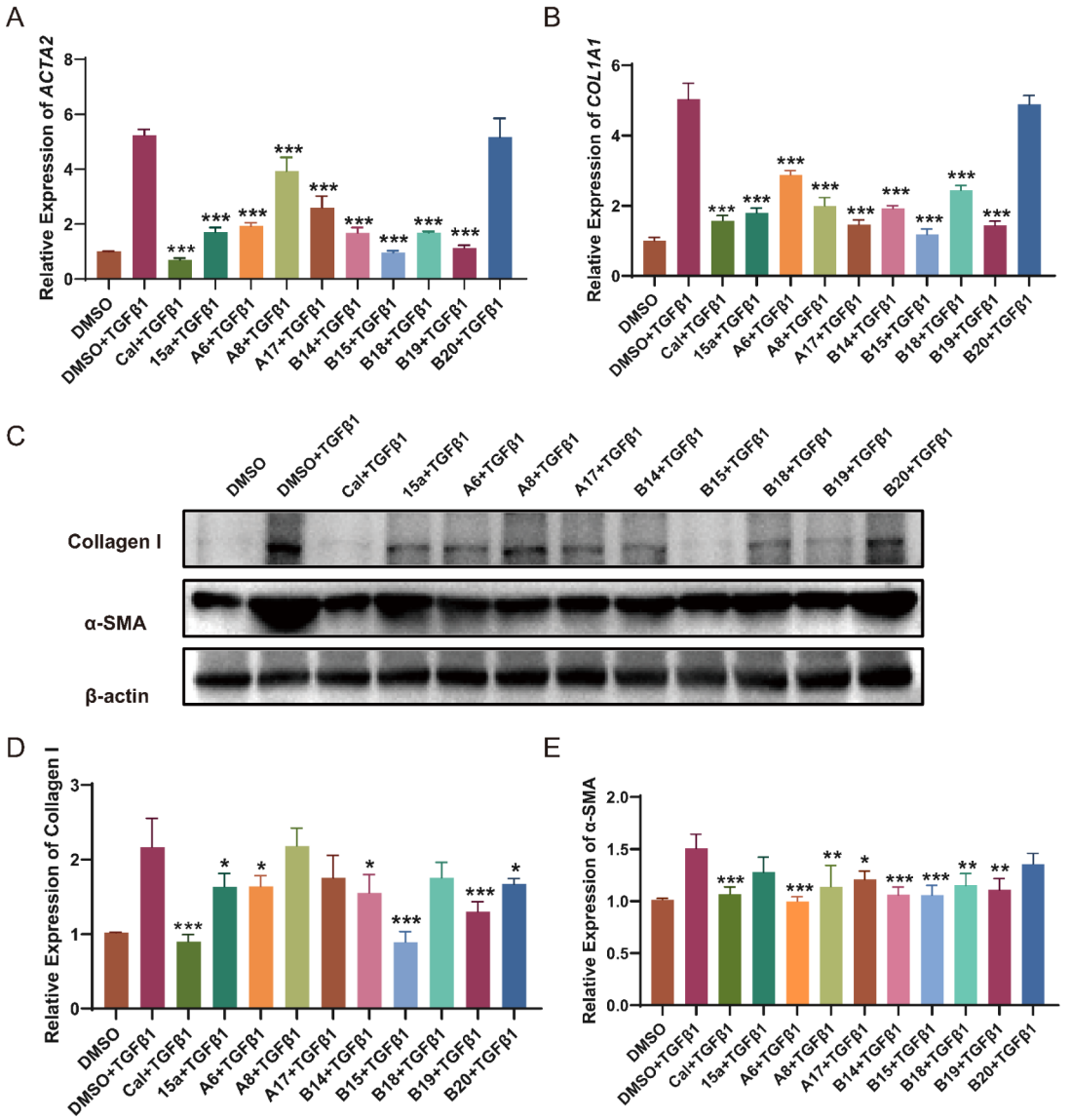

Figure 4. Selected compounds effectively suppressed collagen I and α-SMA expression *in vitro*. LX-2 cells were treated with different compounds at a final concentration of 0.1 μM, with calcipotriol and **15a** as positive controls and DMSO as a negative control. (A) The relative expression of *ACTA2* was detected by qPCR. (B) The relative expression of *COL1A1* was detected by qPCR. (C) The relative expression of collagen I and α-SMA in LX-2 cells was determined by Western blotting. Representative gel electrophoresis bands were shown. (D) Relative protein expression of collagen I was normalized to the protein expression of β-actin. (E) Relative protein expression of α-SMA was normalized to the protein expression of β-actin (mean ± SD; $^{*}p < 0.05$ vs TGFβ1, $^{**}p < 0.01$ vs TGFβ1, $^{***}p < 0.001$ vs DMSO+TGFβ1).

ability to activate the VDR; specifically, the order of the two-bond derivative ≈ cyclopropyl > saturated alkane. These findings align well with the compound's ability to bind to VDR. The length of the side chain is the primary determinant of compound activity. The effects of the A-ring structure and end-substituent on the steric hindrance of the side chain are not readily apparent, thereby providing a reference for subsequent structural optimization.

Based on these previous results, to further enhance the agonistic activity of the compound, its structure was subjected to additional modifications, and active carbon chain lengths of 4, 5, and 6 were selected. As the steric hindrance of the terminal tertiary alcohol substituents increased, there was a significant decrease in VDR activation activity, with methyl > ethyl > n-propyl > *n*-butyl > benzyl; this may be due to the impact of increased terminal substituents on the ability of terminal hydroxyl groups to form hydrogen bonds. However, compounds **B12** and **B24** exhibited a loss of activity due to the absence of dimethyl end-substituents, highlighting the essential role of appropriate steric hindrance from end-substituents. We introduced a series of amide substituents at the terminal position of the compound, exploiting the intrinsic stability and water solubility of the amide bond to improve both the aqueous solubility and stability of the compound. Furthermore, this modification enables the formation of stronger hydrogen bonding interactions, which in turn enhances the activity of the compound. Surprisingly, after amide substituents were incorporated into the side chain, there was a significant increase in *CYP24A1* gene expression; in particular, compounds **B15** and **B20** exhibited significantly better activity than **15a** did, reaching one-third that of the calcipotriol positive control. The activity of amide compounds still relies primarily on the end substituents, with diethyl > dimethyl > other being the preferred choices. The optimal side chain length for the

https://doi.org/10.1021/acs.jmedchem.5c01753
J. Med. Chem. 2025, 68, 20561−20585

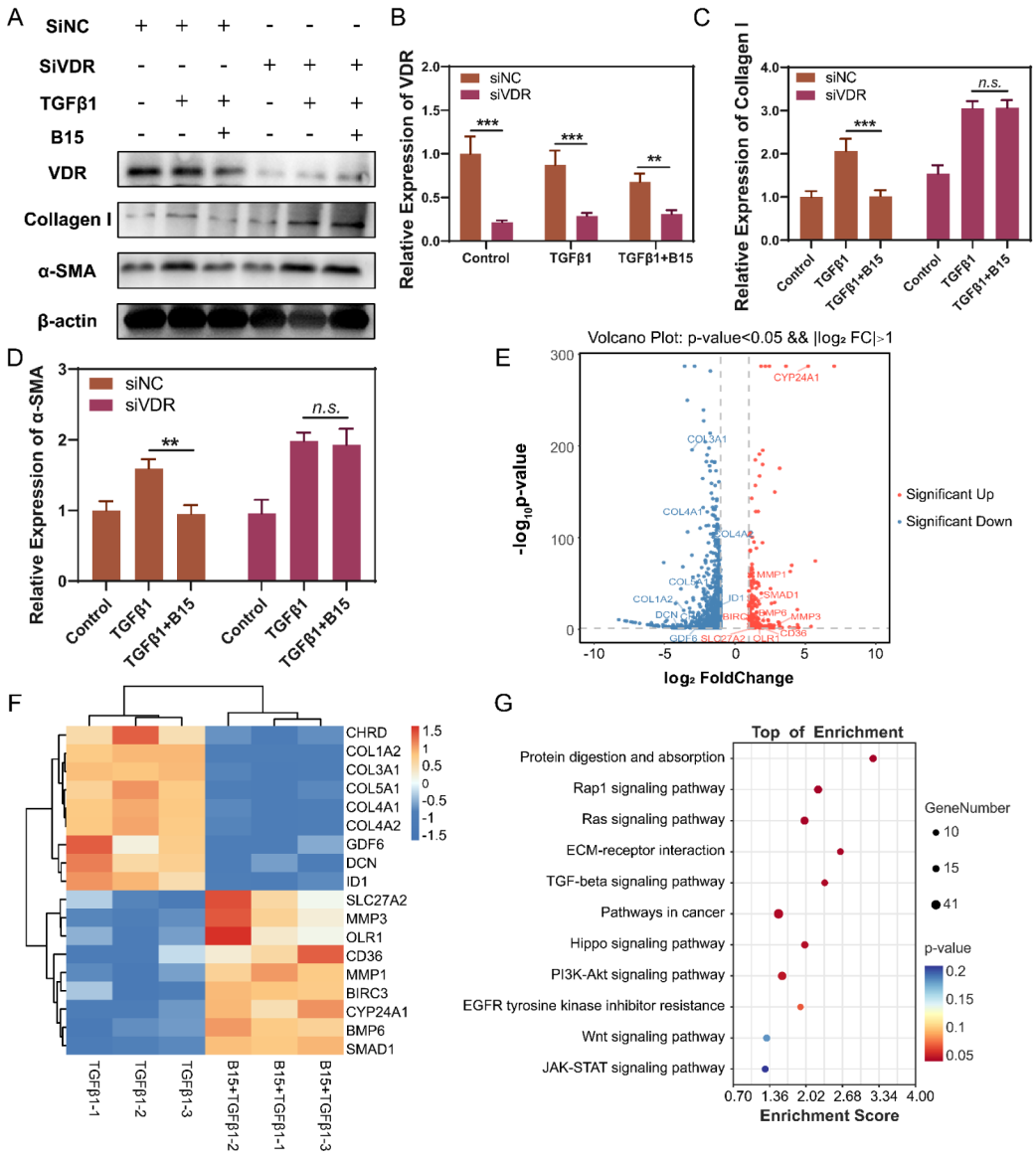

Figure 5. Compound **B15** suppressed fibrosis gene expression through the VDR. (A) VDR Knockout Experiment and RNA-Seq analysis of Compound **B15**. VDR-specific (siVDR) or negative control (siNC) siRNA-transfected LX-2 cells were treated with **B15** (0.1 μM), TGFβ1 (5 ng/mL) or TGFβ1 plus **B15** for 24 h. The expression of VDR, α-SMA, and collagen I in LX-2 cells was tested via Western blotting. Representative gel electrophoresis bands were shown. (B) Relative protein expression of VDR was normalized to the protein expression of β-actin. (C) Relative protein expression of collagen I was normalized to the protein expression of β-actin. (D) Relative protein expression of α-SMA was normalized to the protein expression of β-actin. (E) Compound **B15** elicited differential gene expression in LX-2 cells induced by TGFβ1. RNA-Seq analysis of LX-2 cells treated with TGFβ1 (5 ng/mL) or **B15** (0.1 μM) + TGFβ1 (5 ng/mL) for 48 h (n = 3). RNA-Seq analysis of global mRNA changes in LX-2 cells treated with **B15**. (F) Heatmap of DEGs is shown ($|\log_2$ FCl ≥ 1 and p-value <0.05). (G) KEGG analysis of differentially expressed genes (DEGs) in LX-2 cells treated with **B15**. The top significantly enriched pathways are shown with the number of genes in each category and the corresponding Q value. The quantified densitometry data are shown as the mean ± SD; *p < 0.05 (mean ± SD); **p < 0.01 vs TGFβ1; ***p < 0.001 vs DMSO+TGFβ1.

compound is 5. The A-ring has minimal influence, possibly because of the flexible ether bond connecting it with the CD-ring, which enhances compound stability and facilitates unrestricted rotation within the VDR cavity to establish crucial hydrogen bonding interactions with the hydroxyl groups at C1 and C3.

The incorporation of amide substituents significantly enhanced the activity of the compound. Eight compounds demonstrating notable activity, particularly **B15** and **B20**, were selected for further investigation. To confirm the ability of the compounds to activate the VDR, calcipotriol and **15a** were used as positive controls, whereas DMSO was used as a negative control. The VDR transcriptional activity of the compound was evaluated in HEK293 cells via a dual-luciferase reporter assay (Figure 3B). The concentration-dependent activation of **B15** and **B20** was markedly greater than that of **15a** and approached the efficacy of calcipotriol. These results provide further evidence of the potent agonistic effect of this compound on VDR. The experimental data indicate a strong positive correlation between the agonistic activity of compounds against VDR and their binding affinity for VDR. Notably, a five-carbon side chain length is optimal for

https://doi.org/10.1021/acs.jmedchem.5c01753
J. Med. Chem. 2025, 68, 20561−20585

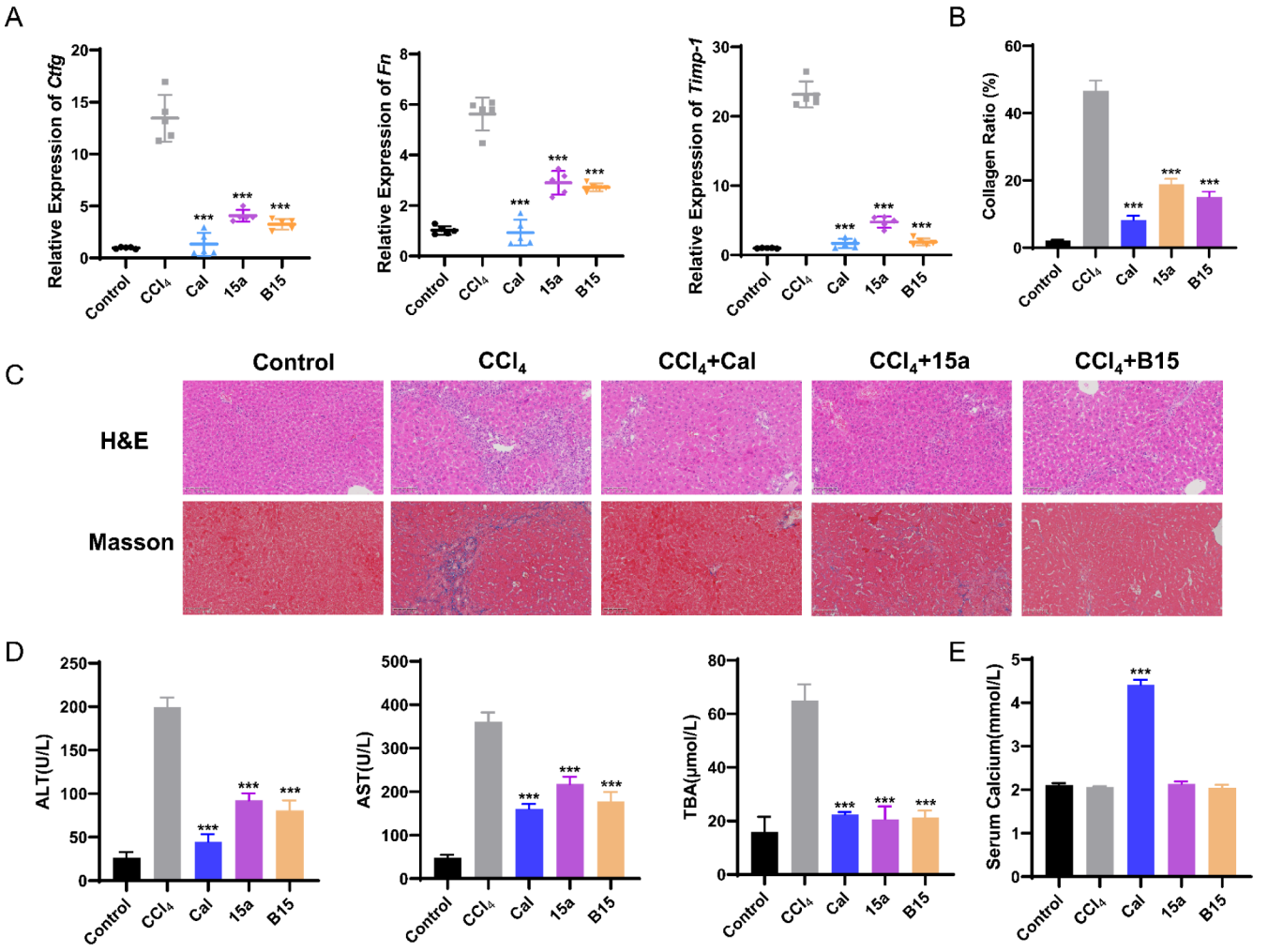

Figure 6. Compound **B15** improved CCl_4-induced hepatic fibrosis in mice. To establish the CCl_4-induced liver fibrosis model, the mice received intraperitoneal injections of a CCl_4/corn oil (1/50, v/v) mixture at a dose of 0.5 mL/kg three times a week for 4 weeks. Treatments began after 2 weeks of CCl_4 injections, when fibrosis typically develops. DMSO, calcipotriol (100 μg/kg body weight), compound **15a** or **B15** (500 μg/kg body weight) was administered by oral gavage five times weekly for 2 weeks (n = 5 per group). (A) The expression levels of *Fn*, *Ctgf*, and *Timp-1* were measured via qPCR (mean ± SD; ***p < 0.001 vs the CCl_4 group). (B) The collagen ratio was determined by Masson's trichrome staining (mean ± SD; *p < 0.05 vs the control group, **p < 0.01 vs the control group). (C) CCl_4-induced hepatic fibrosis lesions were examined via H&E staining (×100), and collagen deposition was determined via Masson's trichrome staining (×100). (D) Serum levels of ALT, AST, and TBA were determined (mean ± SD; ***p < 0.001 vs the CCl_4 group). (E) Serum calcium concentrations were determined with a calcium assay kit (mean ± SD; ***p < 0.001 vs the CCl_4 group).

maximizing agonist activity, which is further enhanced by the inclusion of an amide group at the terminal position.

The Selected Compounds Effectively Suppressed Collagen I and α-SMA Expression *In Vitro*. To evaluate the inhibitory effects of various compounds on HSC activation and their potential therapeutic implications for liver fibrosis, LX-2 cells were incubated with each compound at a concentration of 0.1 μM for 24 h in the presence of 5 ng/mL TGFβ1. Calcipotriol and **15a** served as positive controls, while DMSO was used as a negative control. qPCR was conducted to assess the expression levels of *ACTA2* and *COL1A1*, which are established markers of HSC activation (Figure 4A, B). Among the eight compounds evaluated, **A7**, **A17**, **B15**, and **B20** significantly inhibited *COL1A1* and *ACTA2* expression. Notably, **B15** and **B20** exhibited superior potency compared to **A7** and **A17**, which was attributed to their enhanced agonistic activity against VDR. Furthermore, compounds with an amide side chain showed greater efficacy than those with a tertiary alcohol side chain. Interestingly, despite its greater VDR activation capacity, **B20** resulted in weaker inhibition of *COL1A1* and *ACTA2* expression than **B15**. This discrepancy may be due to the complex recruitment of cofactors during downstream gene transcription mediated by the VDR.[39] Western blot analysis further confirmed that compounds **B15** and **B20** exerted moderate inhibition on α-SMA expression while potently suppressing collagen I, thereby demonstrating their potent antifibrotic activity (Figure 4C,D and E). Both compounds **B15** and **B20**, featuring a five-carbon side chain and diethylamino terminal groups, exhibit high VDR agonistic activity. This structural profile correlates with their display of the most potent antifibrotic activity.

Compound B15 Suppressed Fibrosis Gene Expression through the VDR. To further validate the inhibitory effects of these compounds on collagen I and α-SMA expression via the VDR, we utilized RNA interference (RNAi) in LX-2 cells. The depletion of the VDR resulted in

https://doi.org/10.1021/acs.jmedchem.5c01753
J. Med. Chem. 2025, 68, 20561−20585

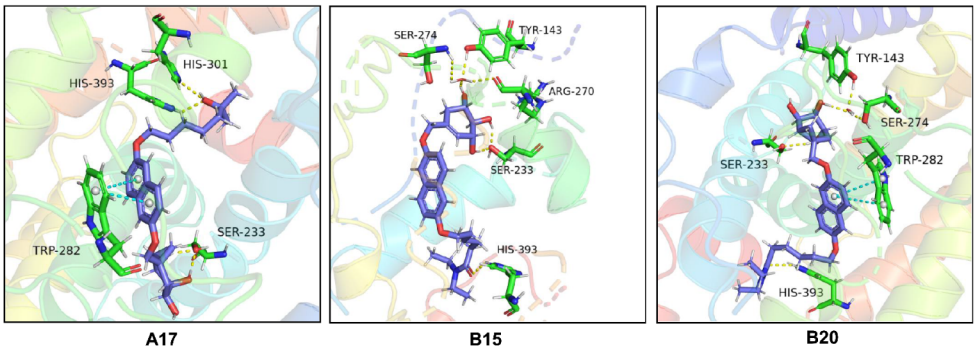

Figure 7. The predicted binding model of **A17**, **B15,** and **B20**. The VDR LBD of PDB reference 2ZFX was used in the molecular-docking analysis. Yellow dashed lines represent hydrogen-bonding interactions, whereas blue dashed lines denote $\pi-\pi$ conjugation interactions.

the loss of compound-mediated inhibition of collagen I and α-SMA expression (Figure 5A–D). These findings unequivocally establish that the biological activity of the compound is mediated through the VDR.

To further delineate the mechanism by which compound **B15** inhibits the activation of HSCs, we performed transcriptome-wide RNA sequencing (RNA-seq) in LX-2 cells treated with either TGFβ1 (5 ng/mL) or **B15** (0.1 μM) + TGFβ1 (5 ng/mL). Our results identified that in LX-2 cells treated with **B15**, 991 differentially expressed genes (DEGs) were downregulated, and 249 DEGs were upregulated (Figure 5E). Notably, there was a marked increase in the expression of *CYP24A1*, suggesting that compound **B15** has potent agonistic effects on the VDR (Figure 5F). Additionally, genes associated with collagen synthesis during fibrosis, such as *COL1A2* and *COL3A1*, were significantly downregulated, indicating that the compound has the capacity to suppress collagen production. Conversely, genes involved in collagen degradation, including *MMP1* and *MMP3*, were upregulated, demonstrating that the compound promotes collagen breakdown. KEGG enrichment analysis further demonstrated that, in addition to those involved in the TGFβ/SMAD3 signaling pathway, genes involved in other liver fibrosis-related pathways, such as the PEGF and JAK signaling pathways,[4] were also partially downregulated (Figure 5G). These findings collectively suggest that compound **B15** effectively inhibits HSC activation and restores HSCs to a quiescent state.

Given that **B15** modulates a broad range of genes *in vitro*, we further investigated its potential off-target toxicities. Inhibition of the human ether-à-go-go–related gene (hERG) potassium channel is a well-known mechanism underlying drug-induced QT interval prolongation,[42] which can predispose patients to life-threatening arrhythmias. To evaluate the cardiac safety of compound **B15** at an early preclinical stage, we performed a hERG assay to detect potential cardiotoxic liabilities. **B15** exhibited an IC_{50} value greater than 30 μM (Figure S3), indicating negligible hERG-mediated toxicity. These results suggest a minimal risk of QT interval prolongation and related proarrhythmic events, supporting the favorable cardiac safety profile of **B15** for further development.

In conclusion, compound **B15**, as a highly potent VDR agonist, regulates multiple fibrosis-related genes, thereby significantly suppressing the production of α-SMA and collagen I, and consequently inhibiting HSC activation. This inhibitory effect is mediated by VDR without detectable cardiotoxicity from off-target effects, thus highlighting its therapeutic potential as a target for liver fibrosis.

Compound B15 Improved CCl_4-Induced Hepatic Fibrosis in Mice. Compound **B15** exhibited the most potent inhibition of collagen I and α-SMA expression *in vitro*, prompting its selection for evaluating antifibrotic efficacy *in vivo*. To determine the optimal administration route and metabolic stability of compound **B15**, we first assessed its stability and permeability profiles. Given the naphthalene moiety in **B15** that may undergo oxidative metabolism, an *in vitro* liver microsomal stability assay was performed to predict its metabolic clearance. **B15** showed a half-life exceeding 6 h (Figure S2), indicating high metabolic stability and supporting its potential to maintain sufficient systemic exposure *in vivo*. To evaluate the intestinal absorption of **B15**, a Caco-2 cell assay was performed. The compound exhibited an apparent permeability (Papp) of 2.96×10^{-6} cm/s in the apical-to-basolateral direction and an efflux ratio of 1.87 (Table S3), indicating moderate permeability with slight efflux. These results suggest that **B15** is likely to achieve acceptable oral absorption. Subsequently, an *in vivo* pharmacokinetic study of compound **B15** was performed to provide a reference for subsequent dosing regimens and timing. Compound **B15** was administered to Sprague–Dawley (SD) rats via intravenous (*i.v.*) and oral (*p.o.*) administration. As shown in Table S2, the oral bioavailability of compound **B15** was 35.17%, with an *in vivo* half-life of approximately 4.5 h following oral administration. Given these findings, it was decided that the *in vivo* pharmacodynamic study would proceed via the oral administration route.

A CCl_4-induced liver fibrosis model was established in C57BL/6 mice. During liver fibrosis, HSCs are activated, resulting in the upregulation of fibrosis-promoting genes such as the myofibroblast marker fibronectin (*Fn*), connective tissue growth factor (*Ctgf*), and tissue inhibitor of metalloproteinase-1 (*Timp-1*). This leads to excessive deposition of ECM, exacerbating liver fibrosis.[4] Therefore, we quantified the expression levels of these genes to assess the severity of liver fibrosis. As illustrated in Figure 6A, compound **B15** exhibited potent inhibitory effects on target gene expression, outperforming compound **15a** (approximately 20%) and achieving efficacy comparable to that of the positive control calcipotriol. Histopathological evaluation of liver tissues through hematoxylin–eosin (H&E) staining confirmed characteristic CCl_4-induced hepatic damage in mice, including inflammatory cell infiltration and structural disorganization. Concurrently, Masson's trichrome staining revealed substantial collagen deposition, indicative of fibrotic progression. Notably, oral administration of compound **B15** resulted in marked

https://doi.org/10.1021/acs.jmedchem.5c01753
J. Med. Chem. 2025, 68, 20561–20585

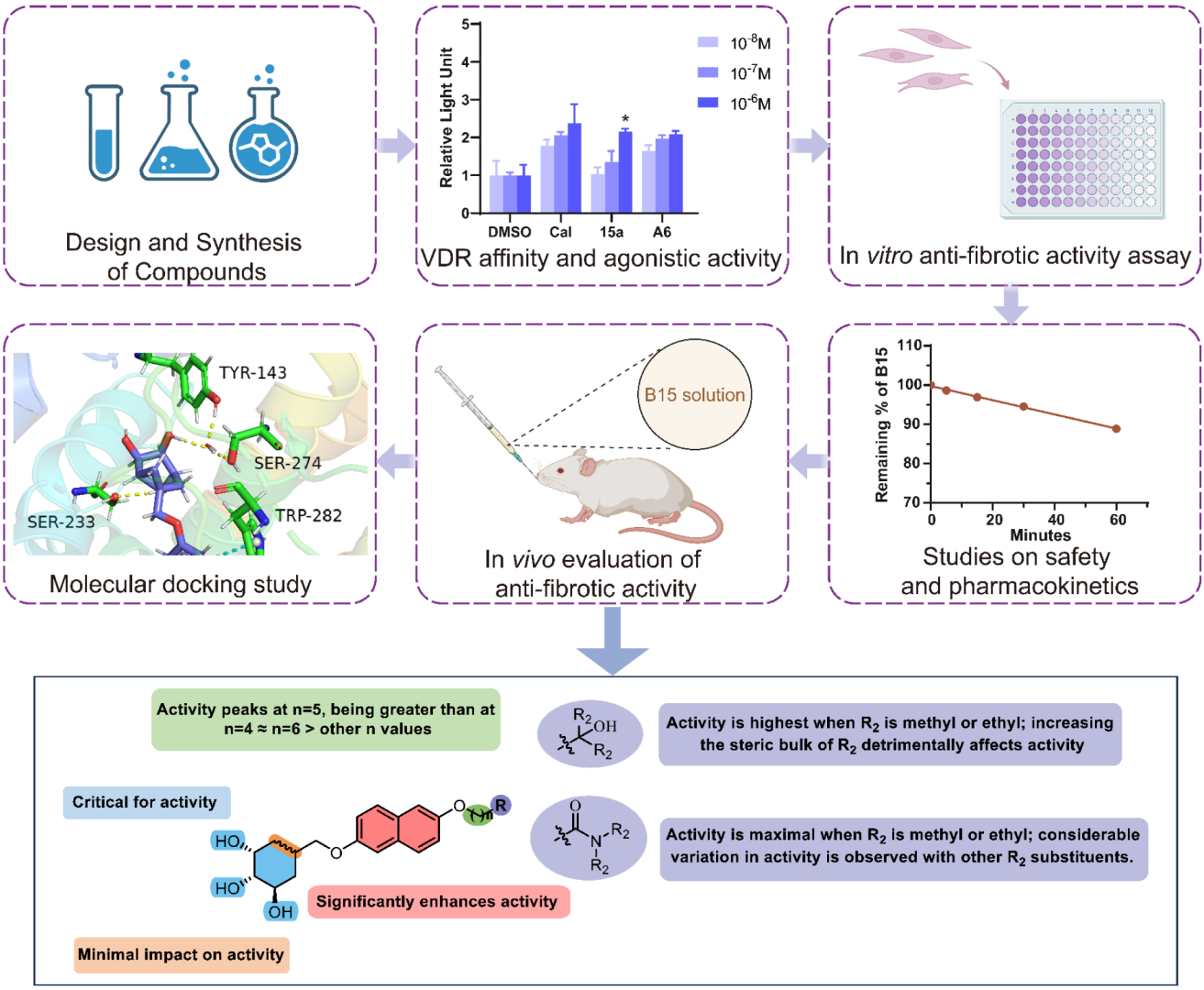

Figure 8. Research workflow for the discovery and antifibrotic activity evaluation of compound **B15** and the structure−activity relationship (SAR) map of the target compounds.

attenuation of hepatic inflammation and significant amelioration of fibrotic lesions, as evidenced by reduced inflammatory markers and collagen accumulation (Figure 6B,C). These findings suggest that compound **B15** effectively mitigates both inflammatory responses and fibrotic remodeling in chemically induced liver injury. The antifibrotic activity of compound **B15** surpassed that of compound **15a** (approximately 25%) and was comparable to that of calcipotriol. The serum levels of alanine aminotransferase (ALT), aspartate aminotransferase (AST), and total bile acid (TBA) serve as critical indicators for the clinical evaluation of liver status. The administration of compound **B15** resulted in a significant decrease in ALT, AST, and TBA levels (Figure 6D), further supporting its beneficial effects on liver function. Notably, in contrast to calcipotriol, compound **B15** did not result in increased serum calcium levels (Figure 6E), thereby demonstrating its favorable safety profile.

Molecular Docking. To further elucidate the interaction mode between compounds and VDR, we prioritize molecular docking studies of compounds **A17**, **B15**, and **B20** with the VDR LBD (PDB: 2ZFX). As shown in Figure 7 and Table S4, the results indicate that the two hydroxyl groups on the A-ring of compound **A17** can establish hydrogen bonds with Ser233, the naphthalene ring can engage in $\pi-\pi$ conjugation interactions with Trp282, and the tertiary alcohol at the end of the side chain can form two critical hydrogen bonds with His301 and His309. These interactions account for the strong agonistic activity of this compound on VDR. Compound **B15** not only establishes hydrogen bonds with Ser233 via both hydroxyl groups on the A-ring but also forms three hydrogen bonds with Ser274, Arg270, and Tyr143, which are mediated by water molecules. Additionally, the tertiary alcohol at the end of the side chain forms a hydrogen bond with His309. Despite the lack of the $\pi-\pi$ conjugation force provided by the naphthalene ring, the increase in hydrogen bonding may be the primary factor contributing to its enhanced agonistic activity. Compound **B20**, which has the strongest VDR agonistic activity, has one hydroxyl group on the A-ring that forms a hydrogen bond with Ser233, whereas the other hydroxyl group, which is mediated by water molecules, forms two hydrogen bonds with Ser274 and Tyr143. Furthermore, the tertiary alcohol at the end of the side chain forms a hydrogen bond with His309. Notably, the naphthalene ring of this compound

https://doi.org/10.1021/acs.jmedchem.5c01753
J. Med. Chem. 2025, 68, 20561−20585

engages in a robust $\pi-\pi$ conjugation interaction with Trp282, which may explain its optimal agonistic activity.

CONCLUSION

In conclusion, we successfully designed and synthesized a series of novel nonsteroidal VDR agonists featuring a 1,6-dihydronaphthalene core structure. The overall research workflow is summarized in Figure 8. These compounds are characterized by relatively straightforward synthetic pathways, ease of preparation, and significantly enhanced *in vivo* stability. *In vitro* studies demonstrated that compounds **B15** and **B20** effectively upregulate *CYP24A1* expression and inhibit HSC activation, with compound **B15** exhibiting particularly promising results. VDR knockout experiments confirmed that these effects are mediated through VDR signaling pathways. Furthermore, *in vivo* efficacy studies showed that **B15** effectively mitigates liver inflammation and collagen deposition in mice, leading to the downregulation of genes associated with liver fibrosis and robust antifibrotic effects. Notably, **B15** does not induce hypercalcemia, the most severe side effect commonly associated with long-term VDR agonist therapy for liver fibrosis. These results highlight **B15** as a promising candidate for the clinical treatment of liver fibrosis.

Furthermore, this study identifies key structural features underpinning the binding affinity and biological activity of novel VDR agonists, advancing the understanding of VDR–ligand interactions and guiding the rational design of more potent analogues. As shown in Figure 8, incorporation of the A-ring markedly increased VDR binding affinity, whereas a terminal side chain amide further enhanced biological activity, likely through additional hydrogen-bonding interactions, optimized hydrophobicity, and improved metabolic stability, collectively augmenting potency.

Leveraging the remarkable antifibrotic efficacy of **B15**, future work will focus on advanced preclinical investigations, particularly on formulation strategies to enhance bioavailability. Such endeavors are expected to accelerate the translational pathway of this candidate toward clinical application.

EXPERIMENTAL SECTION

General Chemistry Methods. All materials and reagents were procured from commercial suppliers and used without further purification unless otherwise specified. High-resolution mass spectrometry (HRMS) data were acquired via a QSTAR XL hybrid mass spectrometer. ^{1}H NMR and ^{13}C NMR spectra were recorded in DMSO on Bruker AV-300 or AV-400 instruments. Chemical shifts are reported in δ (ppm) units relative to tetramethylsilane (TMS) as the internal standard. Column chromatography was performed on silica gel (200–300 mesh). The purity of the synthesized compounds, as determined by high-performance liquid chromatography (HPLC), was $\geq$ 95%.

*Methyl(3R,4S,5R)-3,4,5-trihydroxycyclohex-1-ene-1-carboxylate (**1**).* Shikimic acid (20.0 g, 114.84 mmol) was dissolved in 250 mL of anhydrous methanol. $SOCl_2$ (2 mL) was slowly added dropwise at room temperature. Following the completion of the addition, the reaction mixture was heated to 70 °C and maintained under reflux for 5 h. Upon completion of the reaction, the solvent was removed by evaporation under reduced pressure. Subsequently, 200 mL of ethyl acetate was added, resulting in the precipitation of a white solid. The solid was collected via vacuum filtration, washed with ethyl acetate, and dried to afford Compound **1** as a white solid (19.8 g, yield: 92%). ^{1}H NMR (300 MHz, Chloroform-*d*) δ 6.76–6.66 (m, 1H), 5.37 (d, J = 7.1 Hz, 1H), 4.56–4.42 (m, 2H), 4.13–3.96 (m, 1H), 3.81–3.65 (m, 5H), 2.93–2.79 (m, 1H), 2.68–2.54 (m, 1H). MS (ESI, m/z): 211.05$[M + Na]^+$.

*Methyl(3R,4S,5R)-3,4,5-tris((tert-butyldimethylsilyl)oxy)-cyclohex-1-ene-1-car-box-ylate (**2**).* Compound **1** (19.8 g, 105.22 mmol) was dissolved in 200 mL of DMF. Imidazole (24.7 g, 368.27 mmol) and TBSCl (55.5 g, 368.27 mmol) were subsequently added to the solution at room temperature. The reaction mixture was then heated to 75 °C and incubated for 8 h. Upon completion of the reaction, the solution was poured into 500 mL of water and extracted with ethyl acetate (300 mL × 2). The organic phases were combined, washed with brine and dried over anhydrous Na_2SO_4. The organic solvent was subsequently removed under reduced pressure, and the resulting residue was subsequently purified via column chromatography via petroleum ether/ethyl acetate (20/1, v/v) to afford Compound **2** as a waxy solid (52.1 g, 93% yield). ^{1}H NMR (300 MHz, Chloroform-*d*) δ 6.84 (dt, J = 6.5, 0.9 Hz, 1H), 4.32–4.18 (m, 2H), 3.96 (dd, J = 6.7, 5.2 Hz, 1H), 3.62 (s, 3H), 2.73–2.52 (m, 2H), 0.86 (d, J = 3.4 Hz, 27H), 0.03 (d, J = 6.4 Hz, 18H). MS (ESI, m/z): 553.31$[M + Na]^+$.

*((3R,4S,5R)-3,4,5-tris((tert-butyldimethylsilyl)oxy)-cyclohex-1-en-1-yl)methanol (**3**).* Compound **2** (20.0 g, 37.67 mmol) was dissolved in 250 mL of DCM. The solution was subsequently cooled to −20 °C under an argon atmosphere, followed by the slow addition of 1 M DIBA-H in hexanes (95 mL). The reaction mixture was then gradually warmed to room temperature over a period of 2 h and stirred overnight to ensure complete conversion. Upon completion of the reaction, the mixture was carefully quenched by pouring it into 300 mL of a saturated potassium sodium tartrate aqueous solution. The resulting solution was vigorously stirred for 5 h to facilitate phase separation. The organic layer was extracted with DCM (300 mL × 3), combined, washed with brine and dried over anhydrous Na_2SO_4. The solvent was evaporated under reduced pressure, yielding a crude product which was purified by column chromatography using petroleum ether/ethyl acetate (10/1, v/v) to afford Compound **3** as a waxy solid (15.1 g, 79% yield). ^{1}H NMR (300 MHz, Chloroform-*d*) δ 5.74 (dt, J = 6.6, 1.0 Hz, 1H), 4.22–3.98 (m, 3H), 3.98–3.84 (m, 2H), 3.74 (t, J = 7.6 Hz, 1H), 2.47–2.33 (m, 1H), 2.17–2.00 (m, 1H), 0.86 (d, J = 3.0 Hz, 27H), 0.09–0.00 (m, 18H). MS (ESI, m/z): 503.33$[M + H]^+$.

*Methyl(4R,5S,6R)-4,5,6-tris((tert-butyldimethylsilyl)oxy)-3,3a,4,5,6,7-hexahydro-7aH-indazole-7a-carboxylate (**4**).* Compound **2** (10.0 g, 18.83 mmol) was dissolved in 100 mL of ether. Under continuous stirring, the diazomethane ether solution was slowly added in portions. If the yellow–green color of the reaction mixture did not disappear within 10 min, this indicated the completion of the reaction. Following evaporation of the ether, 200 mL of water was added, and the mixture was extracted with ethyl acetate (200 mL × 3). The organic layers were combined, washed with brine and dried over anhydrous Na_2SO_4. The organic solvent was subsequently removed under reduced pressure, yielding a residue that was purified by column chromatography using a petroleum ether: ethyl acetate (10/1, v/v) to afford Compound **4** as a waxy solid (10.5 g, 97% yield). ^{1}H NMR (300 MHz, Chloroform-*d*) δ 4.41 (dd, J = 7.0, 5.1 Hz, 1H), 4.28 (td, J = 6.7, 4.7 Hz, 1H), 3.95–3.80 (m, 3H), 3.64 (s, 3H), 2.51 (dt, J = 6.9, 5.0 Hz,

https://doi.org/10.1021/acs.jmedchem.5c01753
J. Med. Chem. 2025, 68, 20561–20585

1H), 2.21 (dd, J = 12.1, 4.7 Hz, 1H), 1.97 (dd, J = 12.1, 6.8 Hz, 1H), 0.87 (s, 27H), 0.08−0.01 (m, 18H). MS (ESI, m/z): 595.33[M + Na]$^+$.

*Methyl(3R,4S,5R)-3,4,5-tris((tert-butyldimethylsilyl)oxy)-bicyclo[4.1.0]heptane-1-carboxylate (**5**).* Compound **4** (10.5 g, 18.32 mmol) was degassed under an argon atmosphere and subsequently subjected to a solvent-free reaction at 150 °C for 3 h. Upon completion of the reaction, 200 mL of ethyl acetate was added, and the resulting mixture was filtered to remove any solid impurities. The filtrate was then purified by column chromatography using a petroleum ether: ethyl acetate (10/1, v/v) mixture to afford Compound **5** as a colorless oil (9.5 g, 95% yield). ^{1}H NMR (300 MHz, Chloroform-d) δ 4.18−4.05 (m, 2H), 3.77 (dd, J = 6.7, 5.1 Hz, 1H), 3.61 (s, 3H), 2.32−2.12 (m, 2H), 2.02 (d, J = 6.5 Hz, 2H), 1.86 (dd, J = 13.2, 7.0 Hz, 1H), 0.87 (d, J = 1.3 Hz, 27H), 0.09−0.01 (m, 18H). MS (ESI, m/z): 567.34[M + Na]$^+$.

*((3R,4S,5R)-3,4,5-tris((tert-butyldimethylsilyl)oxy)bicyclo-[4.1.0]heptan-1-yl)methanol (**6**).* The synthesis procedure for compound **6** is identical to that for compound **3**, which was purified by column chromatography using petroleum ether/ethyl acetate (10/1, v/v) to afford compound **6** as a waxy solid (6.1 g, 71% yield). ^{1}H NMR (300 MHz, Chloroform-d) δ 4.12−3.98 (m, 2H), 3.77 (dd, J = 6.7, 5.2 Hz, 1H), 3.49 (dd, J = 10.7, 7.0 Hz, 1H), 3.30−3.09 (m, 2H), 1.88−1.71 (m, 5H), 0.87 (d, J = 0.9 Hz, 27H), 0.11−0.00 (m, 18H). MS (ESI, m/z): 517.36[M + H]$^+$.

General Procedure 1. *Synthesis of Compound 7.* Dissolve 1,6-dinaphthol (5.0 g, 31.22 mmol) in 100 mL of DMF. NaH (1.5 g, 37.46 mmol) was gradually added to the mixture in an ice bath while stirring. The mixture was allowed to react for 1 h. The brominated esters (37.46 mmol) were subsequently introduced slowly in portions. The reaction was maintained at a controlled temperature for 2 h, followed by gradual warming to room temperature. The reaction was continued for an additional 5 h. Upon completion of the reaction, the mixture was quenched by adding it to 200 mL of ice water. The resulting solution was extracted three times with ethyl acetate (200 mL each time). The organic layers were combined, washed with brine and dried over anhydrous Na_2SO_4. The solvent was removed under reduced pressure, and the residue was purified via column chromatography.

*Methyl 3-((6-Hydroxynaphthalen-2-yl)oxy)propanoate (**7**−**1**).* Petroleum ether/ethyl acetate (2/1, v/v), white solid, 55% yield. ^{1}H NMR (300 MHz, Chloroform-d) δ 8.31 (s, 1H), 7.69 (dd, J = 8.4, 1.8 Hz, 1H), 7.61 (dd, J = 8.4, 2.5 Hz, 1H), 7.16 (t, J = 2.3 Hz, 1H), 7.02 (dd, J = 8.4, 2.3 Hz, 1H), 6.97−6.89 (m, 2H), 4.38 (t, J = 7.1 Hz, 2H), 3.67 (s, 3H), 2.69 (t, J = 7.1 Hz, 2H). MS (ESI, m/z): 269.07[M + Na]$^+$.

*Methyl 4-((6-Hydroxynaphthalen-2-yl)oxy)butanoate (**7**−**2**).* Petroleum ether/ethyl acetate (2/1, v/v), white solid, 52% yield. ^{1}H NMR (300 MHz, Chloroform-d) δ 8.31 (s, 1H), 7.65 (ddd, J = 17.4, 8.4, 2.0 Hz, 2H), 7.22−7.10 (m, 1H), 7.05−6.82 (m, 3H), 4.07 (t, J = 6.1 Hz, 2H), 3.68 (s, 3H), 2.47 (t, J = 6.9 Hz, 2H), 2.18−1.93 (m, 2H). MS (ESI, m/z): 283.09[M + Na]$^+$.

*Methyl 5-((6-Hydroxynaphthalen-2-yl)oxy)pentanoate (**7**−**3**).* Petroleum ether/ethyl acetate (3/1, v/v), white solid, 56% yield. ^{1}H NMR (300 MHz, Chloroform-d) δ 8.31 (s, 1H), 7.66 (ddd, J = 24.6, 8.4, 2.0 Hz, 2H), 7.16 (t, J = 2.2 Hz, 1H), 7.06−6.79 (m, 3H), 4.29−3.93 (m, 2H), 3.65 (s, 3H), 2.56−2.21 (m, 2H), 1.88−1.55 (m, 4H). MS (ESI, m/z): 297.12[M + Na]$^+$.

*Methyl 6-((6-Hydroxynaphthalen-2-yl)oxy)hexanoate (**7**−**4**).* Petroleum ether/ethyl acetate (3/1, v/v), white solid, 60% yield. ^{1}H NMR (300 MHz, Chloroform-d) δ 8.29 (s, 1H), 7.68 (ddd, J = 30.4, 8.5, 2.1 Hz, 2H), 7.20−7.12 (m, 1H), 7.07−6.86 (m, 3H), 4.05 (t, J = 6.1 Hz, 2H), 3.65 (s, 3H), 2.32 (t, J = 7.0 Hz, 2H), 1.77−1.38 (m, 6H). MS (ESI, m/z): 311.12[M + Na]$^+$.

*Methyl 7-((6-Hydroxynaphthalen-2-yl)oxy)heptanoate (**7**−**5**).* Petroleum ether/ethyl acetate (4/1, v/v), white solid, 62% yield. ^{1}H NMR (300 MHz, Chloroform-d) δ 8.64 (s, 1H), 7.67 (ddd, J = 27.7, 8.4, 2.1 Hz, 2H), 7.14 (t, J = 2.2 Hz, 1H), 7.07−6.86 (m, 3H), 4.04 (t, J = 6.1 Hz, 2H), 3.65 (s, 3H), 2.32 (t, J = 7.0 Hz, 2H), 1.76 (p, J = 6.6 Hz, 2H), 1.68−1.52 (m, 2H), 1.40 (q, J = 3.7 Hz, 4H). MS (ESI, m/z): 325.14[M + Na]$^+$.

*Methyl 8-((6-Hydroxynaphthalen-2-yl)oxy)octanoate (**7**−**6**).* Petroleum ether/ethyl acetate (4/1, v/v), white solid, 52% yield. ^{1}H NMR (300 MHz, Chloroform-d) δ 8.64 (s, 1H), 7.66 (ddd, J = 23.7, 8.4, 2.0 Hz, 2H), 7.20−7.11 (m, 1H), 7.07−6.86 (m, 3H), 4.03 (t, J = 6.1 Hz, 2H), 3.66 (s, 3H), 2.31 (t, J = 6.9 Hz, 2H), 1.84−1.68 (m, 2H), 1.58 (p, J = 7.0 Hz, 2H), 1.51−1.37 (m, 2H), 1.37−1.19 (m, 4H). MS (ESI, m/z): 339.17[M + Na]$^+$.

General Procedure 2. *Synthesis of Compounds 8 and 10.* Either compound **3** or compound **6** (2.0 g, 3.87 mmol), compound **7**−**1**−**7**−**6** (3.87 mmol), or triphenylphosphine (1.1 g, 4.26 mmol) were dissolved in 50 mL of anhydrous THF under an argon atmosphere. DEAD (0.74 g, 4.26 mmol) was subsequently slowly added to the reaction mixture while maintaining it in an ice bath. The reaction mixture was stirred for 1 h at this temperature before being gradually warmed to room temperature and allowed to proceed overnight. Upon completion of the reaction, the solution was poured into 100 mL of water and extracted three times with ethyl acetate (100 mL each time). The combined organic layers were washed with brine and dried over anhydrous Na_2SO_4. The solvent was then removed under reduced pressure, followed by purification via column chromatography.

*Methyl 3-((6-(((3R,4S,5R)-3,4,5-Tris((tert-butyldimethylsilyl)oxy)bicyclo[4.1.0]heptan-1-yl)methoxy)-naphthalen-2-yl)oxy)propanoate (**8**−**1**).* Petroleum ether/ethyl acetate (10/1, v/v), oil, 87% yield. ^{1}H NMR (300 MHz, Chloroform-d) δ 7.72−7.62 (m, 2H), 7.31 (q, J = 2.3 Hz, 2H), 6.97 (ddd, J = 25.9, 8.4, 2.4 Hz, 2H), 4.22 (t, J = 7.1 Hz, 2H), 4.10−3.97 (m, 2H), 3.89 (d, J = 10.9 Hz, 1H), 3.77 (dd, J = 6.7, 5.1 Hz, 1H), 3.61 (s, 3H), 3.52 (d, J = 11.2 Hz, 1H), 2.80−2.58 (m, 2H), 1.95−1.65 (m, 5H), 0.87 (d, J = 0.9 Hz, 27H), 0.10−0.00 (m, 18H). MS (ESI, m/z): 745.43[M + H]$^+$.

*Methyl 4-((6-(((3R,4S,5R)-3,4,5-Tris((tert-butyldimethylsilyl)oxy)bicyclo[4.1.0]heptan-1-yl)methoxy)-naphthalen-2-yl)oxy)butanoate (**8**−**2**).* Petroleum ether/ethyl acetate (10/1, v/v), and oil, 85% yield. ^{1}H NMR (300 MHz, Chloroform-d) δ 7.66 (dd, J = 8.5, 2.1 Hz, 2H), 7.32 (q, J = 2.3 Hz, 2H), 6.97 (ddd, J = 25.9, 8.4, 2.4 Hz, 2H), 4.13−3.84 (m, 5H), 3.77 (dd, J = 6.7, 5.1 Hz, 1H), 3.61 (s, 3H), 3.51 (d, J = 11.2 Hz, 1H), 2.62−2.30 (m, 2H), 2.24−1.95 (m, 2H), 1.95−1.84 (m, 4H), 1.84−1.67 (m, 2H), 0.87 (d, J = 0.9 Hz, 27H), 0.10−0.00 (m, 18H). MS (ESI, m/z): 759.45[M + H]$^+$.

*Methyl 5-((6-(((3R,4S,5R)-3,4,5-Tris((tert-butyldimethylsilyl)oxy)bicyclo[4.1.0]heptan-1-yl)methoxy)-naphthalen-2-yl)oxy)pentanoate (**8**−**3**).* Petroleum ether/ethyl acetate (10/1, v/v), and oil, 90% yield. ^{1}H NMR (300 MHz, Chloroform-d) δ 7.66 (dt, J = 8.4, 2.3 Hz, 2H), 7.32 (q,

https://doi.org/10.1021/acs.jmedchem.5c01753
J. Med. Chem. 2025, 68, 20561−20585

J = 2.4 Hz, 2H), 6.97 (ddd, J = 26.1, 8.4, 2.3 Hz, 2H), 4.10−3.84 (m, 5H), 3.77 (dd, J = 6.7, 5.1 Hz, 1H), 3.61 (s, 3H), 3.51 (d, J = 10.9 Hz, 1H), 2.46−2.24 (m, 2H), 1.96−1.61 (m, 9H), 0.87 (d, J = 0.9 Hz, 27H), 0.10−0.00 (m, 18H). MS (ESI, m/z): 795.43[M + Na]$^+$.

*Methyl 6-((6-(((3R,4S,5R)-3,4,5-tris((tert-butyldimethylsilyl)oxy)bicyclo[4.1.0]heptan-1-yl)methoxy)-naphthalen-2-yl)oxy)hexanoate (**8−4**).* Petroleum ether/ethyl acetate (10/1, v/v), and oil, 95% yield. ^{1}H NMR (300 MHz, Chloroform-d) δ 7.66 (dd, J = 8.4, 2.1 Hz, 2H), 7.32 (q, J = 2.3 Hz, 2H), 6.97 (ddd, J = 26.1, 8.4, 2.4 Hz, 2H), 4.10−3.84 (m, 5H), 3.77 (dd, J = 6.7, 5.1 Hz, 1H), 3.61 (s, 3H), 3.51 (d, J = 11.2 Hz, 1H), 2.45−2.15 (m, 2H), 1.95−1.79 (m, 4H), 1.79−1.60 (m, 4H), 1.60−1.47 (m, 2H), 1.47−1.35 (m, 1H), 0.87 (d, J = 0.9 Hz, 27H), 0.10−0.00 (m, 18H). MS (ESI, m/z): 809.45[M + Na]$^+$.

*Methyl7-((6-(((3R,4S,5R)-3,4,5-Tris((tert-butyldimethylsilyl)oxy)bicyclo[4.1.0] heptan-1-yl)methoxy)-naphthalen-2-yl)oxy)heptanoate (**8−5**).* petroleum ether/ethyl acetate (10/1, v/v), and oil, 75% yield. ^{1}H NMR (300 MHz, Chloroform-d) δ 7.66 (dd, J = 8.4, 2.1 Hz, 2H), 7.32 (q, J = 2.3 Hz, 2H), 6.97 (ddd, J = 26.1, 8.4, 2.4 Hz, 2H), 4.12−3.84 (m, 5H), 3.77 (dd, J = 6.7, 5.1 Hz, 1H), 3.61 (s, 3H), 3.51 (d, J = 10.9 Hz, 1H), 2.43−2.14 (m, 2H), 1.96−1.82 (m, 4H), 1.82−1.72 (m, 3H), 1.72−1.49 (m, 2H), 1.49−1.40 (m, 2H), 1.40−1.22 (m, 2H), 0.87 (d, J = 0.9 Hz, 27H), 0.10−0.00 (m, 18H). MS (ESI, m/z): 823.48[M + Na]$^+$.

*Methyl 8-((6-(((3R,4S,5R)-3,4,5-Tris((tert-butyldimethylsilyl)oxy)bicyclo[4.1.0]heptan-1-yl)methoxy)-naphthalen-2-yl)oxy)octanoate (**8−6**).* Petroleum ether/ethyl acetate (10/1, v/v), and oil, 91% yield. ^{1}H NMR (300 MHz, Chloroform-d) δ 7.71−7.61 (m, 2H), 7.32 (q, J = 2.3 Hz, 2H), 6.97 (ddd, J = 26.1, 8.4, 2.4 Hz, 2H), 4.12−3.84 (m, 5H), 3.77 (dd, J = 6.7, 5.1 Hz, 1H), 3.61 (s, 3H), 3.50 (d, J = 10.9 Hz, 1H), 2.43−2.14 (m, 2H), 1.97−1.63 (m, 7H), 1.63−1.18 (m, 8H), 0.87 (d, J = 0.9 Hz, 27H), 0.10−0.00 (m, 18H). MS (ESI, m/z): 837.50[M + Na]$^+$.

*Methyl 3-((6-(((3R,4S,5R)-3,4,5-Tris((tert-butyldimethylsilyl)oxy)cyclohex-1-en-1-yl)methoxy)-naphthalen-2-yl)oxy)propanoate (**10−1**).* Petroleum ether/ethyl acetate (10/1, v/v), and oil, 89% yield. ^{1}H NMR (300 MHz, Chloroform-d) δ 7.69 (ddd, J = 8.4, 4.0, 2.2 Hz, 2H), 7.35−7.27 (m, 1H), 7.15 (t, J = 2.1 Hz, 1H), 7.00 (ddd, J = 9.5, 8.4, 2.5 Hz, 2H), 5.47 (dp, J = 6.5, 1.0 Hz, 1H), 4.37 (t, J = 0.9 Hz, 2H), 4.28−4.10 (m, 4H), 3.92 (dd, J = 6.7, 5.2 Hz, 1H), 3.61 (s, 3H), 2.78−2.56 (m, 2H), 2.49 (ddt, J = 14.9, 7.5, 0.9 Hz, 1H), 2.24 (ddt, J = 14.9, 5.0, 0.9 Hz, 1H), 0.86 (d, J = 3.0 Hz, 27H), 0.08−0.00 (m, 18H). MS (ESI, m/z): 755.41[M + Na]$^+$.

*Methyl 4-((6-(((3R,4S,5R)-3,4,5-Tris((tert-butyldimethylsilyl)oxy)cyclohex-1-en-1-yl)methoxy)-naphthalen-2-yl)oxy)butanoate (**10−2**).* Petroleum ether/ethyl acetate (10/1, v/v), oil, 85% yield. ^{1}H NMR (300 MHz, Chloroform-d) δ 7.69 (ddd, J = 8.4, 4.5, 2.0 Hz, 2H), 7.31 (t, J = 2.4 Hz, 1H), 7.16 (t, J = 2.1 Hz, 1H), 7.00 (ddd, J = 9.6, 8.2, 2.3 Hz, 2H), 5.47 (dp, J = 6.5, 1.0 Hz, 1H), 4.37 (t, J = 0.9 Hz, 2H), 4.17−4.00 (m, 3H), 3.92 (dd, J = 6.7, 5.2 Hz, 1H), 3.61 (s, 3H), 2.62−2.42 (m, 2H), 2.37 (dd, J = 15.3, 7.2 Hz, 1H), 2.30−1.88 (m, 3H), 0.86 (d, J = 3.0 Hz, 27H), 0.08−0.00 (m, 18H). MS (ESI, m/z): 745.43[M + H]$^+$.

*Methyl 5-((6-(((3R,4S,5R)-3,4,5-Tris((tert-butyldimethylsilyl)oxy)cyclohex-1-en-1-yl)methoxy)-naphthalen-2-yl)oxy)pentanoate (**10−3**).* Petroleum ether/ethyl acetate (10/1, v/v), and oil, 92% yield. ^{1}H NMR (300 MHz, Chloroform-d) δ 7.68 (dd, J = 8.4, 2.1 Hz, 2H), 7.31 (t, J = 2.6 Hz, 1H), 7.16 (t, J = 2.0 Hz, 1H), 7.07−6.93 (m, 2H), 5.53−5.43 (m, 1H), 4.37 (q, J = 0.9 Hz, 2H), 4.24−4.10 (m, 2H), 4.02−3.86 (m, 3H), 3.61 (s, 3H), 2.58−2.14 (m, 4H), 1.93−1.60 (m, 4H), 0.86 (d, J = 3.0 Hz, 27H), 0.08−0.00 (m, 18H). MS (ESI, m/z): 781.43[M + Na]$^+$.

*Methyl 6-((6-(((3R,4S,5R)-3,4,5-Tris((tert-butyldimethylsilyl)oxy)cyclohex-1-en-1-yl)methoxy)-naphthalen-2-yl)oxy)hexanoate (**10−4**).* Petroleum ether/ethyl acetate (10/1, v/v), and oil, 82% yield. ^{1}H NMR (300 MHz, Chloroform-d) δ 7.66 (dd, J = 8.5, 2.2 Hz, 2H), 7.31 (t, J = 2.2 Hz, 1H), 7.15 (t, J = 2.2 Hz, 1H), 7.00 (ddd, J = 10.6, 8.4, 2.4 Hz, 2H), 5.48 (dt, J = 6.5, 1.1 Hz, 1H), 4.37 (d, J = 0.9 Hz, 2H), 4.26−4.14 (m, 1H), 4.11−3.98 (m, 1H), 3.98−3.86 (m, 3H), 3.61 (s, 3H), 2.54−2.43 (m, 1H), 2.30 (t, J = 6.9 Hz, 2H), 1.75−1.39 (m, 6H), 0.90−0.82 (m, 27H), 0.09−0.00 (m, 18H). MS (ESI, m/z): 773.46[M + H]$^+$.

*Methyl 7-((6-(((3R,4S,5R)-3,4,5-Tris((tert-butyldimethylsilyl)oxy)cyclohex-1-en-1-yl)methoxy)-naphthalen-2-yl)oxy)heptanoate (**10−5**).* Petroleum ether/ethyl acetate (10/1, v/v), and oil, 95% yield. ^{1}H NMR (300 MHz, Chloroform-d) δ 7.66 (dd, J = 8.5, 2.2 Hz, 2H), 7.31 (t, J = 2.3 Hz, 1H), 7.15 (t, J = 2.0 Hz, 1H), 7.00 (ddd, J = 10.6, 8.4, 2.4 Hz, 2H), 5.53−5.43 (m, 1H), 4.37 (d, J = 1.0 Hz, 2H), 4.26−4.11 (m, 2H), 4.02−3.86 (m, 3H), 3.61 (s, 3H), 2.62−2.43 (m, 2H), 2.29 (t, J = 7.0 Hz, 2H), 1.84−1.68 (m, 2H), 1.67−1.51 (m, 2H), 1.47−1.31 (m, 4H), 0.90−0.82 (m, 27H), 0.09−0.00 (m, 18H). MS (ESI, m/z): 809.47[M + Na]$^+$.

*Methyl 8-((6-(((3R,4S,5R)-3,4,5-Tris((tert-butyldimethylsilyl)oxy)cyclohex-1-en-1-yl)methoxy)-naphthalen-2-yl)oxy)octanoate (**10−6**).* Petroleum ether/ethyl acetate (10/1, v/v), and oil, 93% yield. ^{1}H NMR (300 MHz, Chloroform-d) δ 7.66 (dd, J = 8.5, 2.2 Hz, 2H), 7.31 (t, J = 2.3 Hz, 1H), 7.15 (t, J = 2.0 Hz, 1H), 7.00 (ddd, J = 10.6, 8.4, 2.4 Hz, 2H), 5.53−5.43 (m, 1H), 4.37 (d, J = 0.9 Hz, 2H), 4.26−4.11 (m, 2H), 4.11−3.86 (m, 3H), 3.61 (s, 3H), 2.62−2.43 (m, 2H), 2.29 (t, J = 7.0 Hz, 2H), 1.76 (p, J = 6.6 Hz, 2H), 1.54−1.18 (m, 8H), 0.90−0.82 (m, 27H), 0.09−0.00 (m, 18H). MS (ESI, m/z): 823.48[M + Na]$^+$.

General Procedure 3. *Synthesis of Compounds A1−A22, B1−B3, B9−B11, B13, and B21−B23.* Compound **8** or compound **10** (0.33 mmol) was dissolved in 10 mL of anhydrous tetrahydrofuran (THF), the reaction mixture was protected under an argon atmosphere, and 1 M solutions of various Grignard reagents (0.85 mL) were slowly added while the system was maintained in an ice bath. The reaction was allowed to proceed for 1 h, after which the temperature was gradually restored to room temperature, and the mixture was allowed to react for an additional 5 h. Upon completion of the reaction, the mixture was quenched by adding 20 mL of saturated ammonium chloride solution. The resulting mixture was extracted with ethyl acetate (20 mL × 3), the organic layers were combined, the samples were washed with brine and dried over anhydrous Na_2SO_4. The solvent was removed under reduced pressure to obtain compound 9 or compound 11. The product was dissolved in 10 mL of anhydrous methanol, P-toluenesulfonic acid (0.03 mmol) was added, the mixture was protected under an argon atmosphere, and the reaction was allowed to proceed at room temperature for 5 h. After the reaction was complete, the mixture was poured into 20 mL of saturated sodium bicarbonate solution, extracted with dichloromethane (DCM, 30 mL × 3), combined with organic

https://doi.org/10.1021/acs.jmedchem.5c01753
J. Med. Chem. 2025, 68, 20561−20585

layers, washed with brine and dried over anhydrous Na_2SO_4. The solvent was removed under reduced pressure, the residue was purified by flash column chromatography, and the final product was isolated.

*(1R,2S,3R)-5-(((6-(3-Hydroxy-3-methylbutoxy)-naphthalen-2-yl)oxy)methyl)cyclohex-4-ene-1,2,3-triol (**A1**).* Dichloromethane/methanol (20/1, v/v), white solid, 78% yield. ^{1}H NMR (300 MHz, DMSO-d_6) δ 7.71 (dd, J = 11.9, 9.0 Hz, 2H), 7.28 (t, J = 2.4 Hz, 2H), 7.13 (ddd, J = 15.8, 8.9, 2.5 Hz, 2H), 5.76 (q, J = 1.9 Hz, 1H), 4.98 (d, J = 4.3 Hz, 1H), 4.87 (d, J = 4.5 Hz, 1H), 4.52 (s, 2H), 4.42 (s, 1H), 4.16 (t, J = 7.1 Hz, 2H), 3.69 (d, J = 7.2 Hz, 1H), 3.55−3.43 (m, 1H), 3.35 Hz (s, 1H), 3.34−3.25 (m, 1H), 2.37 (dd, J = 17.2, 5.5 Hz, 1H), 2.08−1.95 (m, 1H), 1.90 (t, J = 7.2 Hz, 2H), 1.20 (s, 6H). ^{13}C NMR (75 MHz, DMSO-d_6) δ 155.52, 154.96, 133.89, 130.01, 129.67, 128.57, 128.52, 123.74, 119.51, 119.28, 107.92, 107.27, 81.84, 76.30, 70.44, 69.38, 68.51, 65.00, 56.91, 42.60, 34.44, 30.23. HR-MS (ESI, m/z): 411.2032[M + Na]$^+$. HPLC Purity: 98.6% (Rt: 4.51 min).

*(1R,2S,3R)-5-(((6-((4-Hydroxy-4-methylpentyl)oxy)-naphthalen-2-yl)oxy)methyl)cyclohex-4-ene-1,2,3-triol (**A2**).* Dichloromethane/methanol (20/1, v/v), white solid, 57% yield. ^{1}H NMR (300 MHz, DMSO-d_6) δ 7.71 (dd, J = 9.0, 4.6 Hz, 2H), 7.26 (dd, J = 10.5, 2.5 Hz, 2H), 7.13 (td, J = 9.0, 2.5 Hz, 2H), 5.80−5.72 (m, 1H), 4.73 (d, J = 4.0 Hz, 1H), 4.55 (d, J = 6.0 Hz, 1H), 4.54−4.42 (m, 3H), 4.23 (s, 1H), 4.12 (q, J = 4.7 Hz, 1H), 4.02 (t, J = 6.5 Hz, 2H), 3.89−3.77 (m, 1H), 3.49−3.41 (m, 1H), 2.43 (dd, J = 17.5, 5.2 Hz, 1H), 1.96 (dd, J = 17.5, 6.5 Hz, 1H), 1.87−1.74 (m, 2H), 1.57−1.45 (m, 2H), 1.13 (s, 6H). ^{13}C NMR (75 MHz, DMSO-d_6) δ 155.52, 154.96, 133.89, 130.01, 129.67, 128.57, 128.52, 123.74, 119.51, 119.28, 107.92, 107.27, 81.84, 76.30, 70.44, 69.38, 68.51, 65.00, 56.91, 42.60, 34.44, 30.23. HR-MS (ESI, m/z): 425.1943[M + Na]$^+$. HPLC Purity: 97.0% (Rt: 2.83 min).

*(1R,2S,3R)-5-(((6-((4-Ethyl-4-hydroxyhexyl)oxy)-naphthalen-2-yl)oxy)methyl) cyclohex-4-ene-1,2,3-triol (**A3**).* Dichloromethane/methanol (20/1, v/v), white solid, 45% yield. ^{1}H NMR (300 MHz, DMSO-d_6) δ 7.70 (dd, J = 9.0, 4.4 Hz, 2H), 7.26 (dd, J = 8.2, 2.5 Hz, 2H), 7.12 (td, J = 9.5, 2.5 Hz, 2H), 5.75 (t, J = 2.8 Hz, 1H), 4.70 (d, J = 4.0 Hz, 1H), 4.56−4.37 (m, 4H), 4.14−3.96 (m, 3H), 3.91 (s, 1H), 3.83 (d, J = 12.5 Hz, 1H), 3.43 (dt, J = 8.5, 4.5 Hz, 1H), 2.41 (dd, J = 17.4, 5.2 Hz, 1H), 1.94 (dd, J = 17.8, 6.5 Hz, 1H), 1.74 (dq, J = 13.5, 6.7 Hz, 2H), 1.53−1.43 (m, 2H), 1.37 (q, J = 7.5 Hz, 4H), 0.80 (t, J = 7.5 Hz, 6H). ^{13}C NMR (75 MHz, DMSO-d_6) δ 155.51, 155.14, 133.83, 129.96, 129.72, 128.54, 125.64, 119.43, 119.30, 107.82, 107.36, 72.79, 72.76, 71.11, 68.68, 66.80, 66.21, 34.60, 33.44, 30.99, 23.59, 8.34. HR-MS (ESI, m/z): 453.2241[M + Na]$^+$. HPLC Purity: 99.5% (Rt: 2.79 min).

*(1R,2S,3R)-5-(((6-((5-Hydroxy-5-methylhexyl)oxy)-naphthalen-2-yl)oxy)methyl)cyclohex-4-ene-1,2,3-triol (**A4**).* Dichloromethane/methanol (20/1, v/v), white solid, 66% yield. ^{1}H NMR (300 MHz, DMSO-d_6) δ 7.70 (dd, J = 9.0, 6.1 Hz, 2H), 7.27 (dd, J = 5.6, 2.5 Hz, 2H), 7.13 (ddd, J = 10.0, 7.8, 2.4 Hz, 2H), 5.80−5.69 (m, 1H), 4.70 (d, J = 4.0 Hz, 1H), 4.57−4.39 (m, 4H), 4.21−3.99 (m, 4H), 3.88−3.77 (m, 1H), 3.43 (dt, J = 8.4, 4.5 Hz, 1H), 2.41 (dd, J = 17.4, 5.2 Hz, 1H), 1.94 (dd, J = 17.4, 6.6 Hz, 1H), 1.73 (q, J = 6.8 Hz, 2H), 1.46 (q, J = 10.8, 9.5 Hz, 4H), 1.09 (s, 6H). ^{13}C NMR (75 MHz, DMSO-d_6) δ 155.53, 155.13, 133.82, 129.95, 129.72, 128.55, 125.64, 119.44, 119.30, 107.80, 107.29, 72.76, 71.09, 69.21, 67.99, 66.79, 66.21, 43.83, 33.44, 29.93, 29.79, 21.08. HR-MS (ESI, m/z): 439.2185[M + Na]$^+$. HPLC Purity: 98.7% (Rt: 4.08 min).

*(1R,2S,3R)-5-(((6-((5-Ethyl-5-hydroxyheptyl)oxy)-naphthalen-2-yl)oxy)methyl) cyclohex-4-ene-1,2,3-triol (**A5**).* Dichloromethane/methanol (20/1, v/v), white solid, 75% yield. ^{1}H NMR (300 MHz, DMSO-d_6) δ 7.70 (dd, J = 9.0, 5.9 Hz, 2H), 7.26 (dd, J = 6.2, 2.5 Hz, 2H), 7.13 (td, J = 9.0, 2.5 Hz, 2H), 5.80−5.66 (m, 1H), 4.70 (d, J = 4.0 Hz, 1H), 4.58−4.36 (m, 4H), 4.08 (dt, J = 23.3, 5.4 Hz, 3H), 3.88−3.74 (m, 2H), 3.43 (dt, J = 8.4, 4.5 Hz, 1H), 2.41 (dd, J = 17.6, 5.2 Hz, 1H), 1.94 (dd, J = 17.5, 6.5 Hz, 1H), 1.74 (p, J = 6.4 Hz, 2H), 1.50−1.25 (m, 8H), 0.78 (t, J = 7.4 Hz, 6H). ^{13}C NMR (75 MHz, DMSO-d_6) δ 155.54, 155.15, 133.85, 129.96, 129.74, 128.53, 125.62, 119.42, 119.29, 107.86, 107.36, 72.92, 72.78, 71.12, 67.94, 66.80, 66.22, 38.04, 33.44, 31.01, 29.96, 20.12, 8.33.HR-MS (ESI, m/z): 467.2400[M + Na]$^+$. HPLC Purity: 99.9% (Rt: 3.01 min).

*(1R,2S,3R)-5-(((6-((6-Hydroxy-6-methylheptyl)oxy)-naphthalen-2-yl)oxy)methyl)cyclohex-4-ene-1,2,3-triol (**A6**).* Dichloromethane/methanol (20/1, v/v), white solid, 65% yield. ^{1}H NMR (300 MHz, DMSO-d_6) δ 7.77−7.63 (m, 2H), 7.27 (dd, J = 6.0, 2.5 Hz, 2H), 7.13 (td, J = 8.9, 2.5 Hz, 2H), 5.75 (d, J = 3.8 Hz, 1H), 4.70 (d, J = 4.0 Hz, 1H), 4.56−4.41 (m, 4H), 4.15−4.00 (m, 4H), 3.80 (d, J = 11.6 Hz, 1H), 3.44 (dd, J = 8.2, 4.2 Hz, 1H), 2.41 (dd, J = 17.5, 5.2 Hz, 1H), 1.94 (dd, J = 17.4, 6.6 Hz, 1H), 1.85−1.71 (m, 2H), 1.38 (d, J = 2.5 Hz, 6H), 1.08 (s, 6H). ^{13}C NMR (75 MHz, DMSO-d_6) δ 155.51, 155.14, 133.82, 129.95, 129.73, 128.54, 125.63, 119.44, 119.29, 107.82, 107.29, 72.76, 71.10, 69.21, 67.87, 66.79, 66.21, 44.12, 33.44, 29.78, 29.31, 26.81, 24.18.HR-MS (ESI, m/z):453.2242[M + Na]$^+$. HPLC Purity: 98.4% (Rt: 4.54 min).

*(1R,2S,3R)-5-(((6-((6-Ethyl-6-hydroxyoctyl)oxy)-naphthalen-2-yl)oxy)methyl)cyclohex-4-ene-1,2,3-triol (**A7**).* Dichloromethane/methanol (20/1, v/v), white solid, 60% yield. ^{1}H NMR (300 MHz, DMSO-d_6) δ 7.70 (dd, J = 9.0, 6.3 Hz, 2H), 7.26 (dd, J = 7.1, 2.5 Hz, 2H), 7.13 (td, J = 9.0, 2.5 Hz, 2H), 5.75 (d, J = 3.9 Hz, 1H), 4.71 (d, J = 4.1 Hz, 1H), 4.58−4.31 (m, 4H), 4.07 (dt, J = 25.2, 5.6 Hz, 3H), 3.88−3.72 (m, 2H), 3.50−3.38 (m, 1H), 2.41 (dd, J = 17.5, 5.3 Hz, 1H), 1.95 (dd, J = 17.6, 6.6 Hz, 1H), 1.77 (p, J = 6.6 Hz, 2H), 1.49−1.20 (m, 10H), 0.77 (t, J = 7.4 Hz, 6H). ^{13}C NMR (101 MHz, DMSO-d_6) δ 155.52, 155.15, 133.84, 129.95, 129.73, 128.53, 125.61, 119.42, 119.28, 107.85, 107.32, 72.88, 72.77, 71.12, 67.92, 66.80, 66.21, 38.30, 33.44, 31.01, 29.32, 26.90, 23.25, 8.33.HR-MS (ESI, m/z): 481.2569[M + Na]$^+$. HPLC Purity: 99.8% (Rt: 3.73 min).

*(1R,2S,3R)-5-(((6-((7-Hydroxy-7-methyloctyl)oxy)-naphthalen-2-yl)oxy)methyl)cyclohex-4-ene-1,2,3-triol (**A8**).* Dichloromethane/methanol (20/1, v/v), white solid, 49% yield. ^{1}H NMR (400 MHz, DMSO-d_6) δ 7.70 (dd, J = 8.9, 7.7 Hz, 2H), 7.27 (dd, J = 8.0, 2.5 Hz, 2H), 7.13 (ddd, J = 11.6, 8.9, 2.5 Hz, 2H), 5.75 (dt, J = 3.6, 1.6 Hz, 1H), 4.70 (d, J = 4.1 Hz, 1H), 4.55−4.38 (m, 4H), 4.06 (td, J = 14.6, 13.0, 5.8 Hz, 4H), 3.82 (ddd, J = 11.4, 6.8, 4.9 Hz, 1H), 3.43 (dt, J = 7.9, 4.4 Hz, 1H), 2.41 (dd, J = 17.5, 5.2 Hz, 1H), 1.95 (dd, J = 17.5, 6.6 Hz, 1H), 1.82−1.68 (m, 2H), 1.52−138 (m, 2H), 1.34 (d, J = 3.0 Hz, 6H), 1.06 (s, 6H). ^{13}C NMR (75 MHz, DMSO-d_6) δ 155.51, 155.14, 133.82, 129.95, 129.73, 128.54, 125.63, 119.43, 119.29, 107.82, 107.30, 72.76, 71.10, 69.22, 67.89, 66.79, 66.21, 44.11, 33.44, 30.03, 29.76, 29.19, 26.15, 24.34. HR-MS (ESI, m/z):467.2399[M + Na]$^+$. HPLC Purity: 99.3% (Rt: 3.40 min).

https://doi.org/10.1021/acs.jmedchem.5c01753
J. Med. Chem. 2025, 68, 20561−20585

*(1R,2S,3R)-5-(((6-((7-Ethyl-7-hydroxynonyl)oxy)-naphthalen-2-yl)oxy)methyl)cyclohex-4-ene-1,2,3-triol (**A9**).* Dichloromethane/methanol (20/1, v/v), white solid, 53% yield. ^{1}H NMR (300 MHz, DMSO-d_6) δ 7.70 (dd, J = 9.0, 5.5 Hz, 2H), 7.27 (dd, J = 6.2, 2.5 Hz, 2H), 7.13 (td, J = 9.1, 2.5 Hz, 2H), 5.75 (d, J = 3.8 Hz, 1H), 4.70 (d, J = 4.1 Hz, 1H), 4.57−4.38 (m, 4H), 4.07 (dt, J = 20.7, 5.6 Hz, 3H), 3.86−3.70 (m, 2H), 3.43 (dt, J = 7.9, 4.5 Hz, 1H), 2.41 (dd, J = 17.5, 5.3 Hz, 1H), 1.95 (dd, J = 17.5, 6.5 Hz, 1H), 1.76 (p, J = 6.6 Hz, 2H), 1.32 (dd, J = 14.8, 7.3 Hz, 12H), 0.77 (t, J = 7.4 Hz, 6H). ^{13}C NMR (75 MHz, DMSO-d_6) δ 155.51, 155.15, 133.84, 129.96, 129.74, 128.52, 125.62, 119.41, 119.28, 107.85, 107.34, 72.87, 72.77, 71.12, 67.91, 66.80, 66.21, 38.22, 33.45, 31.03, 30.12, 29.21, 26.12, 23.40, 8.31. HR-MS (ESI, m/z): 495.2711[M + Na]$^+$. HPLC Purity: 99.7% (Rt:3.47 min).

*(1R,2S,3R)-5-(((6-((8-Hydroxy-8-methylnonyl)oxy)-naphthalen-2-yl)oxy)methyl)cyclohex-4-ene-1,2,3-triol (**A10**).* Dichloromethane/methanol (20/1, v/v), white solid, 76% yield. ^{1}H NMR (400 MHz, DMSO-d_6) δ 7.70 (dd, J = 8.9, 7.5 Hz, 2H), 7.26 (dd, J = 8.9, 2.5 Hz, 2H), 7.13 (ddd, J = 12.3, 8.9, 2.5 Hz, 2H), 5.75 (dt, J = 3.6, 1.6 Hz, 1H), 4.70 (d, J = 4.1 Hz, 1H), 4.56−4.37 (m, 4H), 4.14−3.97 (m, 4H), 3.82 (tt, J = 6.6, 4.8 Hz, 1H), 3.43 (dt, J = 7.9, 4.5 Hz, 1H), 2.41 (dd, J = 17.4, 5.2 Hz, 1H), 1.95 (dd, J = 17.5, 6.6 Hz, 1H), 1.76 (p, J = 6.8 Hz, 2H), 1.50−1.20 (m, 10H), 1.06 (s, 6H). ^{13}C NMR (75 MHz, DMSO-d_6) δ 155.51, 155.14, 133.83, 129.95, 129.73, 128.53, 125.63, 119.42, 119.29, 107.81, 107.30, 72.76, 71.10, 69.22, 67.89, 66.79, 66.21, 44.17, 33.45, 30.28, 29.76, 29.40, 29.22, 26.09, 24.33. HR-MS (ESI, m/z): 481.2555[M + Na]$^+$. HPLC Purity: 99.1% (Rt: 5.34 min).

*(1R,2S,3R)-5-(((6-((8-Ethyl-8-hydroxydecyl)oxy)-naphthalen-2-yl)oxy)methyl)cyclohex-4-ene-1,2,3-triol (**A11**).* Dichloromethane/methanol (20/1, v/v), white solid, 79% yield. ^{1}H NMR (300 MHz, DMSO-d_6) δ 7.70 (dd, J = 9.0, 5.3 Hz, 2H), 7.26 (dd, J = 6.8, 2.5 Hz, 2H), 7.13 (ddd, J = 9.9, 8.9, 2.5 Hz, 2H), 5.75 (d, J = 3.9 Hz, 1H), 4.70 (d, J = 4.1 Hz, 1H), 4.57−4.40 (m, 4H), 4.14−3.96 (m, 3H), 3.75 (s, 2H), 3.43 (dt, J = 7.9, 4.5 Hz, 1H), 2.41 (dd, J = 17.4, 5.3 Hz, 1H), 1.95 (dd, J = 17.5, 6.5 Hz, 1H), 1.76 (p, J = 6.7 Hz, 2H), 1.52−1.17 (m, 14H), 0.76 (t, J = 7.4 Hz, 6H). ^{13}C NMR (75 MHz, DMSO-d_6) δ 155.50, 155.13, 133.82, 129.94, 129.73, 128.53, 125.64, 119.41, 119.29, 107.78, 107.27, 72.87, 72.76, 71.09, 67.87, 66.79, 66.21, 38.25, 33.44, 31.02, 30.36, 29.38, 29.21, 26.09, 23.38, 8.31. HR-MS (ESI, m/z): 509.2655[M + Na]$^+$. HPLC Purity: 98.8% (Rt: 3.02 min).

*(2R,3S,4R)-6-(((6-(3-Hydroxy-3-methylbutoxy)-naphthalen-2-yl)oxy)methyl)bicyclo[4.1.0]heptane-2,3,4-triol (**A12**).* Dichloromethane/methanol (20/1, v/v), white solid, 79% yield. ^{1}H NMR (400 MHz, DMSO-d_6) δ 7.69 (dd, J = 15.9, 9.0 Hz, 2H), 7.23 (dd, J = 26.1, 2.5 Hz, 2H), 7.11 (ddd, J = 15.5, 8.9, 2.5 Hz, 2H), 4.53−4.34 (m, 3H), 4.26−4.06 (m, 4H), 3.90 (d, J = 9.6 Hz, 1H), 3.70 (d, J = 9.6 Hz, 1H), 3.50 (dp, J = 7.8, 3.7 Hz, 1H), 3.30 (dt, J = 8.0, 4.1 Hz, 1H), 2.13 (dd, J = 13.5, 4.5 Hz, 1H), 1.90 (t, J = 7.2 Hz, 2H), 1.80−1.70 (m, 1H), 1.20 (s, 7H), 0.82 (d, J = 4.9 Hz, 1H), 0.54 (dd, J = 9.6, 4.4 Hz, 1H). ^{13}C NMR (75 MHz, DMSO-d_6) δ 155.61, 155.42, 129.86, 129.75, 128.46, 119.46, 119.41, 107.61, 107.26, 76.58, 73.73, 68.52, 66.17, 65.29, 64.98, 42.60, 33.42, 30.23, 21.79, 21.42, 12.92. HR-MS (ESI, m/z): 425.1927[M + Na]$^+$. HPLC Purity: 99.8% (Rt: 2.98 min).

*(2R,3S,4R)-6-(((6-((4-Hydroxy-4-methylpentyl)oxy)-naphthalen-2-yl)oxy)methyl)bicyclo[4.1.0]heptane-2,3,4-triol (**A13**).* Dichloromethane/methanol (20/1, v/v), white solid, 60% yield. ^{1}H NMR (300 MHz, DMSO-d_6) δ 7.68 (dd, J = 8.9, 6.3 Hz, 2H), 7.30−7.00 (m, 4H), 4.43 (s, 2H), 4.28−4.09 (m, 3H), 4.02 (t, J = 6.5 Hz, 2H), 3.90 (d, J = 9.5 Hz, 1H), 3.70 (d, J = 9.6 Hz, 1H), 3.50 (d, J = 5.9 Hz, 1H), 3.29 (d, J = 8.3 Hz, 1H), 2.12 (dd, J = 13.6, 4.5 Hz, 1H), 1.79 (tt, J = 14.1, 7.0 Hz, 3H), 1.52 (dd, J = 10.5, 5.8 Hz, 2H), 1.12 (s, 7H), 0.83 (t, J = 4.9 Hz, 1H), 0.54 (dd, J = 9.6, 4.4 Hz, 1H). ^{13}C NMR (101 MHz, DMSO-d_6) δ 155.61, 155.46, 129.83, 129.76, 128.47, 128.44, 119.46, 119.37, 107.62, 107.31, 76.57, 73.74, 69.05, 68.62, 66.16, 65.30, 33.43, 29.80, 24.46, 21.79, 21.43, 12.89.HR-MS (ESI, m/z): 439.2085[M + Na]$^+$. HPLC Purity: 99.2% (Rt: 4.62 min).

*(2R,3S,4R)-6-(((6-((4-Ethyl-4-hydroxyhexyl)oxy)-naphthalen-2-yl)oxy)methyl)bicyclo[4.1.0]heptane-2,3,4-triol (**A14**).* Dichloromethane/methanol (20/1, v/v), white solid, 74% yield. ^{1}H NMR (300 MHz, DMSO-d_6) δ 7.68 (dd, J = 9.0, 5.6 Hz, 2H), 7.34−7.03 (m, 4H), 4.44 (dd, J = 12.5, 4.2 Hz, 2H), 4.17 (d, J = 3.5 Hz, 2H), 4.02 (t, J = 6.5 Hz, 2H), 3.90 (d, J = 9.3 Hz, 2H), 3.70 (d, J = 9.6 Hz, 1H), 3.50 (tt, J = 7.8, 4.2 Hz, 1H), 3.29 (dt, J = 8.0, 4.0 Hz, 1H), 2.12 (dd, J = 13.5, 4.5 Hz, 1H), 1.74 (td, J = 12.3, 10.8, 7.0 Hz, 3H), 1.55−1.30 (m, 6H), 1.27−1.12 (m, 1H), 0.80 (t, J = 7.4 Hz, 7H), 0.59−0.48 (m, 1H). ^{13}C NMR (101 MHz, DMSO-d_6) δ 155.60, 155.42, 129.83, 129.75, 128.47, 128.44, 119.45, 119.36, 107.62, 107.35, 76.57, 73.76, 72.80, 68.66, 66.13, 65.30, 34.60, 33.44, 30.97, 23.58, 21.79, 21.44, 12.87, 8.33.HR-MS (ESI, m/z): 467.1074[M + Na]$^+$. HPLC Purity: 99.8% (Rt: 4.18 min).

*(2R,3S,4R)-6-(((6-((5-Hydroxy-5-methylhexyl)oxy)-naphthalen-2-yl)oxy)methyl)bicyclo[4.1.0]heptane-2,3,4-triol (**A15**).* Dichloromethane/methanol (20/1, v/v), white solid, 75% yield. ^{1}H NMR (300 MHz, DMSO-d_6) δ 7.80−7.63 (m, 2H), 7.37−7.02 (m, 4H), 4.41 (dd, J = 15.7, 4.2 Hz, 2H), 4.15 (dd, J = 9.8, 7.3 Hz, 3H), 4.03 (t, J = 6.5 Hz, 2H), 3.90 (d, J = 9.5 Hz, 1H), 3.70 (d, J = 9.6 Hz, 1H), 3.49 (dd, J = 7.9, 3.9 Hz, 1H), 3.29 (dt, J = 8.1, 4.1 Hz, 1H), 2.12 (dd, J = 13.5, 4.5 Hz, 1H), 1.75 (dd, J = 14.0, 7.5 Hz, 3H), 1.44 (s, 4H), 1.08 (s, 7H), 0.82 (t, J = 5.0 Hz, 1H), 0.54 (dd, J = 9.6, 44 Hz, 1H). ^{13}C NMR (75 MHz, DMSO-d_6) δ 155.63, 155.48, 129.85, 129.78, 128.46, 119.46, 119.38, 107.67, 107.33, 76.58, 73.76, 69.21, 67.99, 66.18, 65.30, 43.83, 33.43, 29.94, 29.79, 21.80, 21.44, 21.08, 12.89.HR-MS (ESI, m/z): 453.2242[M + Na]$^+$. HPLC Purity: 99.3% (Rt: 3.52 min).

*(2R,3S,4R)-6-(((6-((5-Ethyl-5-hydroxyheptyl)oxy)-naphthalen-2-yl)oxy)methyl)bicyclo[4.1.0]heptane-2,3,4-triol (**A16**).* Dichloromethane/methanol (20/1, v/v), white solid, 61% yield. ^{1}H NMR (300 MHz, DMSO-d_6) δ 7.68 (t, J = 8.1 Hz, 2H), 7.28−7.03 (m, 4H), 4.42 (dd, J = 15.7, 4.2 Hz, 2H), 4.20−4.10 (m, 2H), 4.03 (t, J = 6.4 Hz, 2H), 3.94−3.76 (m, 2H), 3.70 (d, J = 9.6 Hz, 1H), 3.49 (dp, J = 8.0, 4.2 Hz, 1H), 3.29 (dt, J = 8.2, 4.1 Hz, 1H), 2.12 (dd, J = 13.6, 4.5 Hz, 1H), 1.84−1.67 (m, 3H), 1.48−1.12 (m, 9H), 0.79 (q, J = 7.7 Hz, 7H), 0.54 (dd, J = 9.8, 4.5 Hz, 1H). ^{13}C NMR (75 MHz, DMSO-d_6) δ 155.63, 155.48, 129.85, 129.78, 128.46, 119.46, 119.37, 107.67, 107.35, 76.58, 73.76, 72.91, 67.93, 66.18, 65.30, 38.04, 33.43, 31.01, 29.96, 21.80, 21.44, 20.12, 12.88, 8.32.HR-MS (ESI, m/z): 481.2253[M + Na]$^+$. HPLC Purity: 99.6% (Rt: 3.51 min).

*(2R,3S,4R)-6-(((6-((6-Hydroxy-6-methylheptyl)oxy)-naphthalen-2-yl)oxy)methyl)bicyclo[4.1.0]heptane-2,3,4-triol (**A17**).* Dichloromethane/methanol (20/1, v/v), white solid, 68% yield. ^{1}H NMR (300 MHz, DMSO-d_6) δ 7.68 (dd, J = 8.9, 7.6 Hz, 2H), 7.29−7.02 (m, 4H), 4.43 (dd, J = 15.4, 4.2 Hz, 2H), 4.24−3.97 (m, 5H), 3.90 (d, J = 9.6 Hz, 1H), 3.70

https://doi.org/10.1021/acs.jmedchem.5c01753
J. Med. Chem. 2025, 68, 20561−20585

(d, J = 9.6 Hz, 1H), 3.49 (dt, J = 7.8, 4.1 Hz, 1H), 3.33−3.24 (m, 1H), 2.12 (dd, J = 13.5, 4.5 Hz, 1H), 1.89−1.67 (m, 3H), 1.50−1.28 (m, 6H), 1.21 (d, J = 8.0 Hz, 1H), 1.07 (s, 6H), 0.82 (d, J = 4.9 Hz, 1H), 0.54 (dd, J = 9.6, 4.4 Hz, 1H). ^{13}C NMR (75 MHz, DMSO-d_6) δ 155.62, 155.45, 129.84, 129.77, 128.46, 119.46, 119.38, 107.64, 107.28, 76.57, 73.76, 69.21, 67.86, 66.17, 65.31, 44.12, 33.44, 29.78, 29.32, 26.81, 24.17, 21.80, 21.44, 12.89.HR-MS (ESI, m/z): 467.2398[M + Na]$^+$. HPLC Purity: 99.7% (Rt: 3.79 min).

*(2R,3S,4R)-6-(((6-((6-Ethyl-6-hydroxyoctyl)oxy)-naphthalen-2-yl)oxy)methyl)bicyclo[4.1.0]heptane-2,3,4-triol (**A18**).* Dichloromethane/methanol (20/1, v/v), white solid, 65% yield. ^{1}H NMR (400 MHz, DMSO-d_6) δ 7.68 (t, J = 9.4 Hz, 2H), 7.27−7.06 (m, 4H), 4.42 (dd, J = 20.8, 4.2 Hz, 2H), 4.22−4.13 (m, 2H), 4.03 (t, J = 6.5 Hz, 2H), 3.90 (d, J = 9.6 Hz, 1H), 3.78 (s, 1H), 3.70 (d, J = 9.6 Hz, 1H), 3.50 (tt, J = 8.0, 4.2 Hz, 1H), 3.30 (dt, J = 8.4, 4.4 Hz, 1H), 2.13 (dd, J = 13.5, 4.5 Hz, 1H), 1.82−1.67 (m, 3H), 1.47−1.14 (m, 11H), 0.86−0.70 (m, 7H), 0.54 (dd, J = 9.6, 4.3 Hz, 1H). ^{13}C NMR (101 MHz, DMSO-d_6) δ 155.62, 155.45, 129.83, 129.77, 128.46, 128.43, 119.45, 119.36, 107.62, 107.27, 76.57, 73.75, 72.87, 67.88, 66.17, 65.30, 38.29, 33.43, 31.00, 29.33, 26.91, 23.25, 21.80, 21.43, 12.89, 8.33. HR-MS (ESI, m/z): 495.2034[M + Na]$^+$. HPLC Purity: 99.9% (Rt: 3.44 min).

*(2R,3S,4R)-6-(((6-((7-Hydroxy-7-methyloctyl)oxy)-naphthalen-2-yl)oxy)methyl)bicyclo[4.1.0]heptane-2,3,4-triol (**A19**).* Dichloromethane/methanol (20/1, v/v), white solid, 47% yield. ^{1}H NMR (400 MHz, DMSO-d_6) δ 7.68 (t, J = 9.68 (t, J = 9.0 Hz, 2H), 7.22 (dd, J = 17.0, 2.5 Hz, 2H), 7.11 (ddd, J = 9.8, 8.9, 2.5 Hz, 2H), 4.47−4.33 (m, 2H), 4.22−4.12 (m, 2H), 4.09−3.98 (m, 3H), 3.90 (d, J = 9.6 Hz, 1H), 3.70 (d, J = 9.6 Hz, 1H), 3.50 (tt, J = 8.1, 4.3 Hz, 1H), 3.30 (dt, J = 8.4, 4.5 Hz, 1H), 2.13 (dd, J = 13.5, 4.5 Hz, 1H), 1.76 (ddt, J = 12.1, 6.6, 3.5 Hz, 3H), 1.52−1.39 (m, 2H), 1.33 (d, J = 3.3 Hz, 6H), 1.24−1.15 (m, 1H), 1.06 (s, 6H), 0.83 (t, J = 4.9 Hz, 1H), 0.54 (dd, J = 9.6, 4.3 Hz, 1H). ^{13}C NMR (75 MHz, DMSO-d_6) δ 155.62, 155.44, 129.83, 129.77, 128.46, 119.46, 119.37, 107.62, 107.29, 76.57, 73.74, 69.21, 67.87, 66.17, 65.29, 44.11, 33.43, 30.03, 29.76, 29.19, 26.16, 24.34, 21.80, 21.43, 12.90.HR-MS (ESI, m/z): 481.2556[M + Na]$^+$. HPLC Purity: 99.8% (Rt: 3.46 min).

*(2R,3S,4R)-6-(((6-((7-Ethyl-7-hydroxynonyl)oxy)-naphthalen-2-yl)oxy)methyl)bicyclo[4.1.0]heptane-2,3,4-triol (**A20**).* Dichloromethane/methanol (20/1, v/v), white solid, 50% yield. ^{1}H NMR (300 MHz, DMSO-d_6) δ 7.68 (dd, J = 9.0, 6.8 Hz, 2H), 7.28−7.05 (m, 4H), 4.42 (dd, J = 15.7, 4.2 Hz, 2H), 4.23−4.11 (m, 2H), 4.03 (t, J = 6.5 Hz, 2H), 3.90 (d, J = 9.6 Hz, 1H), 3.81−3.66 (m, 2H), 3.50 (tt, J = 8.0, 4.3 Hz, 1H), 3.29 (dt, J = 8.3, 4.3 Hz, 1H), 2.12 (dd, J = 13.5, 4.5 Hz, 1H), 1.76 (td, J = 8.2, 7.7, 3.1 Hz, 3H), 1.52−1.14 (m, 13H), 0.88−0.69 (m, 7H), 0.54 (dd, J = 9.7, 4.3 Hz, 1H). ^{13}C NMR (75 MHz, DMSO-d_6) δ 155.62, 155.44, 129.84, 129.77, 128.46, 128.43, 119.45, 119.36, 107.62, 107.28, 76.56, 73.75, 72.87, 67.86, 66.17, 65.30, 38.20, 33.43, 31.02, 30.12, 29.21, 26.13, 23.40, 21.79, 21.43, 12.88, 8.31. HR-MS (ESI, m/z): 509.2585[M + Na]$^+$. HPLC Purity: 99.9% (Rt: 3.17 min).

*(2R,3S,4R)-6-(((6-((8-Hydroxy-8-methylnonyl)oxy)-naphthalen-2-yl)oxy)methyl)bicyclo[4.1.0]heptane-2,3,4-triol (**A21**).* Dichloromethane/methanol (20/1, v/v), white solid, 85% yield. ^{1}H NMR (300 MHz, DMSO-d_6) δ 7.68 (dd, J = 8.9, 6.9 Hz, 2H), 7.30−6.99 (m, 4H), 4.42 (dd, J = 15.5, 4.1 Hz, 2H), 4.26−3.84 (m, 6H), 3.70 (d, J = 9.7 Hz, 1H), 3.51 (q, J = 4.0 Hz, 1H), 3.32−3.23 (m, 1H), 2.13 (dd, J = 13.5, 4.5 Hz, 1H), 1.76 (td, J = 8.1, 3.3 Hz, 3H), 1.51−1.15 (m, 11H), 1.06 (s, 6H), 0.83 (t, J = 5.0 Hz, 1H), 0.54 (dd, J = 9.6, 4.4 Hz, 1H). ^{13}C NMR (75 MHz, DMSO-d_6) δ 155.62, 155.44, 129.83, 129.77, 128.46, 119.46, 119.36, 107.62, 107.29, 76.57, 73.74, 69.21, 67.87, 66.17, 65.29, 44.17, 33.42, 30.27, 29.76, 29.40, 29.22, 26.09, 24.33, 21.79, 21.42, 12.90. HR-MS (ESI, m/z): 495.2712[M + Na]$^+$. HPLC Purity: 99.7% (Rt: 3.63 min).

*(2R,3S,4R)-6-(((6-((8-Ethyl-8-hydroxydecyl)oxy)-naphthalen-2-yl)oxy)methyl)bicyclo[4.1.0]heptane-2,3,4-triol (**A22**).* Dichloromethane/methanol (20/1, v/v), white solid, 80% yield. ^{1}H NMR (300 MHz, DMSO-d_6) δ 7.68 (dd, J = 9.0, 6.6 Hz, 2H), 7.28−7.02 (m, 4H), 4.42 (dd, J = 15.6, 4.2 Hz, 2H), 4.23−4.12 (m, 2H), 4.03 (t, J = 6.5 Hz, 2H), 3.90 (d, J = 9.6 Hz, 1H), 3.77−3.65 (m, 2H), 3.50 (tt, J = 7.9, 4.2 Hz, 1H), 3.29 (dt, J = 8.4, 4.4 Hz, 1H), 2.12 (dd, J = 13.5, 4.5 Hz, 1H), 1.75 (ddt, J = 12.0, 6.7, 4.2 Hz, 3H), 1.51−1.14 (m, 15H), 0.87−0.69 (m, 7H), 0.54 (dd, J = 9.7, 4.3 Hz, 1H). ^{13}C NMR (101 MHz, DMSO-d_6) δ 155.62, 155.44, 129.83, 129.77, 128.45, 128.43, 119.45, 119.35, 107.62, 107.28, 76.56, 73.75, 72.86, 67.87, 66.17, 65.30, 38.25, 33.43, 31.02, 30.35, 29.37, 29.22, 26.09, 23.38, 21.80, 21.43, 12.89, 8.30.HR-MS (ESI, m/z): 523.2735[M + Na]$^+$. HPLC Purity: 99.6% (Rt: 3.29 min).

*(1R,2S,3R)-5-(((6-((5-Allyl-5-hydroxyoct-7-en-1-yl)oxy)-naphthalen-2-yl)oxy)methyl)cyclohex-4-ene-1,2,3-triol (**B1**).* Dichloromethane/methanol (20/1, v/v), white solid, 83% yield. ^{1}H NMR (300 MHz, DMSO-d_6) δ 7.70 (dd, J = 9.0, 5.1 Hz, 2H), 7.42−7.04 (m, 4H), 5.98−5.64 (m, 3H), 5.20−4.89 (m, 4H), 4.70 (d, J = 4.1 Hz, 1H), 4.60−4.36 (m, 4H), 4.28 (s, 1H), 4.18−3.96 (m, 3H), 3.83 (d, J = 11.8 Hz, 1H), 3.44 (dd, J = 8.2, 4.2 Hz, 1H), 2.41 (dd, J = 17.5, 5.2 Hz, 1H), 2.12 (d, J = 7.3 Hz, 4H), 1.94 (dd, J = 17.5, 6.6 Hz, 1H), 1.80−1.64 (m, 2H), 1.60−1.32 (m, 4H). ^{13}C NMR (75 MHz, DMSO-d_6) δ 155.52, 155.15, 135.46, 133.84, 129.95, 129.74, 128.53, 125.62, 119.43, 119.29, 117.49, 107.86, 107.35, 72.77, 72.72, 71.12, 67.88, 66.80, 66.21, 44.08, 39.00, 33.44, 29.82, 19.85.HR-MS (ESI, m/z): 491.2585[M + Na]$^+$. HPLC Purity: 98.8% (Rt: 3.60 min).

*(1R,2S,3R)-5-(((6-((5-Hydroxy-5-propyloctyl)oxy)-naphthalen-2-yl)oxy)methyl)cyclohex-4-ene-1,2,3-triol (**B2**).* Dichloromethane/methanol (20/1, v/v), white solid, 52% yield. ^{1}H NMR (400 MHz, DMSO-d_6) δ 7.70 (dd, J = 9.0, 6.8 Hz, 2H), 7.31−7.08 (m, 4H), 5.75 (dt, J = 3.7, 1.6 Hz, 1H), 4.70 (d, J = 4.1 Hz, 1H), 4.55−4.37 (m, 4H), 4.08 (dt, J = 30.7, 5.6 Hz, 3H), 3.88−3.74 (m, 2H), 3.43 (dt, J = 7.9, 4.5 Hz, 1H), 2.41 (dd, J = 17.5, 5.2 Hz, 1H), 1.95 (dd, J = 17.5, 6.6 Hz, 1H), 1.73 (p, J = 6.5 Hz, 2H), 1.53−1.12 (m, 12H), 0.93−0.74 (m, 6H). ^{13}C NMR (101 MHz, DMSO-d_6) δ 155.53, 155.15, 133.84, 129.96, 129.74, 128.52, 125.62, 119.41, 119.28, 107.85, 107.37, 72.77, 72.76, 71.12, 67.91, 66.80, 66.21, 41.88, 39.09, 33.44, 29.93, 20.18, 16.82, 15.26.HR-MS (ESI, m/z): 523.2448[M + K]$^+$. HPLC Purity: 99.7% (Rt: 3.03 min).

*(1R,2S,3R)-5-(((6-((5-Butyl-5-hydroxynonyl)oxy)-naphthalen-2-yl)oxy)methyl)cyclohex-4-ene-1,2,3-triol (**B3**).* Dichloromethane/methanol (20/1, v/v), white solid, 66% yield. ^{1}H NMR (400 MHz, DMSO-d_6) δ 7.70 (dd, J = 9.0, 6.1 Hz, 2H), 7.35−7.05 (m, 4H), 5.75 (dt, J = 3.6, 1.6 Hz, 1H), 4.70 (d, J = 4.0 Hz, 1H), 4.56−4.38 (m, 4H), 4.08 (dt, J = 29.5, 5.5 Hz, 3H), 3.88−3.76 (m, 2H), 3.43 (dt, J = 8.0, 4.5 Hz, 1H), 2.41 (dd, J = 17.5, 5.2 Hz, 1H), 1.95 (dd, J = 17.5, 6.6 Hz, 1H), 1.73 (p, J = 6.5 Hz, 2H), 1.54−1.08 (m, 16H), 0.96−0.71 (m, 6H). ^{13}C NMR (101 MHz, DMSO-d_6) δ

https://doi.org/10.1021/acs.jmedchem.5c01753
J. Med. Chem. 2025, 68, 20561−20585

155.53, 155.15, 133.84, 129.96, 129.74, 128.51, 125.62, 119.39, 119.28, 107.85, 107.35, 72.77, 72.67, 71.12, 67.84, 66.80, 66.21, 39.06, 39.02, 33.45, 29.89, 25.79, 23.44, 20.11, 14.56.HR-MS (ESI, m/z): 523.3028[M + Na]$^+$. HPLC Purity: 98.5% (Rt: 3.98 min).

(1R,2S,3R)-5-(((6-((6-Allyl-6-hydroxynon-8-en-1-yl)oxy)-naphthalen-2-yl)oxy)methyl)cyclohex-4-ene-1,2,3-triol ***(B9)***. Dichloromethane/methanol (20/1, v/v), white solid, 82% yield. ^{1}H NMR (400 MHz, DMSO-d_6) δ 7.70 (dd, J = 8.9, 7.3 Hz, 2H), 7.26 (dd, J = 13.7, 2.6 Hz, 2H), 7.13 (ddd, J = 13.1, 8.9, 2.5 Hz, 2H), 5.92−5.73 (m, 3H), 5.11−4.94 (m, 4H), 4.71 (d, J = 4.1 Hz, 1H), 4.56−4.41 (m, 4H), 4.25 (s, 1H), 4.12 (q, J = 4.7 Hz, 1H), 4.02 (t, J = 6.5 Hz, 2H), 3.83 (ddt, J = 9.4, 6.6, 4.7 Hz, 1H), 3.44 (dt, J = 8.0, 4.5 Hz, 1H), 2.45−2.36 (m, 1H), 2.19−2.00 (m, 4H), 1.96 (dd, J = 17. 5, 6.6 Hz, 1H), 1.75 (t, J = 6.8 Hz, 2H), 1.46−1.28 (m, 6H). ^{13}C NMR (101 MHz, DMSO-d_6) δ 155.51, 155.14, 135.52, 133.83, 129.94, 129.73, 128.53, 125.62, 119.42, 119.29, 117.44, 107.82, 107.30, 72.76, 72.68, 71.10, 67.83, 66.79, 66.21, 44.09, 39.22, 33.44, 29.20, 26.70, 22.84.HR-MS (ESI, m/z): 491.2705[M + Na]$^+$. HPLC Purity: 99.7% (Rt: 3.93 min).

(1R,2S,3R)-5-(((6-((6-Hydroxy-6-propylnonyl)oxy)-naphthalen-2-yl)oxy)methyl)cyclohex-4-ene-1,2,3-triol ***(B10)***. Dichloromethane/methanol (20/1, v/v), white solid, 58% yield. ^{1}H NMR (300 MHz, DMSO-d_6) δ 7.70 (dd, J = 9.0, 5.7 Hz, 2H), 7.33−7.07 (m, 4H), 5.75 (d, J = 3.9 Hz, 1H), 4.70 (d, J = 4.0 Hz, 1H), 4.55−4.40 (m, 4H), 4.07 (dt, J = 25.8, 5.5 Hz, 3H), 3.81 (s, 2H), 3.43 (dt, J = 8.4, 4.5 Hz, 1H), 2.41 (dd, J = 17.5, 5.2 Hz, 1H), 1.95 (dd, J = 17.7, 6.6 Hz, 1H), 1.77 (p, J = 6.7 Hz, 2H), 1.52−1.11 (m, 14H), 0.84 (q, J = 4.8, 3.4 Hz, 6H). ^{13}C NMR (75 MHz, DMSO-d_6) δ 155.53, 155.16, 133.84, 129.96, 129.74, 128.53, 125.63, 119.42, 119.29, 107.86, 107.34, 72.77, 72.73, 71.12, 67.93, 66.80, 66.21, 41.89, 33.44, 29.29, 26.90, 23.34, 16.82, 15.26HR-MS (ESI, m/z): 509.2873[M + Na]$^+$. HPLC Purity: 98.6% (Rt: 4.09 min).

(1R,2S,3R)-5-(((6-((6-Butyl-6-hydroxydecyl)oxy)-naphthalen-2-yl)oxy)methyl)cyclohex-4-ene-1,2,3-triol ***(B11)***. Dichloromethane/methanol (20/1, v/v), white solid, 62% yield. ^{1}H NMR (300 MHz, DMSO-d_6) δ 7.70 (dd, J = 9.0, 5.2 Hz, 2H), 7.32−7.06 (m, 4H), 5.75 (d, J = 3.8 Hz, 1H), 4.70 (d, J = 4.1 Hz, 1H), 4.55−4.41 (m, 4H), 4.07 (dt, J = 25.4, 5.6 Hz, 3H), 3.92−3.74 (m, 2H), 3.43 (dt, J = 8.4, 4.6 Hz, 1H), 2.41 (dd, J = 17.3, 5.2 Hz, 1H), 1.95 (dd, J = 17.4, 6.6 Hz, 1H), 1.77 (p, J = 6.7 Hz, 2H), 1.59−1.04 (m, 18H), 0.94−0.70 (m, 6H). ^{13}C NMR (75 MHz, DMSO-d_6) δ 155.53, 155.16, 133.84, 129.96, 129.74, 128.52, 125.62, 119.40, 119.28, 107.85, 107.32, 72.78, 72.65, 71.13, 67.91, 66.80, 66.21, 39.37, 39.06, 33.44, 29.27, 26.88, 25.81, 23.44, 23.27, 14.56.HR-MS (ESI, m/z): 537.3181[M + Na]$^+$. HPLC Purity: 99.4% (Rt: 3.45 min).

(1S,2R,3S)-5-(((6-((6-Hydroxy-6,7-diphenylheptyl)oxy)-naphthalen-2-yl)oxy)methyl)cyclohex-4-ene-1,2,3-triol ***(B13)***. Dichloromethane/methanol (20/1, v/v), white solid, 69% yield. ^{1}H NMR (300 MHz, DMSO-d_6) δ 7.70 (dd, J = 9.0, 5.5 Hz, 2H), 7.28−7.10 (m, 14H), 5.75 (d, J = 3.8 Hz, 1H), 4.71 (d, J = 4.1 Hz, 1H), 4.55−4.43 (m, 4H), 4.27 (s, 1H), 4.11 (d, J = 5.1 Hz, 1H), 4.00 (t, J = 6.4 Hz, 2H), 3.81 (d, J = 5.9 Hz, 1H), 3.42 (dd, J = 8.2, 4.3 Hz, 1H), 2.68 (s, 4H), 2.41 (dd, J = 17.4, 5.2 Hz, 1H), 1.95 (dd, J = 17.3, 6.6 Hz, 1H), 1.75−1.66 (m, 2H), 1.48 (s, 2H), 1.31 (d, J = 7.2 Hz, 2H), 1.16 (dd, J = 11.8, 4.9 Hz, 2H). ^{13}C NMR (75 MHz, DMSO-d_6) δ 155.51, 155.15, 138.85, 133.83, 131.06, 129.95, 129.74, 128.54, 128.04, 126.21, 125.65, 119.43, 119.32, 107.84, 107.32, 74.03, 72.77, 71.11, 67.73, 66.80, 66.22, 45.85, 37.92, 33.45, 29.06, 26.64, 23.48. HR-MS (ESI, m/z): 605.2667[M + Na]$^+$. HPLC Purity: 99.3% (Rt: 3.62 min).

(1R,2S,3R)-5-(((6-((7-Allyl-7-hydroxydec-9-en-1-yl)oxy)-naphthalen-2-yl)oxy)methyl)cyclohex-4-ene-1,2,3-triol ***(B21)***. Dichloromethane/methanol (20/1, v/v), white solid, 64% yield. ^{1}H NMR (300 MHz) δ 7.70 (dd, J = 9.0, 5.5 Hz, 2H), 7.27 (dd, J = 6.6, 2.5 Hz, 2H), 7.16−7.09 (m, 2H), 5.91−5.73 (m, 3H), 5.06−4.98 (m, 4H), 4.70 (d, J = 4.1 Hz, 1H), 4.54−4.43 (m, 4H), 4.23 (s, 1H), 4.11−3.99 (m, 3H), 3.81 (q, J = 6.0, 5.5 Hz, 1H), 3.43 (dt, J = 7.9, 4.5 Hz, 1H), 2.44−2.36 (m, 1H), 2.11 (d, J = 7.2 Hz, 4H), 1.94 (dd, J = 17.4, 6.6 Hz, 1H), 1.74 (d, J = 7.4 Hz, 2H), 1.44 (s, 2H), 1.36−1.18 (m, 6H). ^{13}C NMR (75 MHz, DMSO-d_6) δ 155.52, 155.15, 135.53, 133.84, 129.96, 129.74, 128.53, 125.62, 119.42, 119.28, 117.39, 107.85, 107.35, 72.78, 72.69, 71.12, 67.90, 66.80, 66.22, 44.11, 39.22, 33.45, 29.96, 29.17, 26.06, 23.03. HR-MS (ESI, m/z): 519.2712[M + Na]$^+$. HPLC Purity: 99.0% (Rt: 3.14 min).

(1R,2S,3R)-5-(((6-((7-Hydroxy-7-propyldecyl)oxy)-naphthalen-2-yl)oxy)methyl)cyclohex-4-ene-1,2,3-triol ***(B22)***. Dichloromethane/methanol (20/1, v/v), white solid, 72% yield. ^{1}H NMR (300 MHz, DMSO-d_6) δ 7.70 (dd, J = 9.0, 5.3 Hz, 2H), 7.27 (dd, J = 6.6, 2.5 Hz, 2H), 7.13 (td, J = 9.2, 2.5 Hz, 2H), 5.75 (d, J = 3.8 Hz, 1H), 4.70 (d, J = 4.0 Hz, 1H), 4.55−4.41 (m, 4H), 4.07 (dt, J = 25.4, 5.5 Hz, 3H), 3.79 (s, 2H), 3.43 (dt, J = 8.4, 4.5 Hz, 1H), 2.41 (dd, J = 17.5, 5.2 Hz, 1H), 1.94 (dd, J = 17.7, 6.6 Hz, 1H), 1.76 (p, J = 6.6 Hz, 2H), 1.44 (q, J = 7.0 Hz, 2H), 1.26 (t, J = 7.0 Hz, 14H), 0.91−0.74 (m, 6H). ^{13}C NMR (75 MHz, DMSO-d_6) δ 155.50, 155.14, 133.83, 129.95, 129.73, 128.53, 125.63, 119.41, 119.29, 107.81, 107.30, 72.77, 72.72, 71.10, 67.88, 66.79, 66.21, 41.89, 39.31, 33.45, 30.12, 29.22, 26.12, 23.50, 16.81, 15.27.HR-MS (ESI, m/z): 583.5167[M + Na]$^+$. HPLC Purity: 99.7% (Rt: 2.80 min).

(1R,2S,3R)-5-(((6-((7-Butyl-7-hydroxyundecyl)oxy)-naphthalen-2-yl)oxy)methyl)cyclohex-4-ene-1,2,3-triol ***(B23)***. Dichloromethane/methanol (20/1, v/v), white solid, 76% yield. ^{1}H NMR (300 MHz, DMSO-d_6) δ 7.70 (dd, J = 9.0, 5.2 Hz, 2H), 7.26 (dd, J = 6.7, 2.5 Hz, 2H), 7.13 (td, J = 9.3, 2.5 Hz, 2H), 5.75 (d, J = 3.7 Hz, 1H), 4.70 (d, J = 4.1 Hz, 1H), 4.56−4.41 (m, 4H), 4.07 (dt, J = 20.6, 5.9 Hz, 3H), 3.80 (d, J = 10.8 Hz, 2H), 3.43 (dt, J = 8.7, 4.5 Hz, 1H), 2.45−2.36 (m, 1H), 1.94 (dd, J = 17.6, 6.6 Hz, 1H), 1.75 (q, J = 6.9 Hz, 2H), 1.44 (d, J = 9.0 Hz, 2H), 1.38−1.07 (m, 18H), 0.92−0.78 (m, 6H). ^{13}C NMR (75 MHz, DMSO-d_6) δ 155.52, 155.16, 133.84, 129.96, 129.74, 128.52, 125.62, 119.40, 119.28, 107.85, 107.33, 72.78, 72.64, 71.13, 67.90, 66.80, 66.21, 39.31, 39.07, 33.45, 30.10, 29.21, 26.11, 25.80, 23.44, 14.57. HR-MS (ESI, m/z): 555.3762[M + Na]$^+$. HPLC Purity: 99.8% (Rt: 3.02 min).

General Procedure 4. *Synthesis of Compounds A23−A24.* Compound **A4** or **A5** (50 mg, 0.11 mmol) was dissolved in 20 mL of methanol, followed by the addition of Pd/C (10 mg, 0.01 mmol). The mixture was subjected to hydrogenation under atmospheric pressure at room temperature overnight. Upon completion of the reaction, the catalyst was filtered through diatomite, and the filtrate was concentrated via rotary evaporation. The residue was subsequently purified via column chromatography.

(1R,3R)-5-(((6-((5-Hydroxy-5-methylhexyl)oxy)-naphthalen-2-yl)oxy)methyl)cyclohexane-1,2,3-triol ***(A23)***. Dichloromethane/methanol (20/1, v/v), white solid, 70%

https://doi.org/10.1021/acs.jmedchem.5c01753
J. Med. Chem. 2025, 68, 20561−20585

yield. ^{1}H NMR (300 MHz) δ 7.70 (d, J = 8.9 Hz, 2H), 7.24 (q, J = 2.2 Hz, 2H), 7.11 (dd, J = 8.9, 2.4 Hz, 2H), 4.67 (s, 1H), 4.39 (s, 2H), 4.17−4.00 (m, 3H), 3.90−3.71 (m, 4H), 3.59 (q, J = 4.5, 3.2 Hz, 1H), 2.01−1.19 (m, 10H), 1.09 (s, 7H). ^{13}C NMR (75 MHz, DMSO-d_6) δ 155.55, 155.45, 129.82, 128.49, 119.37, 107.41, 107.34, 77.21, 73.01, 72.55, 72.39, 69.72, 69.27, 69.21, 69.01, 68.00, 67.35, 43.83, 36.82, 34.84, 32.23, 30.92, 30.68, 30.63, 29.94, 29.79, 21.08. HR-MS (ESI, m/z): 441.2241[M + Na]$^+$. HPLC Purity: 99.4% (Rt: 3.40 min).

(1R,3R)-5-((((6-((5-Ethyl-5-hydroxyheptyl)oxy)naphthalen-2-yl)oxy)methyl)cyclohexane-1,2,3-triol ***(A24)***. Dichloromethane/methanol (20/1, v/v), white solid, 65% yield. ^{1}H NMR (300 MHz) δ 7.70 (d, J = 8.9 Hz, 2H), 7.24 (d, J = 2.5 Hz, 2H), 7.11 (dt, J = 8.9, 2.2 Hz, 2H), 4.67 (s, 1H), 4.38 (s, 2H), 4.04 (t, J = 6.4 Hz, 2H), 3.95−3.66 (m, 5H), 3.60 (q, J = 4.6, 2.9 Hz, 1H), 2.29−2.08 (m, 1H), 2.00−1.07 (m, 14H), 0.78 (t, J = 7.4 Hz, 6H). ^{13}C NMR (75 MHz, DMSO-d_6) δ 155.55, 155.50, 155.46, 129.83, 129.81, 128.49, 119.37, 107.41, 107.35, 77.21, 73.02, 72.91, 72.55, 72.39, 69.72, 69.27, 69.01, 67.93, 67.34, 38.04, 36.82, 34.84, 32.23, 31.00, 30.92, 30.68, 30.63, 29.97, 20.12, 8.32.HR-MS (ESI, m/z): 469.2555[M + Na]$^+$. HPLC Purity: 99.9% (Rt: 3.13 min).

General Procedure 4. *Synthesis of Compounds B4, B12, and B24.* Compound **10** (0.33 mmol) was dissolved in 20 mL of DCM, and the mixture was cooled to −20 °C under argon protection. Subsequently, 1 M DIBAL-H (1 mL) was slowly added to the reaction mixture. The mixture was stirred at −20 °C for 2 h, after which the reaction mixture was gradually warmed to room temperature, after which it was allowed to react overnight. Upon completion of the reaction, the reaction was carefully quenched by pouring the solution into 20 mL of saturated potassium sodium tartrate aqueous solution. The mixture was stirred vigorously for 5 h to ensure phase separation. The organic layer was extracted with DCM (20 mL × 3), combined with the organic phases, washed with brine and dried over anhydrous Na_2SO_4. The product was dissolved in 10 mL of anhydrous methanol, P-toluenesulfonic acid (0.03 mmol) was added, the mixture was protected under an argon atmosphere, and the reaction was allowed to proceed at room temperature for 5 h. After the reaction was complete, the mixture was poured into 20 mL of saturated sodium bicarbonate solution, extracted with dichloromethane (DCM, 30 mL × 3), combined with organic layers, washed with brine and dried over anhydrous Na_2SO_4. The solvent was removed under reduced pressure, the residue was purified by flash column chromatography, and the final product was isolated.

(1R,2S,3R)-5-((((6-((5-Hydroxypentyl)oxy)naphthalen-2-yl)oxy)methyl)cyclohex-4-ene-1,2,3-triol ***(B4)***. Dichloromethane/methanol (20/1, v/v), white solid, 38% yield. ^{1}H NMR (400 MHz, DMSO-d_6) δ 7.70 (t, J = 9.2 Hz, 2H), 7.27 (dd, J = 5.7, 2.5 Hz, 2H), 7.13 (ddd, J = 15.0, 8.9, 2.5 Hz, 2H), 5.76 (q, J = 2.5 Hz, 1H), 4.98 (d, J = 4.3 Hz, 1H), 4.87 (d, J = 4.3 Hz, 1H), 4.52 (s, 2H), 4.41 (t, J = 5.1 Hz, 1H), 4.03 (d, J = 6.5 Hz, 2H), 3.72−3.63 (m, 1H), 3.46 (dq, J = 23.9, 5.8, 5.3 Hz, 3H), 3.30 (dt, J = 10.7, 4.1 Hz, 2H), 2.37 (dd, J = 17.0, 5.8 Hz, 1H), 2.07−1.94 (m, 1H), 1.77 (t, J = 6.9 Hz, 2H), 1.55−1.38 (m, 4H). ^{13}C NMR (75 MHz, DMSO-d_6) δ 155.54, 154.97, 133.88, 129.98, 129.69, 128.56, 128.52, 123.74, 119.46, 119.28, 107.90, 107.28, 81.84, 76.30, 70.44, 69.38, 67.92, 61.11, 56.91, 34.44, 32.74, 29.10, 22.70.HR-MS (ESI, m/z): 411.1772[M + Na]$^+$. HPLC Purity: 99.5% (Rt: 3.12 min).

(1R,2S,3R)-5-((((6-((6-Hydroxyhexyl)oxy)naphthalen-2-yl)oxy)methyl)cyclohex-4-ene-1,2,3-triol ***(B12)***. Dichloromethane/methanol (20/1, v/v), white solid, 40% yield. ^{1}H NMR (300 MHz, DMSO-d_6) δ 7.70 (dd, J = 9.0, 6.0 Hz, 2H), 7.27 (dd, J = 6.4, 2.5 Hz, 2H), 7.13 (td, J = 8.7, 2.5 Hz, 2H), 5.75 (d, J = 3.9 Hz, 1H), 4.70 (d, J = 4.1 Hz, 1H), 4.57−4.33 (m, 5H), 4.07 (dt, J = 25.0, 5.5 Hz, 3H), 3.87−3.76 (m, 1H), 3.48−3.36 (m, 3H), 2.41 (dd, J = 17.5, 5.3 Hz, 1H), 1.94 (dd, J = 17.4, 6.6 Hz, 1H), 1.75 (q, J = 6.8 Hz, 2H), 1.52−1.31 (m, 6H). ^{13}C NMR (75 MHz, DMSO-d_6) δ 155.51, 155.14, 133.83, 129.95, 129.73, 128.54, 125.64, 119.43, 119.29, 107.82, 107.31, 72.76, 71.10, 67.87, 66.79, 66.21, 61.12, 33.44, 32.98, 29.26, 25.99, 25.80.HR-MS (ESI, m/z):425.1927[M + Na]$^+$. HPLC Purity: 97.8% (Rt: 4.37 min).

(1R,2S,3R)-5-((((6-((7-Hydroxyheptyl)oxy)naphthalen-2-yl)oxy)methyl)cyclohex-4-ene-1,2,3-triol ***(B24)***. Dichloromethane/methanol (20/1, v/v), white solid, 41% yield. ^{1}H NMR (300 MHz, DMSO-d_6) δ 7.70 (dd, J = 9.0, 5.9 Hz, 2H), 7.27 (dd, J = 6.1, 2.5 Hz, 2H), 7.13 (td, J = 8.9, 2.5 Hz, 2H), 5.75 (d, J = 3.8 Hz, 1H), 4.70 (d, J = 4.0 Hz, 1H), 4.57−4.27 (m, 5H), 4.07 (dt, J = 25.1, 5.5 Hz, 3H), 3.82 (p, J = 5.6 Hz, 1H), 3.41 (dtd, J = 11.7, 7.4, 6.5, 4.8 Hz, 3H), 2.41 (dd, J = 17.5, 5.3 Hz, 1H), 1.94 (dd, J = 17.5, 6.5 Hz, 1H), 1.76 (p, J = 6.7 Hz, 2H), 1.51−1.17 (m, 8H). ^{13}C NMR (75 MHz, DMSO-d_6) δ 155.52, 155.16, 133.85, 129.96, 129.74, 128.54, 125.62, 119.42, 119.29, 107.86, 107.34, 72.78, 71.12, 67.90, 66.81, 66.22, 61.18, 33.45, 32.97, 29.19, 26.13, 25.97. HR-MS (ESI, m/z): 425.1930[M + Na]$^+$. HPLC Purity: 97.7% (Rt: 2.90 min).

General Procedure 5. *Synthesis of Compounds 12 and 14.* Compound **8** or compound **10** (2.74 mmol) was dissolved in a mixture of water (50 mL) and methanol (5 mL). Subsequently, NaOH (0.33 g, 8.21 mmol) was added to the solution, and the reaction was conducted at 50 °C for 6 h. Upon completion of the reaction, the solution was neutralized with 1 M hydrochloric acid. The resulting mixture was then extracted with DCM (50 mL × 3). The organic phases were combined, washed with brine and dried over anhydrous Na_2SO_4, and the solvent was evaporated under reduced pressure.

5-((6-(((3R,4S,5R)-3,4,5-Tris((tert-butyldimethylsilyl)oxy)-bicyclo[4.1.0]heptan-1-yl)methoxy)naphthalen-2-yl)oxy)-pentanoic acid ***(12−1)***. White solid, 85% yield. ^{1}H NMR (300 MHz, Chloroform-d) δ 10.31 (s, 1H), 7.67 (dt, J = 8.4, 2.6 Hz, 2H), 7.32 (q, J = 2.4 Hz, 2H), 6.97 (ddd, J = 26.1, 8.4, 2.3 Hz, 2H), 4.12−3.84 (m, 5H), 3.77 (dd, J = 6.6, 5.3 Hz, 1H), 3.51 (d, J = 10.9 Hz, 1H), 2.46−2.29 (m, 2H), 1.95−1.59 (m, 9H), 0.87 (d, J = 0.9 Hz, 27H), 0.10−0.00 (m, 18H). MS (ESI, m/z): 781.42[M + Na]$^+$.

6-((6-(((3R,4S,5R)-3,4,5-Tris((tert-butyldimethylsilyl)oxy)-bicyclo[4.1.0]heptan-1-yl)methoxy)naphthalen-2-yl)oxy)-hexanoic acid ***(12−2)***. White solid, 90% yield. ^{1}H NMR (300 MHz, Chloroform-d) δ 10.31 (s, 1H), 7.67 (dd, J = 8.4, 2.1 Hz, 2H), 7.32 (q, J = 2.4 Hz, 2H), 6.97 (ddd, J = 26.1, 8.3, 2.4 Hz, 2H), 4.12−3.84 (m, 5H), 3.77 (dd, J = 6.6, 5.3 Hz, 1H), 3.53 (d, J = 10.9 Hz, 1H), 2.31 (td, J = 7.0, 2.2 Hz, 2H), 2.06−1.35 (m, 11H), 0.87 (d, J = 0.9 Hz, 27H), 0.10−0.00 (m, 18H). MS (ESI, m/z): 795.45[M + Na]$^+$.

7-((6-(((3R,4S,5R)-3,4,5-Tris((tert-butyldimethylsilyl)oxy)-bicyclo[4.1.0]heptan-1-yl)methoxy)naphthalen-2-yl)oxy)-heptanoic acid ***(12−3)***. White solid, 82% yield. ^{1}H NMR (300 MHz, Chloroform-d) δ 10.31 (s, 1H), 7.72−7.61 (m, 2H), 7.32 (q, J = 2.3 Hz, 2H), 6.97 (ddd, J = 26.1, 8.4, 2.3 Hz, 2H), 4.12−3.84 (m, 5H), 3.77 (dd, J = 6.6, 5.3 Hz, 1H), 3.54 (d, J = 10.9 Hz, 1H), 2.41−2.20 (m, 2H), 1.95−1.76 (m, 6H),

https://doi.org/10.1021/acs.jmedchem.5c01753
J. Med. Chem. 2025, 68, 20561−20585

1.76−1.51 (m, 3H), 1.47−1.26 (m, 4H), 0.87 (d, J = 0.9 Hz, 27H), 0.10−0.00 (m, 18H). MS (ESI, m/z): 809.45[M + Na]$^+$.

*5-((6-(((3R,4S,5R)-3,4,5-Tris((tert-butyldimethylsilyl)oxy)-cyclohex-1-en-1-yl)methoxy)naphthalen-2-yl)oxy)pentanoic acid (**14−1**).* White solid, 91% yield. ^{1}H NMR (300 MHz, Chloroform-d) δ 10.31 (s, 1H), 7.67 (ddd, J = 8.4, 3.6, 2.0 Hz, 2H), 7.35−7.27 (m, 1H), 7.13 (t, J = 2.2 Hz, 1H), 7.00 (ddd, J = 9.5, 8.4, 2.4 Hz, 2H), 5.52−5.42 (m, 1H), 4.37 (t, J = 1.1 Hz, 2H), 4.17 (td, J = 6.8, 5.1 Hz, 2H), 4.00−3.86 (m, 3H), 2.55−2.30 (m, 4H), 1.93−1.77 (m, 2H), 1.77−1.62 (m, 2H), 0.86 (d, J = 3.0 Hz, 27H), 0.08−0.00 (m, 18H). MS (ESI, m/z): 767.40[M + Na]$^+$.

*6-((6-(((3R,4S,5R)-3,4,5-Tris((tert-butyldimethylsilyl)oxy)-cyclohex-1-en-1-yl)methoxy)naphthalen-2-yl)oxy)hexanoic acid (**14−2**).* White solid, 89% yield. ^{1}H NMR (300 MHz, Chloroform-d) δ 10.31 (s, 1H), 7.73−7.63 (m, 2H), 7.35−7.27 (m, 1H), 7.16 (t, J = 2.1 Hz, 1H), 7.00 (ddd, J = 9.5, 8.4, 2.4 Hz, 2H), 5.53−5.43 (m, 1H), 4.37 (q, J = 0.9 Hz, 2H), 4.24−4.10 (m, 2H), 4.02−3.86 (m, 3H), 2.55−2.40 (m, 1H), 2.40−2.20 (m, 3H), 1.80−1.35 (m, 6H), 0.86 (d, J = 3.0 Hz, 27H), 0.08−0.00 (m, 18H). MS (ESI, m/z): 781.43[M + Na]$^+$.b

*7-((6-(((3R,4S,5R)-3,4,5-Tris((tert-butyldimethylsilyl)oxy)-cyclohex-1-en-1-yl)methoxy)naphthalen-2-yl)oxy)heptanoic acid (**14−3**).* White solid, 86% yield. ^{1}H NMR (300 MHz, Chloroform-d) δ 10.31 (s, 1H), 7.67 (dt, J = 8.4, 2.3 Hz, 2H), 7.31 (td, J = 2.2, 0.7 Hz, 1H), 7.13 (td, J = 2.1, 1.1 Hz, 1H), 7.00 (ddd, J = 9.5, 8.4, 2.4 Hz, 2H), 5.53−5.43 (m, 1H), 4.37 (q, J = 0.9 Hz, 2H), 4.24−4.10 (m, 2H), 4.05−3.86 (m, 3H), 2.43−2.20 (m, 3H), 1.87−1.68 (m, 2H), 1.68−1.53 (m, 2H), 1.53−1.27 (m, 5H), 0.86 (d, J = 3.0 Hz, 27H), 0.08−0.00 (m, 18H). MS (ESI, m/z): 795.46[M + Na]$^+$.

General Procedure 6. *Synthesis of Compounds B5−B8, B14−B20, and B25−B28.* Either compound **12** or compound **14** (0.34 mmol) was dissolved in 30 mL of dichloromethane. Triethylamine (66 mg, 0.66 mmol), various amines (0.39 mmol), and HATU (66 mg, 0.66 mmol) were subsequently added. The mixture was allowed to react at room temperature for 6 h. Upon completion of the reaction, the mixture was poured into a 1 M citric acid aqueous solution (30 mL). The resulting solution was extracted three times with DCM (50 mL × 3). The organic phases were combined, washed with brine and dried over anhydrous Na_2SO_4. Finally, the organic solvent was removed under reduced pressure. The product was dissolved in 10 mL of anhydrous methanol, P-toluenesulfonic acid (0.03 mmol) was added, the mixture was protected under an argon atmosphere, and the reaction was allowed to proceed at room temperature for 5 h. After the reaction was complete, the mixture was poured into 20 mL of saturated sodium bicarbonate solution, extracted with dichloromethane (DCM, 30 mL × 3), combined with organic layers, washed with brine and dried over anhydrous Na_2SO_4. The solvent was removed under reduced pressure, the residue was purified by flash column chromatography, and the final product was isolated.

*N,N-Dimethyl-5-((6-(((3R,4S,5R)-3,4,5-trihydroxycyclohex-1-en-1-yl)methoxy)naphthalen-2-yl)oxy)pentanamide (**B5**),.* Dichloromethane/methanol (10/1, v/v), white solid, 35% yield. ^{1}H NMR (400 MHz) δ 7.68 (dd, J = 8.9, 7.5 Hz, 2H), 7.23 (dd, J = 18.3, 2.5 Hz, 2H), 7.14−7.09 (m, 2H), 4.45 (dd, J = 3.9, 1.0 Hz, 1H), 4.39 (dd, J = 4.6, 1.0 Hz, 1H), 4.18 (d, J = 9.9 Hz, 2H), 4.05 (t, J = 6.3 Hz, 2H), 3.90 (d, J = 9.6 Hz, 1H), 3.70 (d, J = 9.6 Hz, 1H), 3.50 (dq, J = 8.0, 4.0 Hz, 1H), 3.29 (dd, J = 8.2, 4.2 Hz, 1H), 2.96 (s, 3H), 2.81 (s, 3H), 2.36 (d, J = 7.3 Hz, 2H), 2.13 (dd, J = 13.6, 4. Five Hz, 1H), 1.80−1.65 (m, 5H), 1.20 (dd, J = 9.9, 6.0 Hz, 1H), 0.83 (t, J = 4.9 Hz, 1H), 0.54 (dd, J = 9.6, 4.4 Hz, 1H). ^{13}C NMR (75 MHz, DMSO-d_6) δ 172.21, 155.61, 155.39, 129.81, 129.77, 128.47, 128.43, 119.47, 119.36, 107.60, 107.32, 76.59, 73.71, 67.71, 66.18, 65.27, 37.13, 35.24, 33.41, 32.42, 28.80, 21.84, 21.79, 21.41, 12.93. HR-MS (ESI, m/z): 452.2037[M + Na]$^+$. HPLC Purity: 99.9% (Rt: 2.98 min).

*N,N-Diethyl-5-((6-(((3R,4S,5R)-3,4,5-trihydroxycyclohex-1-en-1-yl)methoxy)naphthalen-2-yl)oxy)pentanamide (**B6**).* Dichloromethane/methanol (10/1, v/v), white solid, 36% yield. ^{1}H NMR (300 MHz, DMSO-d_6) δ 7.70 (dd, J = 9.0, 3.9 Hz, 2H), 7.27 (dd, J = 5.2, 2.5 Hz, 2H), 7.13 (td, J = 9.1, 2.5 Hz, 2H), 5.75 (d, J = 3.8 Hz, 1H), 4.70 (d, J = 4.1 Hz, 1H), 4.56−4.36 (m, 4H), 4.08 (dt, J = 18.3, 5.4 Hz, 3H), 3.86−3.73 (m, 1H), 3.43 (dt, J = 8.4, 4.5 Hz, 1H), 3.27 (dt, J = 13.9, 7.0 Hz, 4H), 2.48−2.32 (m, 3H), 1.94 (dd, J = 17.4, 6.5 Hz, 1H), 1.74 (dq, J = 25.8, 7.8, 7.2 Hz, 4H), 1.05 (dt, J = 28.0, 7.1 Hz, 6H). ^{13}C NMR (75 MHz, DMSO-d_6) δ 171.24, 155.47, 155.15, 133.81, 129.94, 129.74, 128.53, 125.63, 119.40, 119.30, 107.84, 107.36, 72.76, 71.11, 67.79, 66.79, 66.20, 41.73, 33.44, 32.19, 28.80, 22.16, 14.78, 13.60. HR-MS (ESI, m/z): 458.2534[M + H]$^+$. HPLC Purity: 98.0% (Rt: 4.51 min).

*N,N-Dimethyl-5-((6-(((3R,4S,5R)-3,4,5-trihydroxybicyclo-[4.1.0]heptan-1-yl)methoxy)naphthalen-2-yl)oxy)-pentanamide (**B7**).* Dichloromethane/methanol (10/1, v/v), white solid, 38% yield. ^{1}H NMR (400 MHz) δ 7.68 (dd, J = 8.9, 7.5 Hz, 2H), 7.23 (dd, J = 18.3, 2.5 Hz, 2H), 7.14−7.09 (m, 2H), 4.42 (ddd, J = 21.4, 4.3, 1.0 Hz, 2H), 4.19−4.14 (m, 2H), 4.04 (d, J = 6.4 Hz, 2H), 3.90 (d, J = 9.6 Hz, 1H), 3.70 (d, J = 9.6 Hz, 1H), 3.50 (dq, J = 8.0, 4.0 Hz, 1H), 3.30 (dt, J = 8.3, 4.2 Hz, 1H), 2.96 (s, 3H), 2.81 (s, 3H), 2.36 (d, J = 7.3 Hz, 2H), 2.13 (dd, J = 13.6, 4.5 Hz, 1H), 1.81−1.65 (m, 5H), 1.21 (dt, J = 9.8, 5.9 Hz, 1H), 0.83 (t, J = 4.9 Hz, 1H), 0.57−0.51 (m, 1H). ^{13}C NMR (75 MHz, DMSO-d_6) δ 172.21, 155.61, 155.39, 129.81, 129.77, 128.47, 128.43, 119.47, 119.36, 107.60, 107.32, 76.59, 73.71, 67.71, 66.18, 65.27, 37.13, 35.24, 33.41, 32.42, 28.80, 21.84, 21.79, 21.41, 12.93. HR-MS (ESI, m/z): 444.2374[M + H]$^+$. HPLC Purity: 99.6% (Rt: 3.71 min).

*N,N-Diethyl-5-((6-(((3R,4S,5R)-3,4,5-trihydroxybicyclo-[4.1.0]heptan-1-yl)methoxy)naphthalen-2-yl)oxy)-pentanamide (**B8**).* Dichloromethane/methanol (10/1, v/v), white solid, 35% yield. ^{1}H NMR (300 MHz, DMSO-d_6) δ 7.69 (dd, J = 9.0, 5.1 Hz, 2H), 7.31−7.01 (m, 4H), 4.42 (dd, J = 15.5, 4.2 Hz, 2H), 4.23−4.11 (m, 2H), 4.05 (t, J = 6.2 Hz, 2H), 3.90 (d, J = 9.6 Hz, 1H), 3.70 (d, J = 9.7 Hz, 1H), 3.50 (tt, J = 8.0, 4.3 Hz, 1H), 3.27 (dt, J = 13.9, 6.9 Hz, 5H), 2.36 (t, J = 7.2 Hz, 2H), 2.12 (dd, J = 13.5, 4.5 Hz, 1H), 1.85−1.56 (m, 5H), 1.27−1.15 (m, 1H), 1.05 (dt, J = 28.0, 7.1 Hz, 6H), 0.83 (t, J = 4.9 Hz, 1H), 0.54 (dd, J = 9.6, 4.3 Hz, 1H). ^{13}C NMR (75 MHz, DMSO-d_6) δ 171.24, 155.63, 155.41, 129.83, 129.78, 128.46, 119.47, 119.34, 107.64, 107.35, 76.58, 73.74, 67.77, 66.18, 65.29, 41.73, 33.42, 32.19, 28.80, 22.16, 21.80, 21.42, 14.78, 13.60, 12.91. HR-MS (ESI, m/z): 472.2690[M + H]$^+$. HPLC Purity: 98.7% (Rt: 4.86 min).

*N,N-Dimethyl-6-((6-(((3R,4S,5R)-3,4,5-trihydroxycyclohex-1-en-1-yl)methoxy)naphthalen-2-yl)oxy)hexanamide (**B14**).* Dichloromethane/methanol (10/1, v/v), white solid, 43% yield. ^{1}H NMR (400 MHz, DMSO-d_6) δ 7.70 (t, J = 8.3 Hz, 2H), 7.27 (dd, J = 8.4, 2.5 Hz, 2H), 7.13 (ddd, J = 12.5, 8.9, 2.5 Hz, 2H), 5.75 (dt, J = 3.7, 1.6 Hz, 1H), 4.68 (d, J = 4.1 Hz,

https://doi.org/10.1021/acs.jmedchem.5c01753
J. Med. Chem. 2025, 68, 20561−20585

1H), 4.55−4.36 (m, 4H), 4.14−3.98 (m, 3H), 3.87−3.73 (m, 1H), 3.43 (dt, J = 8.0, 4.5 Hz, 1H), 2.96 (s, 3H), 2.81 (s, 3H), 2.41 (dd, J = 17.5, 5.3 Hz, 1H), 2.31 (t, J = 7.3 Hz, 2H), 1.99−1.90 (m, 1H), 1.78 (p, J = 6.7 Hz, 2H), 1.61−1.42 (m, 4H). ^{13}C NMR (75 MHz, DMSO-d_6) δ 172.29, 155.49, 155.14, 133.81, 129.94, 129.73, 128.54, 125.64, 119.41, 119.29, 107.79, 107.30, 72.76, 71.09, 67.85, 66.79, 66.21, 37.15, 35.23, 33.44, 32.75, 29.11, 25.93, 24.94. HR-MS (ESI, m/z): 444.2374[M + H]$^+$. HPLC Purity: 98.2% (Rt: 3.75 min).

*N,N-Diethyl-6-((6-(((3R,4S,5R)-3,4,5-trihydroxycyclohex-1-en-1-yl)methoxy)naphthalen-2-yl)oxy)hexanamide (**B15**).* Dichloromethane/methanol (10/1, v/v), white solid, 41% yield. ^{1}H NMR (400 MHz, DMSO-d_6) δ 7.70 (dd, J = 8.9, 7.4 Hz, 2H), 7.27 (dd, J = 8.3, 2.5 Hz, 2H), 7.13 (ddd, J = 13.7, 9.0, 2.5 Hz, 2H), 5.75 (dt, J = 3.6, 1.6 Hz, 1H), 4.69 (d, J = 4.1 Hz, 1H), 4.58−4.34 (m, 4H), 4.18−3.96 (m, 3H), 3.82 (tt, J = 6.6, 4.7 Hz, 1H), 3.43 (dt, J = 7.9, 4.5 Hz, 1H), 3.27 (dq, J = 14.2, 7.1 Hz, 4H), 2.41 (dd, J = 17.5, 5.2 Hz, 1H), 2.29 (d, J = 7.4 Hz, 2H), 1.95 (dd, J = 17.5, 6.6 Hz, 1H), 1.78 (p, J = 6.7 Hz, 2H), 1.59 (p, J = 7.2 Hz, 2H), 1.46 (tt, J = 9.8, 5.9 Hz, 2H), 1.14−0.91 (m, 6H). ^{13}C NMR (75 MHz, DMSO-d_6) δ 171.31, 155.49, 155.14, 133.81, 129.94, 129.73, 128.54, 125.64, 119.40, 119.29, 107.80, 107.30, 72.78, 71.10, 67.85, 66.77, 66.20, 41.75, 33.45, 32.47, 29.13, 25.92, 25.24, 14.81, 13.60. HR-MS (ESI, m/z): 472.2689[M + H]$^+$. HPLC Purity: 99.6% (Rt: 3.24 min).

*N-(2-(Dimethylamino)ethyl)-6-((6-(((3R,4S,5R)-3,4,5-trihydroxycyclohex-1-en-1-yl)methoxy)naphthalen-2-yl)oxy)hexanamide (**B16**).* Dichloromethane/methanol (6/1, v/v), white solid, 32% yield. ^{1}H NMR (400 MHz) δ 7.70 (dd, J = 8.9, 6.9 Hz, 3H), 7.26 (dd, J = 10.0, 2.5 Hz, 2H), 7.13 (ddd, J = 14.2, 8.9, 2.5 Hz, 2H), 5.75 (dt, J = 3.6, 1.6 Hz, 1H), 4.69 (d, J = 4.0 Hz, 1H), 4.58−4.34 (m, 4H), 4.18−3.93 (m, 4H), 3.82 (d, J = 6.2 Hz, 1H), 3.48−3.41 (m, 1H), 3.19−3.03 (m, 2H), 2.41 (dd, J = 17.5, 5.3 Hz, 1H), 2.28 (t, J = 6.8 Hz, 2H), 2.15 (s, 8H), 1.95 (dd, J = 17.9, 6.9 Hz, 1H), 1.76 (p, J = 6.7 Hz, 2H), 1.57 (p, J = 7.4 Hz, 2H), 1.43 (qd, J = 7.5, 6.8, 4.0 Hz, 2H). ^{13}C NMR (75 MHz, DMSO-d_6) δ 172.41, 155.48, 155.14, 133.82, 129.94, 129.73, 128.54, 125.64, 119.41, 119.30, 107.80, 107.29, 72.76, 71.09, 67.80, 66.79, 66.21, 58.73, 45.59, 37.02, 35.78, 33.44, 28.97, 25.74, 25.57.HR-MS (ESI, m/z): 487.2800[M + H]$^+$. HPLC Purity: 98.9% (Rt: 3.97 min).

*N-(2-(4-Methylpiperazin-1-yl)ethyl)-6-((6-(((3R,4S,5R)-3,4,5-trihydroxycyclohex-1-en-1-yl)methoxy)naphthalen-2-yl)oxy)hexanamide (**B17**).* Dichloromethane/methanol (8/1, v/v), white solid, 34% yield. ^{1}H NMR (400 MHz) δ 7.70 (dd, J = 8.9, 6.2 Hz, 3H), 7.26 (dd, J = 11.2, 2.5 Hz, 2H), 7.15−7.09 (m, 2H), 5.75 (dt, J = 3.7, 1.6 Hz, 1H), 4.70 (d, J = 4.0 Hz, 1H), 4.52−4.42 (m, 4H), 4.16−3.97 (m, 4H), 3.85−3.79 (m, 1H), 3.44 (dd, J = 8.1, 4.2 Hz, 1H), 3.14 (q, J = 6.6 Hz, 2H), 2.37 (ddd, J = 32.7, 15.7, 6.1 Hz, 10H), 2.11 (d, J = 13.5 Hz, 5H), 1.98−1.88 (m, 1H), 1.79−1.73 (m, 2H), 1.60−1.54 (m, 2H), 1.46−1.38 (m, 2H). ^{13}C NMR (75 MHz, DMSO-d_6) δ 172.40, 155.49, 155.16, 133.84, 129.95, 129.74, 128.53, 125.62, 119.39, 119.29, 107.86, 107.34, 72.80, 71.13, 67.84, 66.78, 66.20, 57.48, 55.00, 52.91, 45.98, 36.52, 35.83, 33.46, 28.98, 25.71, 25.59.HR-MS (ESI, m/z): 542.3220[M + H]$^+$. HPLC Purity: 99.3% (Rt: 3.38 min).

*N-(2-(Pyrrolidin-1-yl)ethyl)-6-((6-(((3R,4S,5R)-3,4,5-trihydroxycyclohex-1-en-1-yl)methoxy)naphthalen-2-yl)oxy)hexanamide (**B18**).* Dichloromethane/methanol (7/1, v/v), white solid, 30% yield. ^{1}H NMR (400 MHz, DMSO-d_6) δ 7.80 (t, J = 5.7 Hz, 1H), 7.70 (dd, J = 9.0, 6.7 Hz, 2H), 7.26 (dd, J = 10.6, 2.6 Hz, 2H), 7.13 (ddd, J = 14.5, 9.0, 2.5 Hz, 2H), 5.75 (dt, J = 3.6, 1.6 Hz, 1H), 4.69 (d, J = 4.1 Hz, 1H), 4.57−4.33 (m, 4H), 4.17−3.97 (m, 3H), 3.81 (ddd, J = 11.9, 5.3, 3.3 Hz, 1H), 3.43 (dt, J = 8.3, 4.4 Hz, 1H), 3.23−3.09 (m, 2H), 2.51−2.45 (m, 6H), 2.44−2.37 (m, 1H), 2.11 (t, J = 7.3 Hz, 2H), 1.99−1.88 (m, 1H), 1.75 (q, J = 7.0 Hz, 2H), 1.67 (p, J = 3.1 Hz, 4H), 1.58 (p, J = 7.4 Hz, 2H), 1.48−1.38 (m, 2H). ^{13}C NMR (75 MHz, DMSO-d_6) δ 172.43, 155.48, 155.14, 133.81, 129.93, 129.73, 128.53, 125.64, 119.40, 119.30, 107.80, 107.28, 72.77, 71.09, 67.80, 66.78, 66.20, 55.36, 54.02, 38.05, 35.79, 33.45, 28.97, 25.73, 25.55, 23.52. HR-MS (ESI, m/z): 513.2957[M + H]$^+$. HPLC Purity: 99.2% (Rt: 4.92 min).

*N,N-Dimethyl-6-((6-(((3R,4S,5R)-3,4,5-trihydroxybicyclo[4.1.0]heptan-1-yl)methoxy)naphthalen-2-yl)oxy)hexanamide (**B19**).* Dichloromethane/methanol (10/1, v/v), white solid, 39% yield. ^{1}H NMR (400 MHz, DMSO-d_6) δ 7.68 (t, J = 9.1 Hz, 2H), 7.22 (dd, J = 16.9, 2.5 Hz, 2H), 7.11 (ddd, J = 11.0, 8.9, 2.5 Hz, 2H), 4.40 (s, 2H), 4.18 (dd, J = 7.5, 4.7 Hz, 1H), 4.03 (t, J = 6.5 Hz, 2H), 3.90 (d, J = 9.6 Hz, 1H), 3.71 (d, J = 9.6 Hz, 1H), 3.50 (dt, J = 7.7, 3.9 Hz, 1H), 3.30 (dd, J = 8.0, 4.6 Hz, 2H), 2.95 (s, 3H), 2.81 (s, 3H), 2.31 (t, J = 7.3 Hz, 2H), 2.12 (dd, J = 13.6, 4.5 Hz, 1H), 1.81−1.72 (m, 3H), 1.62−1.52 (m, 2H), 1.46 (tt, J = 10.4, 6.0 Hz, 2H), 1.21 (ddd, J = 9.6, 7.3, 5.4 Hz, 1H), 0.83 (t, J = 4.9 Hz, 1H), 0.54 (dd, J = 9.6, 4.3 Hz, 1H). ^{13}C NMR (75 MHz, DMSO-d_6) δ 172.30, 155.63, 155.44, 129.84, 129.78, 128.46, 119.46, 119.36, 107.64, 107.32, 76.58, 73.75, 67.85, 66.18, 65.30, 37.15, 35.23, 33.43, 32.74, 29.11, 25.94, 24.94, 21.80, 21.43, 12.90. HR-MS (ESI, m/z): 458.2531[M + H]$^+$. HPLC Purity: 98.0% (Rt: 4.06 min).

*N,N-Diethyl-6-((6-(((3R,4S,5R)-3,4,5-trihydroxybicyclo[4.1.0]heptan-1-yl)methoxy)naphthalen-2-yl)oxy)hexanamide (**B20**).* Dichloromethane/methanol (10/1, v/v), white solid, 30% yield. ^{1}H NMR (400 MHz) δ 7.68 (t, J = 9.0 Hz, 2H), 7.22 (dd, J = 17.1, 2.5 Hz, 2H), 7.11 (ddd, J = 11.5, 8.8, 2.5 Hz, 2H), 4.36 (s, 2H), 4.18 (dd, J = 7.5, 4.7 Hz, 1H), 4.03 (t, J = 6.5 Hz, 2H), 3.90 (d, J = 9.6 Hz, 1H), 3.70 (d, J = 9.6 Hz, 1H), 3.50 (dt, J = 7.9, 4.0 Hz, 1H), 3.27 (dq, J = 14.2, 7.1, 6.5 Hz, 6H), 2.29 (t, J = 7.3 Hz, 2H), 2.12 (dd, J = 13.5, 4.5 Hz, 1H), 1.80−1.72 (m, 3H), 1.58 (q, J = 7.5 Hz, 2H), 1.46 (t, J = 7.5 Hz, 2H), 1.23−1.17 (m, 1H), 1.04 (dt, J = 36.2, 7.0 Hz, 6H), 0.83 (t, J = 5.0 Hz, 1H), 0.54 (dd, J = 9.7, 4.4 Hz, 1H). ^{13}C NMR (101 MHz, DMSO-d_6) δ 171.31, 155.62, 155.43, 129.82, 128.46, 119.46, 119.35, 107.61, 107.30, 76.57, 73.73, 67.83, 66.18, 65.29, 41.74, 33.42, 32.47, 29.13, 25.92, 25.24, 21.79, 21.42, 14.80, 13.59, 12.91. HR-MS (ESI, m/z): 486.2847[M + H]$^+$. HPLC Purity: 98.6% (Rt: 5.32 min).

*N,N-Dimethyl-7-((6-(((3R,4S,5R)-3,4,5-trihydroxycyclohex-1-en-1-yl)methoxy)naphthalen-2-yl)oxy)heptanamide (**B25**).* Dichloromethane/methanol (10/1, v/v), white solid, 46% yield. ^{1}H NMR (400 MHz) δ 7.70 (t, J = 8.4 Hz, 2H), 7.27 (dd, J = 8.3, 2.5 Hz, 2H), 7.13 (ddd, J = 11.2, 8.9, 2.5 Hz, 2H), 5.78−5.70 (m, 1H), 4.69 (s, 1H), 4.48 (s, 4H), 4.12−4.01 (m, 3H), 3.82 (q, J = 6.5 Hz, 1H), 3.43 (dd, J = 7.9, 4.1 Hz, 1H), 2.95 (s, 3H), 2.80 (s, 3H), 2.41 (dd, J = 17.5, 5.2 Hz, 1H), 2.27 (d, J = 7.4 Hz, 2H), 1.95 (dd, J = 17.4, 6.5 Hz, 1H), 1.76 (p, J = 6.8 Hz, 2H), 1.54−1.26 (m, 6H). ^{13}C NMR (101 MHz, DMSO-d_6) δ 172.33, 155.50, 155.14, 133.82, 129.95, 129.73, 128.53, 125.63, 119.43, 119.29, 107.81, 107.30, 72.76, 71.10, 67.84, 66.79, 66.21, 37.14, 35.22, 33.44, 32.73, 29.13, 29.06, 25.96, 25.11. HR-MS (ESI, m/z): 458.2530[M + H]$^+$. HPLC Purity: 99.0% (Rt: 3.17 min).

https://doi.org/10.1021/acs.jmedchem.5c01753
J. Med. Chem. 2025, 68, 20561−20585

*N,N-Diethyl-7-((6-(((3R,4S,5R)-3,4,5-trihydroxycyclohex-1-en-1-yl)methoxy)naphthalen-2-yl)oxy)heptanamide (**B26**).* Dichloromethane/methanol (10/1, v/v), white solid, 51% yield. ^{1}H NMR (400 MHz) δ 7.70 (dd, J = 8.9, 7.7 Hz, 2H), 7.27 (dd, J = 8.7, 2.5 Hz, 2H), 7.16−7.09 (m, 2H), 5.75 (dt, J = 3.5, 1.5 Hz, 1H), 4.68 (s, 1H), 4.48 (s, 2H), 4.16−4.01 (m, 3H), 3.82 (q, J = 6.6 Hz, 1H), 3.43 (dd, J = 7.9, 4.1 Hz, 1H), 3.26 (dq, J = 14.1, 7.1 Hz, 6H), 2.41 (dd, J = 17.5, 5.3 Hz, 1H), 2.27 (t, J = 7.4 Hz, 2H), 1.94 (dd, J = 17.5, 6.5 Hz, 1H), 1.76 (p, J = 6.7 Hz, 2H), 1.61−1.23 (m, 6H), 1.09 (t, J = 7.1 Hz, 3H), 0.99 (t, J = 7.1 Hz, 3H). ^{13}C NMR (101 MHz, DMSO-d_6) δ 171.35, 155.50, 155.14, 133.82, 129.95, 129.73, 128.53, 125.64, 119.42, 119.29, 107.81, 107.30, 72.76, 71.10, 67.83, 66.79, 66.21, 41.74, 33.44, 32.44, 29.12, 29.02, 25.97, 25.41, 14.81, 13.59. HR-MS (ESI, m/z): 486.2847[M + H]$^+$. HPLC Purity: 98.8% (Rt: 2.96 min).

*N,N-Dimethyl-7-((6-(((3R,4S,5R)-3,4,5-trihydroxybicyclo-[4.1.0]heptan-1-yl)methoxy)naphthalen-2-yl)oxy)-heptanamide (**B27**).* Dichloromethane/methanol (10/1, v/v), white solid, 42% yield. ^{1}H NMR (300 MHz, DMSO-d_6) δ 7.68 (dd, J = 8.9, 7.2 Hz, 2H), 7.22 (dd, J = 12.8, 2.5 Hz, 2H), 7.11 (ddd, J = 9.1, 6.7, 2.5 Hz, 2H), 4.18 (dd, J = 7.4, 4.7 Hz, 1H), 4.03 (t, J = 6.5 Hz, 2H), 3.89 (s, 1H), 3.71 (d, J = 9.6 Hz, 2H), 3.55−3.45 (m, 2H), 3.29 (dd, J = 8.0, 4.6 Hz, 1H), 2.95 (s, 3H), 2.80 (s, 3H), 2.28 (t, J = 7.3 Hz, 2H), 2.13 (dd, J = 13.5, 4.5 Hz, 1H), 1.76 (ddt, J = 11.2, 6.5, 3.3 Hz, 3H), 1.60−1.10 (m, 8H), 0.83 (t, J = 5.0 Hz, 1H), 0.54 (dd, J = 9.7, 4.4 Hz, 1H). ^{13}C NMR (75 MHz, DMSO-d_6) δ 172.33, 155.62, 155.44, 129.84, 129.78, 128.46, 119.46, 119.37, 107.63, 107.30, 76.58, 73.75, 67.83, 66.18, 65.30, 37.15, 35.22, 33.43, 32.73, 29.14, 29.06, 25.96, 25.11, 21.80, 21.43, 12.90. HR-MS (ESI, m/z): 472.2689[M + H]$^+$. HPLC Purity: 99.8% (Rt: 2.79 min).

*N,N-Diethyl-7-((6-(((3R,4S,5R)-3,4,5-trihydroxybicyclo-[4.1.0]heptan-1-yl)methoxy)naphthalen-2-yl)oxy)-heptanamide (**B28**).* Dichloromethane/methanol (10/1, v/v), white solid, 37% yield. ^{1}H NMR (400 MHz) δ 7.68 (t, J = 9.0 Hz, 2H), 7.22 (dd, J = 16.7, 2.5 Hz, 2H), 7.15−7.09 (m, 2H), 4.39 (s, 1H), 4.18 (dd, J = 7.5, 4.7 Hz, 1H), 4.03 (t, J = 6.5 Hz, 2H), 3.90 (d, J = 9.6 Hz, 1H), 3.70 (d, J = 9.6 Hz, 1H), 3.53−3.48 (m, 1H), 3.26 (dq, J = 14.1, 7.3 Hz, 6H), 2.27 (t, J = 7.4 Hz, 2H), 2.12 (dd, J = 13.5, 4.5 Hz, 1H), 1.76 (ddt, J = 11.9, 6.7, 3.4 Hz, 3H), 1.58−1.17 (m, 8H), 1.08 (d, J = 7.0 Hz, 3H), 0.99 (t, J = 7.0 Hz, 3H), 0.83 (t, J = 5.0 Hz, 1H), 0.54 (dd, J = 9.6, 4.4 Hz, 1H). ^{13}C NMR (75 MHz, DMSO-d_6) δ 171.35, 155.62, 155.44, 129.84, 129.78, 128.46, 128.43, 119.45, 119.36, 107.63, 107.29, 76.58, 73.75, 67.81, 66.18, 65.30, 41.74, 39.73, 33.43, 32.44, 29.12, 29.03, 25.97, 25.75, 25.41, 21.80, 21.43, 14.80, 13.59, 12.90. HR-MS (ESI, m/z): 500.3003[M + H]$^+$. HPLC Purity: 99.9% (Rt: 3.06 min).

VDR Binding Assay. The VDR binding affinity assay was conducted via the PolarScreen Vitamin D Receptor Competitor Assay Red Kit (Thermo Fisher, Massachusetts, USA), which is designed to determine the IC_{50} values of compounds that bind to the full-length VDR. This assay measures the decrease in the polarization value that occurs when the binding of the full-length VDR to the Fluormone Tracer is disrupted by the presence of a competitor compound. All test compounds were prepared in a 1% DMSO solution and evaluated for their binding affinity at a concentration of 1 μM, with each measurement performed in triplicate. Fluorescence polarization was measured via a BioTek Cytation 5 Multiscan Spectrum instrument equipped with a 535 nm excitation filter (25 nm bandwidth) and a 590 nm emission filter (20 nm bandwidth). The fluorescence polarization value of calcipotriol was set as the standard at 100%, and the relative binding affinity of each test compound was calculated via the following formula: $(mP_{DMSO} - mP_{test\ compound})/(mP_{DMSO} - mP_{calcipotriene}) \times 100\%$.

RNA Extraction and Quantitative Real-Time Polymerase Chain Reaction (QPCR). cDNA was generated from RNA extracts derived from cultured LX-2 cells or liver tissues via HiScript II Q RT SuperMix for Q-PCR (+ gDNA wiper mix) (Vazyme, Nanjing, China). β-actin (human) or β-actin (mouse) was used as an internal control. Q-PCR was performed using Hieff Q-PCR SYBR Green Master Mix (High Rox Plus) (Vazyme, Nanjing, China). The primer pairs used for the mRNAs are listed in Table S1.

Transcription Assay. The luciferase activity assay was conducted via the Dual-Luciferase Reporter Assay System (Vazyme, Nanjing, China) following the manufacturer's guidelines. HEK293 cells at 50−60% confluence were seeded in 48-well plates. For each well, the transfection mixture included 140 ng of TK-SPP × 3-Luci reporter plasmid, 20 ng of pCMX-Renilla, 30 ng of pENTER-CMV-hRXRα, and 100 ng of pCMX-VDR, and Lipofectamine 2000 Reagent (Thermo Fisher, Massachusetts, USA) was used. Six hours posttransfection, test compounds were added, and luciferase activity was measured 48 h later with the Dual-Luciferase Assay System. Firefly luciferase activity was normalized to Renilla luciferase activity. All the experiments were repeated three times under the same conditions.

Western Blot. The cell or tissue samples were lysed with radioimmunoprecipitation assay buffer. The protein concentrations of the samples were determined via a BCA protein assay kit (Beyotime, Shanghai, China) according to the manufacturer's instructions. The protein mixture was diluted with SDS−PAGE sample loading buffer (5×) containing the reducing reagent and heated at 95 °C for 5 min. Proteins were separated on 4−20% SDS−polyacrylamide gels (Yeasen, Shanghai, China) and then transferred onto polyvinylidene fluoride (PVDF) membranes. The membranes were blocked with 5% bovine serum albumin at 37 °C for 1 h, followed by overnight incubation with primary antibodies at 4 °C. After washing, the membranes were incubated with a secondary antibody at room temperature for 1 h, and the proteins were detected via Tanon 5200. The primary antibodies used were mouse anti-α-SMA (Boster, Wuhan, China), rabbit anticollagen I (Boster, Wuhan, China), and mouse anti-β-actin (Boster, Wuhan, China). Horseradish peroxidase-conjugated goat antirabbit/mouse IgG (Boster, Wuhan, China) was used as the secondary antibody. Images were acquired with Image Lab 6.0.1, and cumulative densitometric analyses of the Western blot images were performed via ImageJ 1.54a.

mRNA Sequencing Experimental Methods. Total RNA was extracted via TRIzol reagent (Invitrogen, CA, USA) according to the manufacturer's protocol. RNA purity and quantification were evaluated via a NanoDrop 2000 spectrophotometer (Thermo Scientific, USA). RNA integrity was assessed via an Agilent 2100 Bioanalyzer (Agilent Technologies, Santa Clara, CA, USA). The libraries were subsequently constructed via the VAHTS Universal V10 RNA-seq Library Prep Kit (Premixed Version) according to the manufacturer's instructions. Transcriptome sequencing and analysis were conducted by OE Biotech Co., Ltd. (Shanghai, China).

https://doi.org/10.1021/acs.jmedchem.5c01753
J. Med. Chem. 2025, 68, 20561−20585

CCl_4-Induced Mouse Hepatic Fibrosis Model. Male C57BL/6 mice (8 weeks old) were obtained from the Medical School of Yangzhou University (Yangzhou, China). All the animal experiments were conducted in strict compliance with the Guide for the Care and Use of Laboratory Animals of the National Institutes of Health and were approved by the Experimentation Ethics Review Committee of China Pharmaceutical University (Ethics Approval Number: 2024-03-033). The animals were housed in a specific-pathogen-free facility at a temperature of 24 ± 2 °C, humidity of 40−70%, and a 12-h dark/light cycle. To establish the CCl_4-induced liver fibrosis model, the mice received intraperitoneal injections of a CCl_4/corn oil (1/50, v/v) mixture at a dose of 0.5 mL/kg three times a week for 4 weeks. Treatments began after 2 weeks of CCl_4 injections, when fibrosis typically develops. DMSO, calcipotriol (100 μg/kg body weight), compound **15a**, or **B15** (500 μg/kg body weight) was administered by oral gavage five times weekly for 2 weeks (n = 5 per group). The mice were sacrificed 4 h after the final treatment, and serum and liver samples were collected for blood chemistry analysis, immunofluorescence and histological staining, Western blotting, and qPCR.

Blood Chemistry Analysis. To assess liver function changes in each group of mice, serum was obtained by centrifuging whole blood samples at 12,000 rpm for 10 min at 4 °C. The levels of serum alanine aminotransferase (ALT), aspartate transaminase (AST), total bile acid (TBA), and calcium were measured via commercial kits from Rayto (Shenzhen, China).

Histological Staining. For histological staining, liver tissues were fixed in 4% (w/v) neutral phosphate-buffered paraformaldehyde for 24 h, followed by dehydration, clearing, and embedding in paraffin. The tissues were then sectioned at a thickness of 5 μm and stained with hematoxylin−eosin (H&E) for structural observation or with Masson's Trichrome staining to detect collagen deposits.

Statistical Analysis. The data are expressed as the means ± standard deviations (SD). Statistical significance was assessed via a two-tailed unpaired Student's t test for comparisons between two sets of values or ANOVA for comparisons among multiple groups via GraphPad Prism 8. Exact p values are provided in the figures or their legends. No exclusion criteria were applied in the design of the experiments for this study.

Molecular Docking. The docking experiments were conducted using the hVDR crystal structure (PDB ID: 2ZFX). The protein structure was prepared via the Protein Preparation Wizard module with default parameters. The workflow included preprocessing the structure, optimizing hydrogen bonds, and performing restrained minimization. The ligand structures were prepared via the LigPrep module with the default settings. Receptor grids were generated via the Receptor Grid Generation module, which centers the grid on the cocrystallized ligand and employs default parameters. Docking was performed via the ligand docking module in extra precision (XP) mode with default settings.

■ ASSOCIATED CONTENT

Supporting Information

The Supporting Information is available free of charge at https://pubs.acs.org/doi/10.1021/acs.jmedchem.5c01753.

Binding model of **B20** with 2ZFX (PDB)
Binding model of **B15** with 2ZFX (PDB)
Binding model of **A17** with 2ZFX (PDB)
Molecular formula stings (CSV)
^{1}H NMR and ^{13}C NMR of all target compounds, HR−MS of all target compounds, HPLC analysis of all target compounds and experimental procedures for biological assays (PDF)

■ AUTHOR INFORMATION

Corresponding Authors

Can Zhang − *State Key Laboratory of Natural Medicines, Jiangsu Key Laboratory of Drug Discovery for Metabolic Diseases, Center of Advanced Pharmaceuticals and Biomaterials, China Pharmaceutical University, Nanjing 211198, P. R. China*; orcid.org/0000-0003-3529-5438; Email: zhangcan@cpu.edu.cn

Cong Wang − *State Key Laboratory of Natural Medicines, Jiangsu Key Laboratory of Drug Discovery for Metabolic Diseases, Center of Advanced Pharmaceuticals and Biomaterials, China Pharmaceutical University, Nanjing 211198, P. R. China*; Email: wangcong@cpu.edu.cn

Authors

Yi Gao − *State Key Laboratory of Natural Medicines, Jiangsu Key Laboratory of Drug Discovery for Metabolic Diseases, Center of Advanced Pharmaceuticals and Biomaterials, China Pharmaceutical University, Nanjing 211198, P. R. China*

Yue Wu − *State Key Laboratory of Natural Medicines, Jiangsu Key Laboratory of Drug Discovery for Metabolic Diseases, Center of Advanced Pharmaceuticals and Biomaterials, China Pharmaceutical University, Nanjing 211198, P. R. China*

Chun Guan − *State Key Laboratory of Natural Medicines, Jiangsu Key Laboratory of Drug Discovery for Metabolic Diseases, Center of Advanced Pharmaceuticals and Biomaterials, China Pharmaceutical University, Nanjing 211198, P. R. China*

Nuo Cheng − *State Key Laboratory of Natural Medicines, Jiangsu Key Laboratory of Drug Discovery for Metabolic Diseases, Center of Advanced Pharmaceuticals and Biomaterials, China Pharmaceutical University, Nanjing 211198, P. R. China*

Yu Tong − *State Key Laboratory of Natural Medicines, Jiangsu Key Laboratory of Drug Discovery for Metabolic Diseases, Center of Advanced Pharmaceuticals and Biomaterials, China Pharmaceutical University, Nanjing 211198, P. R. China*

Complete contact information is available at: https://pubs.acs.org/10.1021/acs.jmedchem.5c01753

Author Contributions

[#]Y.G.and Y.W.contributed equally to this study. The manuscript was written through the contributions of all the authors. All the authors approved the final version of the manuscript.

Notes

The authors declare no competing financial interest.

■ ACKNOWLEDGMENTS

We thank the Public Platform of the State Key Laboratory of Natural Medicines for assisting with pathological section imaging. This work was supported by the National Natural

Science Foundation of China (Nos. 82130102, 92159304, 81930099, and 81773664), the Natural Science Foundation of Jiangsu Province (No. BK20212011), the Natural Science Foundation of Chongqing (CSTB2023NSCQMSX0607), and the "Open Competition to Select the Best Candidates" Key Technology Program for Nucleic Acid Drugs of NCTIB (No. NCTIB2022HS01014).

■ ABBREVIATIONS

α-SMA, α-Smooth actin; CH_2N_2, diazomethane; DCM, dichloromethane; DEAD, diethyl azodicarboxylate; DIBAL-H, diisobutyl aluminum hydride; DIPEA, *N*,N-diisopropylethylamine; DMF, *N*,*N*-dimethylformamide; DMSO, dimethyl sulfoxide; ECM, Extracellular matrix; Et_2O, ether; HATU, 2-(7-azabenzotriazol-1-yl)-*N*,*N*",*N*"-tetramethyluronium hexafluorophosphate; HSCs, Hepatic stellate cells; NaH, sodium hydride; NaOH, sodium hydroxide; PPh_3, triphenylphosphine; SAR, structure−activity relationship; $SOCl_2$, thionyl chloride; TBSCl, t-butyldimethylchlorosilane; TGFβ1, Transforming growth factor-β1; TIMP-1, Tissue inhibitor of metalloproteinase-1; THF, tetrahydrofuran; VD, Vitamin D; VDR, Vitamin D receptor

■ REFERENCES

(1) Hernandez-Gea, V.; Friedman, S. L. Pathogenesis of Liver Fibrosis. *Annu. Rev. Pathol.: Mech. Dis.* **2011**, *6* (1), 425−456.
(2) Pinzani, M.; Rombouts, K.; Colagrande, S. Fibrosis in chronic liver diseases: Diagnosis and management. *J. Hepatol.* **2005**, *42* (1), S22−S36.
(3) Bataller, R.; Brenner, D. A. Liver fibrosis. *J.Clin.Invest.* **2005**, *115* (2), 209−218.
(4) Kisseleva, T.; Brenner, D. Molecular and cellular mechanisms of liver fibrosis and its regression. *Nat. Rev. Gastroenterol. Hepatol.* **2021**, *18* (3), 151−166.
(5) Hammerich, L.; Tacke, F. Hepatic inflammatory responses in liver fibrosis. *Nat. Rev. Gastroenterol. Hepatol.* **2023**, *20* (10), 633−646.
(6) Horn, P.; Tacke, F. Metabolic reprogramming in liver fibrosis. *Cell Metab.* **2024**, *36* (7), 1439−1455.
(7) Inagaki, Y.; Okazaki, I. Emerging insights into Transforming growth factor Smad signal in hepatic fibrogenesis. *Gut* **2007**, *56* (2), 284−292.
(8) Schwabe, R. F.; Tabas, I.; Pajvani, U. B. Mechanisms of Fibrosis Development in Nonalcoholic Steatohepatitis. *Gastroenterology* **2020**, *158* (7), 1913−1928.
(9) Fondevila, M. F.; Novoa, E.; Gonzalez-Rellan, M. J.; Fernandez, U.; Heras, V.; Porteiro, B.; Parracho, T.; Dorta, V.; Riobello, C.; Lima, N. D. S. p63 controls metabolic activation of hepatic stellate cells and fibrosis via an HER2-ACC1 pathway. *Cell Rep. Med.* **2024**, *5* (2), 101401.
(10) Odagiri, N.; Matsubara, T.; Sato-Matsubara, M.; Fujii, H.; Enomoto, M.; Kawada, N. Anti-fibrotic treatments for chronic liver diseases: The present and the future. *Clini. Mol.Hepatol.* **2021**, *27* (3), 413−424.
(11) Tan, Y.; Sun, X.; Xu, Y.; Tang, B.; Xu, S.; Lu, D.; Ye, Y.; Luo, X.; Diao, X.; Li, F.; Wang, T.; Chen, J.; Xu, Q.; Wu, X. Small molecule targeting CELF1 RNA-binding activity to control HSC activation and liver fibrosis. *Nucleic Acids Res.* **2022**, *50* (5), 2440−2451.
(12) Meng, X.-M.; Nikolic-Paterson, D. J.; Lan, H. Y. TGFβ: The master regulator of fibrosis. *Nat. Rev. Nephrol.* **2016**, *12* (6), 325−338.
(13) Fabre, T.; Molina, M. F.; Soucy, G.; Goulet, J.-P.; Willems, B.; Villeneuve, J.-P.; Bilodeau, M.; Shoukry, N. H. Type 3 cytokines IL-17A and IL-22 drive TGF-β−dependent liver fibrosis. *Sci. Immunol.* **2018**, *3* (28), No. eaar7754.
(14) Crouchet, E.; Dachraoui, M.; Jühling, F.; Roehlen, N.; Oudot, M. A.; Durand, S. C.; Ponsolles, C.; Gadenne, C.; Meiss-Heydmann, L.; Moehlin, J.; Martin, R.; Brignon, N.; Del Zompo, F.; Teraoka, Y.; Aikata, H.; Abe-Chayama, H.; Chayama, K.; Saviano, A.; Heide, D.; Onea, M.; Geyer, L.; Wolf, T.; Felli, E.; Pessaux, P.; Heikenwälder, M.; Chambon, P.; Schuster, C.; Lupberger, J.; Mukherji, A.; Baumert, T. F. Targeting the liver clock improves fibrosis by restoring TGFβ signaling. *J. Hepatol.* **2025**, *82* (1), 120−133.
(15) Song, Y.; Wei, J.; Li, R.; Fu, R.; Han, P.; Wang, H.; Zhang, G.; Li, S.; Chen, S.; Liu, Z.; Zhao, Y.; Zhu, C.; Zhu, J.; Zhang, S.; Pei, H.; Cheng, J.; Wu, J.; Dong, L.; Song, G.; Shen, X.; Yao, Q. Tyrosine kinase receptor B attenuates liver fibrosis by inhibiting TGFβ/SMAD signaling. *Hepatology* **2023**, *78* (5), 1433−1447.
(16) Meng, X. M.; Huang, X. R.; Xiao, J.; Chen, H. Y.; Zhong, X.; Chung, A. C. K.; Lan, H. Y. Diverse roles of TGFβ receptor II in renal fibrosis and inflammation *in vivo* and *in vitro*. *J.Pathol.* **2012**, *227* (2), 175−188.
(17) Beilfuss, A.; Sowa, J.-P.; Sydor, S.; Beste, M.; Bechmann, L. P.; Schlattjan, M.; Syn, W.-K.; Wedemeyer, I.; Mathé, Z.; Jochum, C.; Gerken, G.; Gieseler, R. K.; Canbay, A. Vitamin D counteracts fibrogenic TGFβ signaling in human hepatic stellate cells both receptor-dependently and independently. *Gut* **2015**, *64* (5), 791−799.
(18) Zerr, P.; Vollath, S.; Palumbo-Zerr, K.; Tomcik, M.; Huang, J.; Distler, A.; Beyer, C.; Dees, C.; Gela, K.; Distler, O.; et al. Vitamin D receptor regulates TGF-β signalling in systemic sclerosis. *Ann. Rheum. Dis.* **2015**, *74* (3), No. e20.
(19) Bouillon, R.; Marcocci, C.; Carmeliet, G.; Bikle, D.; White, J. H.; Dawson-Hughes, B.; Lips, P.; Munns, C. F.; Lazaretti-Castro, M.; Giustina, A.; Bilezikian, J. Skeletal and Extraskeletal Actions of Vitamin D: Current Evidence and Outstanding Questions. *Endocr. Rev.* **2019**, *40* (4), 1109−1151.
(20) Christakos, S.; Dhawan, P.; Verstuyf, A.; Verlinden, L.; Carmeliet, G. Vitamin D: Metabolism, Molecular Mechanism of Action, and Pleiotropic Effects. *Physiol. Rev.* **2016**, *96* (1), 365−408.
(21) Ding, N.; Yu, R. T.; Subramaniam, N.; Sherman, M. H.; Wilson, C.; Rao, R.; Leblanc, M.; Coulter, S.; He, M.; Scott, C.; Lau, S. L.; Atkins, A. R.; Barish, G. D.; Gunton, J. E.; Liddle, C.; Downes, M.; Evans, R. M. A Vitamin D Receptor/SMAD Genomic Circuit Gates Hepatic Fibrotic Response. *Cell* **2013**, *153* (3), 601−613.
(22) Ito, I.; Waku, T.; Aoki, M.; Abe, R.; Nagai, Y.; Watanabe, T.; Nakajima, Y.; Ohkido, I.; Yokoyama, K.; Miyachi, H.; Shimizu, T.; Murayama, A.; Kishimoto, H.; Nagasawa, K.; Yanagisawa, J. A nonclassical vitamin D receptor pathway suppresses renal fibrosis. *J Clin.Invest.* **2013**, *123* (11), 4579−4594.
(23) Eisman, J. A. Genetics of Osteoporosis. *Endocr. Rev.* **1999**, *20* (6), 788−804.
(24) Nagpal, S.; Na, S.; Rathnachalam, R. Noncalcemic Actions of Vitamin D Receptor Ligands. *Endocr. Rev.* **2005**, *26* (5), 662−687.
(25) Jones, G.; Kaufmann, M. Update on pharmacologically-relevant vitamin D analogs. *Br. J. Clin. Pharmacol.* **2019**, *85* (6), 1095−1102.
(26) Ma, Y. Identification and characterization of noncalcemic, tissue-selective, nonsecosteroidal vitamin D receptor modulators. *J.Clin.Invest.* **2006**, *116* (4), 892−904.
(27) Yamada, S.; Makishima, M. Structure−activity relationship of nonsecosteroidal vitamin D receptor modulators. *Trends Pharmacol. Sci* **2014**, *35* (7), 324−337.
(28) Hakamata, W.; Sato, Y.; Okuda, H.; Honzawa, S.; Saito, N.; Kishimoto, S.; Yamashita, A.; Sugiura, T.; Kittaka, A.; Kurihara, M. 2′R)-Analog of LG190178 is a major active isomer. *Bioorg. Med. Chem. Lett.* **2008**, *18* (1), 120−123.
(29) Shen, W.; Xue, J.; Zhao, Z.; Zhang, C. Novel nonsecosteroidal VDR agonists with phenyl-pyrrolyl pentane skeleton. *Eur. J. Med. Chem.* **2013**, *69*, 768−778.
(30) Peräkylä, M.; Malinen, M.; Herzig, K.-H.; Carlberg, C. Gene Regulatory Potential of Nonsteroidal Vitamin D Receptor Ligands. *Mol. Endocrinol.* **2005**, *19* (8), 2060−2073.
(31) Fujii, S.; Masuno, H.; Taoda, Y.; Kano, A.; Wongmayura, A.; Nakabayashi, M.; Ito, N.; Shimizu, M.; Kawachi, E.; Hirano, T.; Endo, Y.; Tanatani, A.; Kagechika, H. Boron Cluster-based Development of Potent Nonsecosteroidal Vitamin D Receptor Ligands: Direct

https://doi.org/10.1021/acs.jmedchem.5c01753
J. Med. Chem. 2025, 68, 20561−20585

Observation of Hydrophobic Interaction between Protein Surface and Carborane. *J. Am. Chem. Soc.* **2011**, *133* (51), 20933−20941.
(32) Hao, M.; Hou, S.; Xue, L.; Yuan, H.; Zhu, L.; Wang, C.; Wang, B.; Tang, C.; Zhang, C. Further Developments of the Phenyl-Pyrrolyl Pentane Series of Nonsteroidal Vitamin D Receptor Modulators as Anticancer Agents. *J. Med. Chem.* **2018**, *61* (7), 3059−3075.
(33) Kang, Z.; Wang, C.; Tong, Y.; Li, Y.; Gao, Y.; Hou, S.; Hao, M.; Han, X.; Wang, B.; Wang, Q.; Zhang, C. Novel Nonsecosteroidal Vitamin D Receptor Modulator Combined with Gemcitabine Enhances Pancreatic Cancer Therapy through Remodeling of the Tumor Microenvironment. *J. Med. Chem.* **2021**, *64* (1), 629−643.
(34) Wang, C.; Wang, B.; Xue, L.; Kang, Z.; Hou, S.; Du, J.; Zhang, C. Design, Synthesis, and Antifibrosis Activity in Liver of Non-secosteroidal Vitamin D Receptor Agonists with Phenyl-pyrrolyl Pentane Skeleton. *J. Med. Chem.* **2018**, *61* (23), 10573−10587.
(35) Liu, X.; Wu, Y.; Guan, C.; Cheng, N.; Wang, X.; Liu, Y.; et al. Vitamin D receptor agonists inhibit liver fibrosis by disrupting the interaction between hepatic stellate cells and neutrophil extracellular traps. *Biochem. Pharmacol.* **2025**, *240*, 117059.
(36) Gao, F.; Guan, C.; Cheng, N.; Liu, Y.; Wu, Y.; Shi, B.; et al. Design, synthesis, and anti-liver fibrosis activity of novel non-steroidal vitamin D receptor agonists based on open-ring steroid scaffold. *Eur. J. Med. Chem.* **2025**, *286*, 117250.
(37) Jurutka, P. W.; Remus, L. S.; Whitfield, G. K.; Thompson, P. D.; Hsieh, J. C.; Zitzer, H.; Tavakkoli, P.; Galligan, M. A.; Dang, H. T. L.; Haussler, C. A.; Haussler, M. R. The Polymorphic N Terminus in Human Vitamin D Receptor Isoforms Influences Transcriptional Activity by Modulating Interaction with Transcription Factor IIB. *Mol. Endocrinol.* **2000**, *14* (3), 401−420.
(38) Rochel, N.; Wurtz, J. M.; Mitschler, A.; Klaholz, B.; Moras, D. Crystal structure of the nuclear receptor for vitamin D bound to its natural ligand. *Mol. Cell* **2000**, *5*, 173−179.
(39) Seoane, S.; Gogoi, P.; Zárate-Ruíz, A.; Peluso-Iltis, C.; Peters, S.; Guiberteau, T.; Maestro, M. A.; Pérez-Fernández, R.; Rochel, N.; Mouriño, A. Design, Synthesis, Biological Activity, and Structural Analysis of Novel Des-C-Ring and Aromatic-D-Ring Analogues of 1α,25-Dihydroxyvitamin D 3. *J. Med. Chem.* **2022**, *65* (19), 13112−13124.
(40) Kawagoe, F.; Mendoza, A.; Hayata, Y.; Asano, L.; Kotake, K.; Mototani, S.; Kawamura, S.; Kurosaki, S.; Akagi, Y.; Takemoto, Y.; Nagasawa, K.; Nakagawa, H.; Uesugi, M.; Kittaka, A. Discovery of a Vitamin D Receptor-Silent Vitamin D Derivative That Impairs Sterol Regulatory Element-Binding Protein *In Vivo*. *J. Med. Chem.* **2021**, *64* (9), 5689−5709.
(41) Carlberg, C. Molecular basis of the selective activity of vitamin D analogues. *J. Cell. Biochem.* **2003**, *88* (2), 274−281.
(42) Siramshetty, V. B.; Shah, P.; Kerns, E.; Nguyen, K.; Yu, K. R.; Kabir, M.; Williams, J.; Neyra, J.; Southall, N. N.; Nguyen, Đ.-T.; et al. Retrospective assessment of rat liver microsomal stability at NCATS: Data and QSAR models. *Sci. Rep.* **2020**, *10* (1), 20713.

https://doi.org/10.1021/acs.jmedchem.5c01753
J. Med. Chem. 2025, 68, 20561−20585